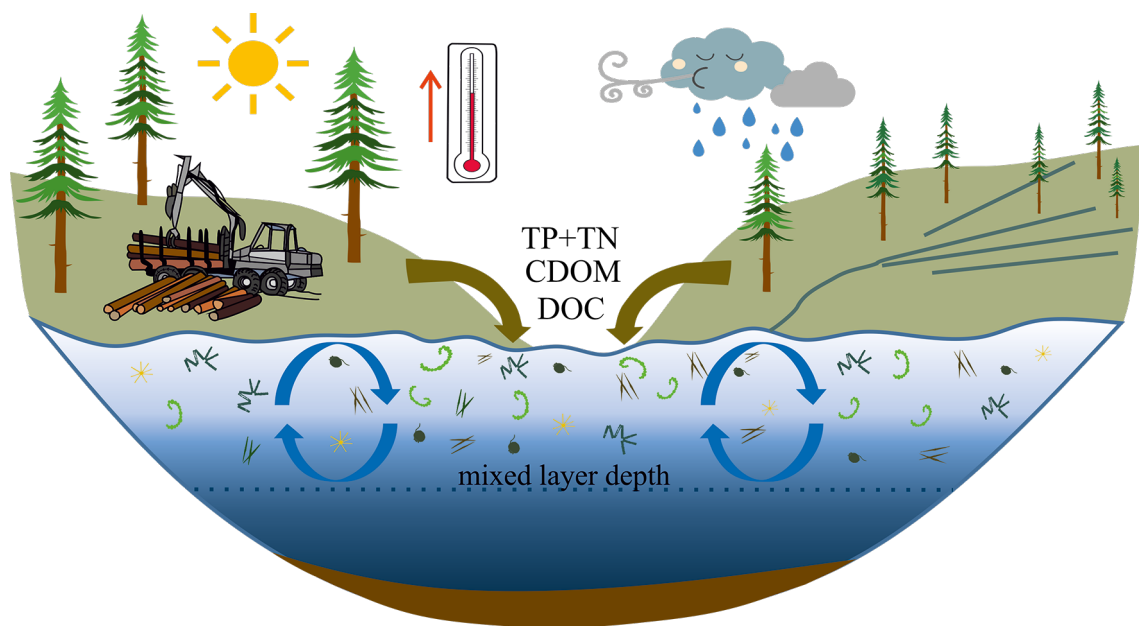Salla Ahonen

The Impact of Optical Properties on Spectral Light Availability and Biomass of Phytoplankton in Boreal Lakes

TP+TN
CDOM
DOC

mixed layer depth

UNIVERSITY OF JYVÄSKYLÄ

FACULTY OF MATHEMATICS
AND SCIENCE

Salla Ahonen

The Impact of Optical Properties on Spectral Light Availability and Biomass of Phytoplankton in Boreal Lakes

JYVÄSKYLÄN YLIOPISTO
UNIVERSITY OF JYVÄSKYLÄ

JYVÄSKYLÄ 2024

Editors
Anssi Lensu
Department of Biological and Environmental Science, University of Jyväskylä
Päivi Vuorio
Open Science Centre, University of Jyväskylä

ABSTRACT

Ahonen, Salla
The impact of optical properties on spectral light availability and biomass of phytoplankton in boreal lakes
Jyväskylä: University of Jyväskylä, 2024, 57 p.
(JYU Dissertations
ISSN 2489-9003; 781)
ISBN 978-952-86-0150-0 (PDF)

Many boreal lakes have a high content of chromophoric dissolved organic matter (CDOM), which affects light attenuation and thermal structure of water columns, with poorly known consequences on phytoplankton that are essential energy source in aquatic food webs. In this thesis, I used water samples from 128 boreal Finnish lakes and water column monitoring of one lake to study the impact of CDOM on the spectral underwater light field and responses of phytoplankton to the changes in light availability and mixed layer. In most study lakes, CDOM was the highest light absorbing component and strongly controlled the attenuation of solar radiation in water columns. Higher CDOM content in lakes was associated to shallower euphotic layer and a shift in the most available waveband towards red waveband of visible light. Consequently, red light covered > 50 % of the total absorption of visible light by phytoplankton in most study lakes. There was no photoacclimation through the regulation of chlorophyll a (Chl$a$) content by phytoplankton in response to the lower light availability in high-CDOM lakes, but both Chl$a$ concentration and phytoplankton biomass were higher in lakes with higher CDOM. A browning scenario assuming increases in both CDOM and nutrients decreased the fraction of light absorbed by phytoplankton but only moderately, presumably due to a compensatory effect of nutrients by promoting higher phytoplankton biomass. In the daily monitoring of Lake Jyväsjärvi during summer stratification, phytoplankton biomass was higher on windy and colder days when mixed layer was deeper. Improving light availability increased the biomass only when light levels were low. Collectively, these findings suggest that despite the strong control of light field by CDOM, phytoplankton biomass can be high even in CDOM-rich lakes, likely owing to higher nutrient export to the lakes. Hence, nutrient availability appears to have a key role in limiting phytoplankton biomass in boreal non-eutrophic lakes. A shallow mixed layer due to a combined effect of browning and climate warming have the potential to limit phytoplankton biomass in stratified lakes during summer heatwave periods, if nutrient availability is low.

Keywords: Browning; CDOM; climate change; mixed layer; phytoplankton; spectral absorption.

Salla Ahonen, University of Jyväskylä, Department of Biological and Environmental Science, P.O. Box 35, FI-40014 University of Jyväskylä, Finland

TIIVISTELMÄ

Boreaalisissa järvissä on usein runsaasti värillistä liuennutta orgaanista ainesta (CDOM), joka vaikuttaa valon vaimenemiseen ja lämpökerrostuneisuuteen, mutta jonka vaikutuksista kasviplanktoniin tiedetään vähän. Tässä väitöskirjassa tutkin CDOM:in vaikutuksia järvien valosaatavuuteen ja spektriin sekä kasviplanktonin vasteita muuttuneeseen valosaatavuuteen ja sekoittuvan kerroksen paksuuteen hyödyntäen vesinäytteitä 128 järvestä ja seuraamalla yhtä järveä kesän kerrostuneisuuden aikana. Lähes kaikissa järvissä suurin valoa absorboiva tekijä oli CDOM, jonka suurempi määrä oli yhteydessä matalampaan eufoottiseen kerrokseen, sekä syvimmälle tunkeutuvan valon siirtymiseen vihreästä kohti punaista aallonpituusaluetta. Samalla kasviplanktonin absorboimasta valosta punaisen valon osuus kasvoi. Klorofyllipitoisuus ja kasviplanktonbiomassa olivat suurempia CDOM:ia paljon sisältävissä järvissä, mutta kasviplanktonin ei havaittu nostavan solunsisäistä klorofyllipitoisuutta vasteena pienempään valosaatavuuteen. Veden tummuminen tyypillisessä boreaalisessa järvessä, olettaen että CDOM ja ravinnesaatavuus kasvavat samanaikaisesti, vähensi kasviplanktonin absorboimaa osuutta saatavilla olevasta valosta vesipatsaassa vain vähän, johtuen ravinnesaatavuuden kompensoivasta vaikutuksesta. Järven vesipatsaan seurannassa kesän kerrostuneisuuden aikana kasviplanktonbiomassa oli suurempi järven sekoittuvan kerroksen syvetessä, kun taas parempi valosaatavuus nosti biomassaa vain valon ollessa vähäinen. Tulosten mukaan kasviplanktonin biomassa voi olla suuri boreaalisissa runsaastikin CDOM:ia sisältävissä järvissä, jos samalla ravinnesaatavuus maalta tulevasta alloktonisesta aineesta kasvaa, olettaen että valoa on tarpeeksi saatavilla. Vaikka CDOM rajoittaa valosaatavuutta boreaalisissa järvissä, ravinteet vaikuttavat olevan tärkeä kasviplanktonin biomassaa rajoittava tekijä tummissakin järvissä. Matala sekoittuva kerros kesän hellejaksojen aikana ilmaston lämpenemisen ja tummumisen yhteisvaikutuksesta voikin rajoittaa kasviplanktonin biomassaa kerrostuneessa järvessä, jos ravinnesaatavuus on heikkoa.

Avainsanat: Absorptiospektri; humus; ilmastonmuutos; kasviplankton; sekoittuminen; tummuminen

Salla Ahonen, Jyväskylän yliopisto, Bio- ja ympäristötieteiden laitos PL 35, 40014 Jyväskylän yliopisto

Author's address   Salla Ahonen
Department of Biological and Environmental Science
P.O. Box 35
FI-40014 University of Jyväskylä
Finland
salla.a.ahonen@jyu.fi

Supervisors   Senior Lecturer Anssi Vähätalo
Department of Biological and Environmental Science
P.O. Box 35
FI-40014 University of Jyväskylä
Finland

Dr Jukka Seppälä
Research Infrastructure
Finnish Environment Institute SYKE
Latokartanonkaari 11
FI-00790 Helsinki
Finland

Reviewers   Professor Jukka Horppila
Ecosystems and Environment Research Programme
Faculty of Biological and Environmental Sciences
University of Helsinki
PO Box 65 (Viikinkaari 1)
FI-00014 Helsinki
Finland

Associate Professor Alo Laas
Chair of Hydrobiology and Fishery
Institute of Agricultural and Environmental Sciences
Estonian University of Life Sciences
Kreutzwaldi 5
Tartu 51006
Estonia

Opponent   Professor Sebastian Diehl
Department of Ecology and Environmental Science
Umeå University
Linnaeus väg 6
90187 Umeå
Sweden

CONTENTS

LIST OF ORIGINAL PUBLICATIONS

The thesis is based on the following original papers, which will be referred to in the text by their Roman numerals I–III. The responsibilities and contributions of authors are given in Table 1.

I   Ahonen S. A., Seppälä J., Jones R. I., Vuorio K. M., Tiirola, M., & Vähätalo A. V. Phytoplankton in boreal lakes mainly absorb red light. Submitted manuscript.

II   Ahonen S. A., Vuorio K. M., Jones R. I., Hämäläinen H., Rantamo K., Tiirola M., & Vähätalo A. V. 2024. Assessing and predicting the influence of chromophoric dissolved organic matter on light absorption by phytoplankton in boreal lakes. *Limnology and Oceanography* 69: 422–433.

III   Ahonen S. A., Seppälä J., Karjalainen J. S., Kuha J. & Vähätalo A. V. 2023. Increasing air temperature relative to water temperature makes the mixed layer shallower, reducing phytoplankton biomass in a stratified lake. *Freshwater Biology* 68: 577–587.

TABLE 1   Author contribution to original papers. Author abbreviations: AVV = Anssi V. Vähätalo, HH = Heikki Hämäläinen, JK = Jonna Kuha, JS = Jukka Seppälä, JSK = Juha S. Karjalainen, KMV = Kristiina M. Vuorio, KR = Krista Rantamo, MT = Marja Tiirola, RIJ= Roger I. Jones, SAA = Salla A. Ahonen

	I	II	III
Planning	SAA, AVV, JS	SAA, AVV, KMV, RIJ	AVV, JS, SAA
Field work	KMV	KMV	SAA, AVV, JSK, JK
Laboratory work	KMV, KR, SAA	KMV, KR, SAA	SAA, AVV
Data analysis	SAA	SAA	SAA
Manuscript draft	SAA	SAA	SAA
Manuscript revisions	SAA, AVV, JS, KMV, RIJ, MT	SAA, AVV, RIJ, KMV, HH, KR, MT	SAA, AVV, JS, JSK, JK
Correspondence	SAA	SAA	SAA

ABBREVIATIONS

$a_{CDOM}(\lambda)$	light absorption coefficient of CDOM at wavelength λ, m^{-1}
$a_{H2O}(\lambda)$	light absorption coefficient of water at wavelength λ, m^{-1}
$a_{phyto}(\lambda)$	light absorption coefficient of phytoplankton at wavelength λ, m^{-1}
$a_{NAP}(\lambda)$	light absorption coefficient of NAP at wavelength λ, m^{-1}
$a_{tot}(\lambda)$	total light absorption coefficient at wavelength λ, m^{-1}
$b(\lambda)$	light scattering coefficient at wavelength λ, m^{-1}
CDOM	chromophoric dissolved organic matter
$CDOM_{mix}$	CDOM in the mixed layer, relative fluorescence units
$Chla_{vol}$	chlorophyll a concentration per volume, mg m^{-3} or µg l^{-1}
$Chla_{area}$	areal chlorophyll a concentration in mixed layer, mg m^{-2}
GR	global radiation, kW m^{-2}
GR_{mix}	global radiation in the mixed layer, kW m^{-2}
$\lambda_{z1\%,max}$	deepest penetrating wavelength of $z_{1\%}(\lambda)$, nm
K_d	attenuation coefficient of light, m^{-1}
NAP	non-algal particles
$O_2\%_{mix}$	oxygen saturation in the mixed layer, %
P_{air}	atmospheric pressure, mbar
PAR	photosynthetically active radiation (400–700 nm)
PUR	rate of photon absorption by phytoplankton over the water column and summed over PAR spectrum, mol m^{-2} d^{-1}
$PUR_{z=0-\infty}(\lambda)$	rate of photon absorption by phytoplankton over the water column at wavelength λ, mol m^{-2} d^{-1}
$PUR_{z=10\%-\infty}(\lambda)$	rate of photon absorption by phytoplankton in the lower half of the euphotic layer at wavelength λ, mol m^{-2} d^{-1}
$\bar{Q}_{mix}(PAR)$	mean photon flux density of PAR at z_{mix}, mol m^{-2} d^{-2}
$Q_{z=1\%}(\lambda)$	photon flux density at $z_{1\%}$ at wavelength λ, mol m^{-2} d^{-1}
$Q_{z=10\%}(\lambda)$	photon flux density at $z_{10\%}$ at wavelength λ, mol m^{-2} d^{-1}
T_{air}	air temperature, °C
T_{mix}	mixed layer temperature, °C
z_{eu}	depth of a euphotic layer, m
z_{mix}	depth of a mixed layer, m
z_{thermo}	depth of a seasonal thermocline, m
$z_{1\%}(\lambda)$	depth where subsurface radiation is attenuated to 1% at wavelength λ, m
$z_{1\%}(PAR)$	depth where subsurface PAR is attenuated to 1 %, m
$z_{10\%}(\lambda)$	depth where subsurface radiation is attenuated to 10 % at wavelength λ, m

1 INTRODUCTION

1.1 Boreal lakes under environmental changes

Aquatic systems are influenced by various anthropogenically induced environmental stressors, such as the ongoing global climate change and land use in the catchments, affecting physical, chemical, and biological processes in the aquatic environments as well as the interaction with surrounding catchments (Adrian *et al.* 2009, Creed *et al.* 2018). The ongoing climate change has globally increased the mean air temperature by more than 1 °C since industrial revolution (IPCC 2021). In arctic and boreal regions, warming is faster than the global average, and therefore the effects on the millions of lakes in these regions have already been particularly intense (Wrona *et al.* 2006, Prowse *et al.* 2009, IPCC 2021). Furthermore, the climate change-induced changes in lakes are entangled with various and more locally observed human-affected stressors on lakes, such as acidification, urbanisation, intensive forestry and agriculture, pollution and introduction of invasive species, which together alter the hydrology, biogeochemistry and ecological processes within the aquatic systems.

The boreal region is predicted to become warmer with higher annual precipitation and experience more frequent and intensive extreme weather events, such as heatwaves, floods, and storms (Jentsch *et al.* 2007, Kivinen *et al.* 2017). In boreal lakes, warming will cause earlier ice breakup and later freezing of lakes, which prolongs the open-water and stratification periods (Moss *et al.* 2009, Woolway *et al.* 2017, 2021a). This lengthens the overall growing season of primary producers at the base of aquatic food webs, and thereby can further affect organisms at higher trophic levels. Longer stratification period can also prolong the period of limited material and gas exchange between the layers of stratified water columns, which can intensify nutrient limitation in the epilimnion as well as oxygen depletion in the hypolimnion (Boehrer and Schultze 2008). Warming and reduced oxygen concentration in hypolimnion can increase

releases of carbon, methane, and nitrogen from lakes to the atmosphere (Moss 2012).

Warming in the northern latitudes will thaw vast areas of permafrost, which together with potentially increasing precipitation (de Wit *et al.* 2016, Lenard and Ejankowski 2017) enhances terrestrial vegetation and mobilizes organic carbon pools in the catchments, increasing the export of allochthonous material from catchments into lakes (Camill 2005, DeLuca and Boisvenue 2012). Over the recent decades, lakes in the northern hemisphere have been experiencing increased terrestrial loading of the chromophoric fraction of dissolved organic matter (CDOM) and iron from the catchments (Xiao *et al.* 2013, Škerlep *et al.* 2020). This phenomenon is called browning and is observed as darker and browner water in lakes (Evans *et al.* 2005, Monteith *et al.* 2007, Kritzberg and Ekström 2012, de Wit *et al.* 2016). Browning is often reported as an increase in the concentrations of dissolved or total organic carbon (DOC and TOC) and water colour (Evans *et al.* 2005, Monteith *et al.* 2007, Ylöstalo *et al.* 2014, Thrane *et al.* 2016). In the past three decades, water colour or DOC/TOC concentrations have been reported to have increased from 8 to over 100 %, but on average by 25 % (Räike *et al.* 2016, Kritzberg 2017, Lepistö *et al.* 2021). Besides higher temperature and precipitation, browning of lakes is driven by increased land use and peatland ditching for forestry purposes (Nieminen *et al.* 2015, Kritzberg 2017, Škerlep *et al.* 2020, Finér *et al.* 2021), and recovery from acid deposition (Monteith *et al.* 2007, Strock *et al.* 2014). Browning of lakes reduces the penetration of light in lakes but also affects the thermal structure of lakes (Sherbo *et al.* 2023, Caplanne and Laurion 2008).

Freshwater ecosystems have a key role in the regional and likely also in the global carbon cycle, as being active spots in transporting, transforming, and storing of carbon (Tranvik *et al.* 2009). Lake density is high especially in the boreal forest region, where the importance of lakes in the carbon cycle can be thus particularly high (Benoy *et al.* 2007, Anas *et al.* 2015). Climate change likely affects the carbon cycle in northern lakes, as warmer climate may increase the proportion of carbon released to the atmosphere as carbon dioxide or methane from boreal lakes, which would enhance further warming (Tranvik *et al.* 2009). Increased allochthonous terrestrial loading can also bring more nutrients to lakes (Corman *et al.* 2018). This thesis focuses on lakes over the boreal zone, where warming and increased CDOM export to lakes are the major environmental stressors on lakes, but relatively little is still known about their effects on the spectral light availability and biomass of pelagic phytoplankton.

1.2 Phytoplankton

Phytoplankton are aquatic photosynthetic organisms that comprise less than 1 % of the global photosynthetic biomass but due to their fast turnover rates are responsible for half of the fixation of carbon dioxide into biomass on Earth (Field *et al.* 1998, Falkowski and Raven 2014). Phytoplankton have a major role in aquatic food webs as the basis for primary production, which is an essential

energy source for consumers in aquatic ecosystems (Field *et al.* 1998). Owing to the importance of phytoplankton for the carbon cycle and as the base energy in aquatic food webs, it is vital to understand the main factors influencing the phytoplankton communities. Human-induced environmental changes, such as the global climate warming (Dokulil *et al.* 2021, Woolway *et al.* 2022) and browning of lakes especially in the northern hemisphere (Evans *et al.* 2006, Monteith *et al.* 2007, Škerlep *et al.* 2020) have various effects on aquatic systems and consequently also phytoplankton communities by shaping their physical and chemical environment.

Phytoplankton are very diverse in terms of their motility, light utilization, nutrient uptake and storing, and morphology, and these species-specific strategies determine their competitiveness in aquatic systems with various environmental conditions (Litchman and Klausmeier 2008). Primary production by phytoplankton is primarily controlled by the supplies of light, temperature and nutrients, which are heterogeneously distributed in a water column (Diehl 2002, Diehl *et al.* 2002). Most phytoplankton float freely in the water and are hence prone to the turbulent and convective mixing that alter their nutrient and light supplies. Differences between phytoplankton species in their requirements of light intensity as well as pigment composition, including chlorophylls, phycobilins and carotenoids, alter their ability to utilize the light spectrum available (Litchman and Klausmeier 2008, Croce and Van Amerongen 2014, Falkowski and Raven 2014). All phytoplankton have the major light harvesting pigment chlorophyll *a*. The content of accessory pigments varies among species and determine the overall waveband range of photons that can be absorbed and hence potentially used as energy in photosynthesis (Falkowski and LaRoche 1991, Grossman *et al.* 1993, Stomp *et al.* 2004). Some pigments are also used in photoprotection against harmful ultraviolet radiation (Choudhury and Behera 2001). Among taxonomic groups, diatoms, dinoflagellates and cyanobacteria are generally efficient in utilizing low light and thus can dominate in low-light conditions, whereas green algae require higher light intensities but are less sensitive to photoinhibition (Richardson *et al.* 1983, Litchman and Klausmeier 2008, Schwaderer *et al.* 2011). The ability of phytoplankton to alter their cellular pigment content in response to the light intensity influences their ability to live under fluctuating light (Richardson *et al.* 1983, Falkowski and LaRoche 1991).

Phytoplankton species differ in their ability and efficiency of nutrient uptake and utilization as well as storing capacity, which influence their ability to live in nutrient-rich versus nutrient-limiting conditions (Litchman *et al.* 2007, Litchman and Klausmeier 2008, Yoshiyama *et al.* 2009). The ability of some cyanobacteria species to fix atmospheric nitrogen (Falkowski and Raven 2008) make them less dependent on the nitrogen supplies available in the water. Vertical gradients of light and nutrients in the water column can favour motile phytoplankton that can control their vertical position with gas vacuoles of flagella (Jöhnk *et al.* 2008, Wagner and Adrian 2011). Mixotrophic phytoplankton, such as some dinoflagellates and cryptophytes, can utilize both autotrophic and heterotrophic pathways for their biomass growth, which can be a favourable strategy in low-nutrient conditions (Modenutti *et al.* 2008, Hansson *et al.* 2019).

Smaller-sized species have generally lower sinking rates and utilize light energy and nutrients more efficiently but are often more prone to grazing (Ptacnik *et al.* 2003, Litchman *et al.* 2007). Temperature has a major role for example in photosynthesis, respiration, and growth of phytoplankton, while temperature optima and tolerance are species-specific (Litchman and Klausmeier 2008). Both temperature and light have high seasonal variability and therefore the competitiveness of different strategies vary according to the season (Sommer *et al.* 1986, Berger *et al.* 2007). All in all, the different strategies among taxonomic groups allow the composition and functioning of phytoplankton communities to effectively adapt to various environmental conditions.

1.3   Optical properties in boreal lakes

Light has a fundamental role in aquatic systems in terms of both intensity and spectral distribution, affecting the physical, chemical, and biological processes in aquatic ecosystems. Distribution of aquatic organisms is controlled by light, as light impacts their visual orientation, predation and reproduction in water columns (Mcfarland 1986). Most importantly, light in the spectral band of photosynthetically active radiation (PAR, 400–700 nm) provides the energy for phytoplankton to produce new biomass through photosynthesis. Within a water column, solar radiation attenuates exponentially with depth at a wavelength-specific rate determined by the spectral absorption and scattering properties of optically active components in the water, including water itself (H_2O), CDOM, non-algal particles (NAP), and phytoplankton (Kirk 1977). The sum of the absorbing and scattering properties of all components can be used to estimate the spectral underwater light field with radiative transfer models (Kirk 1981a, 1984). The depth where 1 % ($z_{1\%}$) or 10 % ($z_{10\%}$) of the incident PAR at water surface is left is often used to describe the lower limit or mid-point of a euphotic layer (z_{eu}) (Falkowski 1994, Wu *et al.* 2021). The euphotic layer estimates the part of the water column where light is sufficient for the net photosynthesis of phytoplankton (Falkowski 1994). The lower limit of the euphotic layer approximates a compensation depth, i.e., the depth where net primary production is zero, but it ignores the amount of light incident at water surface (Banse 2004, Wu *et al.* 2021). However, accounting for the practical challenges in determining the compensation depth, the 1 % light level is often considered as an estimate (Reinart *et al.* 2000, Wu *et al.* 2021). Mid-point of the euphotic layer divides the euphotic layer into upper and lower halves, which absorb 90 % and 9 % of the incident radiation, respectively.

Light absorption properties of the optical components are wavelength dependent. Within the PAR spectrum, light absorption by water increases towards longer wavelengths, i.e., the red part of the spectrum (Buiteveld *et al.* 1994). Consequently, in clear waters such as oceans and ultraoligotrophic lakes where water is the major absorbing component, blue waveband penetrates deepest and red waveband is attenuated most rapidly (Holtrop *et al.* 2021). In

addition, pure water has absorption peaks and shoulders at certain wavelengths, which are caused by harmonics and subharmonics of molecular vibrations (Stomp *et al*. 2007a, Holtrop *et al*. 2021). In freshwater systems, the contents of CDOM, NAP and phytoplankton are generally higher than in marine systems and alter the attenuation of light, resulting in greenish, yellowish or brownish water (Kirk 1977, Eloranta 1978, Arst *et al*. 2008). CDOM strongly absorbs light in the PAR band, where the absorption by CDOM increases exponentially towards shorter wavelengths, i.e., blue light (Bricaud et al. 1981, Kallio 2006, Thrane et al. 2014). Non-algal particles suspended in the water comprise mineral particles, living non-algal organisms and non-living detritus, which absorb mostly in the shorter wavelengths of PAR, and contribute to the scattering of light (Kirk 1981b, Binding *et al*. 2008). In phytoplankton, the main light harvesting pigment chlorophyll *a* has absorption peaks in the blue and red wavebands of PAR, in addition to which various species-specific accessory pigments broaden the absorption spectrum of phytoplankton (Dubinsky and Stambler 2009). Thus, the particulate and dissolved constituents in water with various optical properties control both the intensity and the spectral composition of light that is available in aquatic systems. Environmental stressors, such as the climate warming and intensive land use, can alter the allochthonous loading from surrounding catchments to receiving lakes and thereby the amount and composition of the optical constituents in waterbodies.

CDOM is the chromophoric fraction of dissolved organic matter that absorbs radiation in the ultraviolet and visible wavebands of the spectrum (Bricaud *et al.* 1981). In boreal lakes, CDOM is often the major light absorbing component, which causes the brownish colour of many lakes and restricts the depth of the euphotic layer (Morris *et al*. 1995, Thrane *et al*. 2014). Owing to the strong light absorption by CDOM, it can also impact the thermal structure of lakes particularly in smaller and sheltered lakes that are less susceptible to meteorological forcing (Fee *et al*. 1996, Snucins and Gunn 2000, Caplanne and Laurion 2008). In high-CDOM lakes, a restricted depth of the euphotic layer can limit benthic primary producers to shallow depths (Chambers and Kalff 1985, Godwin *et al*. 2014). Less is known about the impact of CDOM on the light availability to pelagic phytoplankton, but it is often considered to be negative (Karlsson and Byström 2005, Ask *et al*. 2012, Thrane *et al*. 2014). CDOM alters not only the intensity of PAR in lakes, but also the spectral availability of light within a water column, due to its strong absorption of blue light (Kutser *et al.* 2005, Kallio 2006, Thrane *et al*. 2014). Studies based on simulation (Holtrop *et al*. 2021) and underwater light measures of seven water types (Stomp *et al.* 2007a) have demonstrated how light field shifts from the dominance of blue towards red light along a gradient from ocean to peatland lake. As chlorophyll *a* has an absorption peak in the blue part of the PAR spectrum, CDOM could be expected to shade light absorption by phytoplankton most in the shorter wavelength region of PAR. On the other hand, CDOM effectively absorbs ultraviolet radiation, and hence phytoplankton are less exposed to the harmful effects of UV light in lakes with high CDOM content.

The content of CDOM, often quantified as the absorption coefficient at a specific wavelength λ (e.g., $a_{CDOM}(\lambda = 400)$), has a high natural variation among lakes (Kallio 2006, Thrane *et al.* 2014). A primary source of CDOM is a terrestrial loading from the surrounding catchments (Kortelainen and Saukkonen 1998, Corman *et al.* 2018). The allochthonous material from the catchment not only brings CDOM and dissolved organic carbon (DOC) to the lakes but often also nutrients (Kortelainen 1993, Kortelainen and Saukkonen 1998, Corman *et al.* 2018). Hence, elevated contents of CDOM or DOC in lakes can be associated to higher nutrients supplies (Corman *et al.* 2018, Bergström and Karlsson 2019, Hamdan *et al.* 2021, Lepistö *et al.* 2021). In CDOM-rich lakes, elevated nutrient levels can increase Chl*a* concentration or phytoplankton biomass, which can compensate for the lowered light availability caused by CDOM (Bergström and Karlsson 2019, Sherbo *et al.* 2023). Hence, it is still largely unknown, how much light eventually limits phytoplankton in lakes with varying content of CDOM.

1.4 Spectral light absorption by phytoplankton

The light availability to phytoplankton can be assessed by measuring spectral absorption coefficient of phytoplankton pigments ($a_{phyto}(\lambda)$) over PAR band from water samples, which can be compared to the absorption of H_2O ($a_{H2O}(\lambda)$), NAP ($a_{NAP}(\lambda)$), and CDOM ($a_{CDOM}(\lambda)$), or the sum of all components ($a_{tot}(\lambda)$). The fraction of total light absorbed by phytoplankton tends to be lower in freshwater systems with higher content of CDOM (2–28 %; Thrane *et al.* 2014, Watanabe *et al.* 2015), compared to clear water marine systems (5–39 %; Smith *et al.* 1989, Murray *et al.* 2015). Hence, the content of CDOM in aquatic systems may have a major impact on the PAR available for phytoplankton to absorb. In comparison, photosynthetic plants in terrestrial systems can absorb most of the arriving PAR. As an example, the pigments of leaves and needles in a terrestrial forest are the major absorbing component and have basically no competing absorbing components equivalent to CDOM in lakes (Majasalmi *et al.* 2014). Therefore, the contribution of plants to the absorption of PAR in terrestrial forests is typically between 40 to 80 % in needleleaf forests (Xiao *et al.* 2015). The major differences in the fractions of PAR absorbed by terrestrial plants compared to freshwater phytoplankton are further reflected in primary production rates. For example, the gross primary production by Scots pine forest is ca. 1000 g C m^{-2} a^{-1} (Ilvesniemi *et al.* 2009), while phytoplankton production in a boreal Lake Valkea Kotinen is only 28 g C m^{-2} a^{-1} (Einola *et al.* 2011).

The light available for photosynthesis can be also assessed by calculating photosynthetically usable radiation (PUR), i.e., the photons over PAR absorbed by phytoplankton, which considers the variation in the spectra of both solar radiation and $a_{phyto}(\lambda)$ (Morel 1978). PUR can be defined for a specific depth in clear waters, where phytoplankton is distributed heterogeneously with depth and where a deep chlorophyll maximum can occur below the mixed layer (Morel 1978, Pérez *et al.* 2007). In lakes where PAR is absorbed within the mixed layer,

like many boreal lakes (Donis *et al.* 2021, Horppila *et al.* 2023) and where phytoplankton and other absorbing components are homogenously mixed, PUR can be estimated over the entire water column. PUR divided by PAR entering to the lake (PUR/PAR) describes the light availability as a fraction of PAR absorbed by phytoplankton but is poorly documented in freshwater lakes.

The spectral underwater light field experienced by phytoplankton fluctuates according to water movements (Huisman *et al.* 2004, Monismith and MacIntyre 2009). In addition, environmental changes can cause long-term changes in the spectral light field in lakes. Phytoplankton can respond many ways to the intensity and spectral availability of light field to ensure effective light absorption and to minimize damage. Phytoplankton can increase their cellular pigment content to capture light at low light intensities (Dimier *et al.* 2009, Dubinsky and Stambler 2009). This photoacclimation by phytoplankton can be exemplified by high Chl*a* content of cells typically found in communities below a seasonal thermocline (i.e., deep chlorophyll maxima) in transparent aquatic systems (Pérez *et al.* 2002, 2007, Cornec *et al.* 2021). Higher cellular Chl*a* content can also be associated to higher DOC concentration in lakes like shown in a study of eight boreal lakes (Sherbo *et al.* 2023). Photoacclimation can also be assessed through a chlorophyll-specific absorption coefficient by phytoplankton at wavelength of 676 nm ($a_{\text{phyto}}*(676)$). Increasing Chl*a* content of cells causes shading of Chl*a* molecules by each other, and this pigment packaging causes a decrease in $a_{\text{phyto}}*(676)$ value (Pérez *et al.* 2002).

As an acclimation to changes in the spectral composition of light field, phytoplankton can adjust the amount and ratio of accessory photosynthetic and photoprotective pigments in their cells (Wang and Chen 2022). As a chromatic adaptation, different groups of phytoplankton have specific pigments that allow them to utilize different wavelengths of light (Álvarez *et al.* 2022). Photosynthetic accessory pigments absorb the underwater photon flux outside the blue and red absorption maxima of Chl*a* (Holtrop *et al.* 2021). Those photosynthetic accessory pigments are often the most abundant whose absorption maxima corresponds to the deepest penetrating spectral band of underwater PAR (Stomp *et al.* 2007a). As an example, oceanic strains of the cyanobacterium *Synechococcus* produce phycourobilin pigments, which absorbs the most available blue light, whereas in coastal waters, the *Synechococcus* strains contain phycocyanobilin absorbing the most available orange light (Stomp *et al.* 2007b, Holtrop *et al.* 2021). Similarly, phytoplankton in the metalimnion of transparent lakes can produce accessory pigments that absorb the most intense green light (Pérez *et al.* 2007). Some accessory pigments also act as photoprotective pigments to protect the cells from harmful UV light under high light intensities (Pérez *et al.* 2007). Due to the strong short-wavelength absorption by CDOM, phytoplankton communities might respond to an increase in CDOM content of lakes by altering their pigmentation to decrease their absorption in the blue relative to red waveband of PAR.

1.5   Phytoplankton in the surface mixed layer of boreal lakes

The physical structure of water columns is controlled by meteorological forcing acting on water surface, including solar radiation, wind and air temperature, and lake morphological characteristics, which alter the susceptibility of lakes to the meteorological forcing (Imberger and Parker 1985, MacIntyre 1993, Persson and Jones 2008, Monismith and MacIntyre 2009). In general, the larger and less sheltered the lake is, the less impact CDOM or transparency of a lake has on the mixing dynamics of the water column (Fee et $al.$ 1996). In small and sheltered high-CDOM lakes, the restricted penetration of solar radiation caused by high absorption by CDOM can induce steep thermal gradients and strong water column stability (Snucins and Gunn 2000, Caplanne and Laurion 2008, Kirillin and Shatwell 2016).

Most boreal lakes are stratified during the summer, when density gradients caused by temperature differences across the water column form layers that are separated by diurnal and seasonal thermoclines (MacIntyre 1993, Monismith and MacIntyre 2009). Pelagic phytoplankton mainly reside within a surface mixed layer (z_{mix}), which is the top-most, turbulently mixed layer above a diurnal thermocline, and where water is relatively homogenous (Imberger 1985, MacIntyre 1993, Monismith and MacIntyre 2009). The depth of z_{mix} fluctuates frequently, according to the balance between the buoyancy created by the flux of surface and the rate at which wind action and convection cause turbulence (Imberger 1985, Spigel and Imberger 1987, Imboden and Wuest 1995). The z_{mix} depth is also impacted by lake morphometry and water transparency (Hutchinson and Löffler 1956, Imberger 1985, Kirillin and Shatwell 2016).

The z_{mix} influences phytoplankton by affecting their supplies of light and nutrients, grazing pressure, and sedimentation rates (Huisman et $al.$ 1999, Diehl 2002, Winder and Sommer 2012). The ratio of the euphotic and mixed layer depths (z_{mix}:z_{eu}) has a key role in determining the light field experienced by phytoplankton in the z_{mix} (Spigel and Imberger 1987). When z_{mix} is shallower than z_{eu}, phytoplankton reside in a well-lit layer despite the turbulent water mixing (Huisman et $al.$ 1999). However, a shallower mixed layer is often associated with lower nutrient supplies and higher sinking losses of phytoplankton (Weithoff et $al.$ 2000, Ptacnik et $al.$ 2003, Berger et $al.$ 2006, Yang et $al.$ 2016). In contrary, deepening of z_{mix} relative to z_{eu} decreases light supplies but can bring nutrient rich water from deeper layers into the mixed layer. In addition, deepening of z_{mix} can decrease the encounter rates of phytoplankton and zooplankton as their densities are diluted in higher volume of water (Berger et $al.$ 2006).

In sheltered CDOM-rich lakes, nutrient depletion can occur relatively rapidly in the spring after the onset of stratification and lead to a steep vertical gradient of the light and nutrients needed by phytoplankton (Caplanne and Laurion 2008), where light is restricted to the shallow euphotic layer and nutrients below the thermocline (Livingstone 2003, Winder and Sommer 2012). Warm temperatures and stable stratification can favour motile species, such as

cyanobacteria and dinoflagellates, capable of vertical movements to access both sufficient light and nutrients (Jöhnk *et al.* 2008, Winder and Cloern 2010). In addition, mixotrophy can be an advantageous strategy in high-CDOM lakes with reduced light penetration, where mixotrophic species can obtain energy and nutrients through a combination of autotrophic and heterotrophic pathways (Jones 2000, Hansson *et al.* 2019, Calderini *et al.* 2022).

1.6 Responses of phytoplankton to environmental stressors

Diversity, community composition and seasonal dynamics of phytoplankton are altered by the changes for example in the physical structure, nutrient inputs, and grazing pressure in aquatic systems. Browning of lakes influences phytoplankton directly by increasing water colour and reducing the penetration of light in water columns (Thrane *et al.* 2014). Increasing inputs of allochthonous material can also provide more nutrients to lakes, depending on the cause of the browning and the constituents in the allochthonous input originated from the surrounding catchment, and hence enhance nutrient supplies to phytoplankton (Corman *et al.* 2018, Lepistö *et al.* 2021, Stetler *et al.* 2021a). Therefore, forecasting the general effects of browning on phytoplankton communities can be challenging. In nutrient-limited systems, where nutrient supplies increase concurrently with the CDOM content, phytoplankton biomass can be promoted by the higher nutrient supplies, helping to compensate for the light limitation. Brown lakes are predicted to become globally more common in the future (Yang *et al.* 2022), and therefore more understanding about the effect of CDOM and browning on the light availability for phytoplankton is needed.

The global climate change is documented to affect aquatic systems via increasing air temperature, which strengthens the summertime stratification and reduces the z_{mix} in a water column. The stability of stratification is further intensified by heatwaves that have become more frequent and severe in many continents (Snucins and Gunn 2000, Coumou and Rahmstorf 2012, Stetler *et al.* 2021b, Woolway *et al.* 2021b). Climate change has also been documented as an overall reduced wind speeds over the continents, a phenomenon called atmospheric stilling, which tends to increase the strength of the summertime thermal stratification (Magee and Wu 2017, Woolway and Merchant 2019, Stetler *et al.* 2021b). On the other hand, increased frequency and severity of episodic storms have also been reported, inducing mixing of lake water and thus weaking the stratification in lakes (Stockwell *et al.* 2020). In addition, climate warming alters the overall mixing regimes of lakes, as the onset of summertime stratification has been advanced and the overall stratification period has prolonged (Shatwell *et al.* 2019, Stetler *et al.* 2021b, Woolway *et al.* 2021a). The various changes in the meteorological forcing acting on lake surface and thus altering the physical and chemical properties of lakes likely have various and complex consequences on phytoplankton communities (Findlay *et al.* 2001, Winder and Sommer 2012). Browning of lakes can further promote the effects of

climate change on the lake stratification. A rapid attenuation of incoming solar radiation within the surface layer in high-CDOM lakes may create steep thermal density gradients within the water column (Caplanne and Laurion 2008, Heiskanen *et al*. 2015), which increases light availability of phytoplankton but possibly reduces nutrient availability. The effect of CDOM on the physical structure of lakes is more pronounced in small and sheltered lakes which are less susceptible to wind forces that would weaken the accumulated heat energy (Caplanne and Laurion 2008, Fee *et al*. 1996).

In oceans, it has been shown that increased stratification strength caused by climate change has declined the nutrient transport from deeper layers to the water surface, resulting in lower phytoplankton biomass (Behrenfeld *et al*. 2006, Siemer *et al*. 2021, Mishra *et al*. 2022). Due to a high local variation among lakes, there is not as clear evidence of similar reduction of biomass as in oceans, and studies have reported both negative and positive responses of phytoplankton biomass to the warming and diminished lake water mixing (Straile *et al*. 2003, Lepori *et al*. 2018, Gray *et al*. 2019). In non-eutrophic lakes, where nutrients limit phytoplankton production, warming of surface water and consequently reduced z_{mix} can decrease phytoplankton biomass (Kraemer *et al.* 2017). In contrary, phytoplankton biomass in eutrophic lakes can increase in response to the limited mixing, as increased light availability and nutrient supplies from the catchment can promote phytoplankton production (Kraemer *et al.* 2017).

2   AIMS OF THE STUDY

The overall aim of this thesis was to examine the optical properties of boreal lakes and their role in controlling the spectral underwater light field, spectral light absorption by phytoplankton and phytoplankton biomass. More specifically, the specific objectives were:

i) to examine the impact of CDOM content on the spectral underwater light field, photoacclimation and chromatic adaptation by phytoplankton and spectral photon absorption by phytoplankton in boreal lakes (I);

ii) to assess and predict the effects of CDOM content and typical browning scenarios on the fraction of incoming PAR absorbed by phytoplankton in boreal lakes (II);

iii) to examine the impact of mixed layer depth and light availability on daily phytoplankton biomass and the main factors controlling the depth of the mixed layer of a boreal lake during a summer stratification period (III).

3   MATERIAL AND METHODS
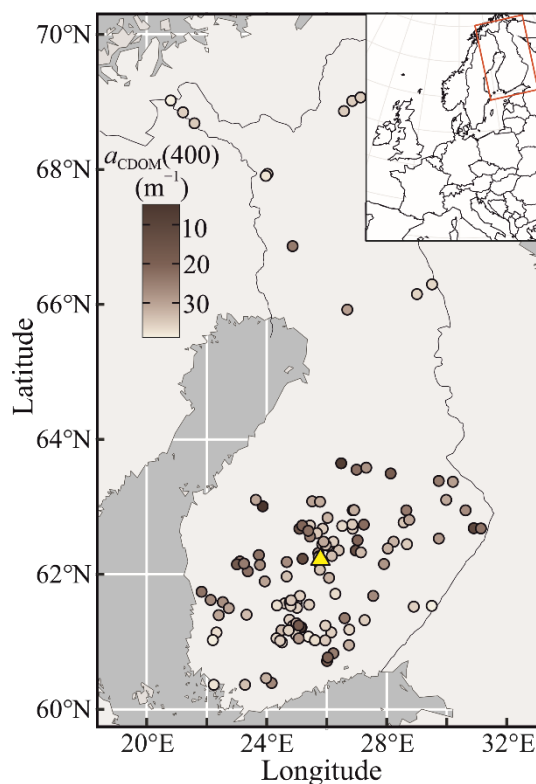
3.1   Study region and data collection

FIGURE 1   A map showing the location of the 128 study lakes (I, II, III). The colour scale indicates a CDOM content of a lake. The location of the monitoring study lake is denoted with a yellow triangle (III).

This study comprises two datasets. The first dataset covers 128 mostly boreal and a few subarctic lakes in Finland, that were sampled between May and August in 2014–2018 (Fig. 1; I, II). The second dataset consists of continuous monitoring of

water column and weather, and weekly water sampling in one of the study lakes, Lake Jyväsjärvi, from May to July 2019, described separately in section 3.5 (Fig. 1; III). Composite water samples were taken with Limnos water sampler from 0–2 m, representing the water in the homogenous mixed layer, to determine water chemistry and optical parameters (I, II, III). In addition, a dataset of 2250 regularly monitored Finnish lakes retrieved from the Hertta database portal (https://www.syke.fi/en-US/Open_information) maintained by the Finnish Environment Institute was used as reference lakes of boreal lakes (II).

3.2 Determination of water chemistry and optical parameters

Composite water samples were used to determine water chemistry, including concentrations of Chl$a$ (μg l^{-1} or mg m^{-3}; I, II, III), total nitrogen and phosphorus (TN and TP, μg l^{-1}; I, II), and water colour (mg Pt l^{-1}; II) that were analysed according to standard methods (international standards SFS-EN ISO 10260 1992, SFS-EN ISO 11905-1 1997, SFS-EN ISO 15681-2 2018, SFS-EN ISO 7887 2011). Concentration of dissolved organic carbon (DOC, mg l^{-1}; I, II) was analysed according to high-temperature catalytic oxidation method using a total organic carbon analyser (TOC-L, Shimadzu, Japan). Phytoplankton biomass (μg fresh weight l^{-1}) was determined by microscopy according to the Utermöhl technique (Utermöhl 1958; BS EN 15204 2006). Turbidity values (FTU) were derived from the Hertta database portal. For 10 % of the study lakes, which lacked water chemistry measures, the data were retrieved from Hertta database.

The absorption coefficients of CDOM ($a_{\mathrm{CDOM}}(\lambda)$), non-algal particles ($a_{\mathrm{NAP}}(\lambda)$) and phytoplankton ($a_{\mathrm{phyto}}(\lambda)$) at wavelength λ across the PAR band (400–700 nm) were determined from the water samples (I, II). Values of $a_{\mathrm{CDOM}}(\lambda)$ were determined from filtered water sample according to Neeley and Mannino (2018) using Shimadzu UV-1800 or PerkinElmer Lambda™ 650 UV/Vis. The value of a_{CDOM} at wavelength of 400 nm ($a_{\mathrm{CDOM}}(400)$) was used to describe a CDOM content in lake water. Absorption of total particles ($a_{\mathrm{p}}(\lambda)$) was determined from the particles collected on GF/F filters using an integrating sphere connected to a PerkinElmer Lambda™ 650 UV/Vis spectrophotometer according to Neeley and Mannino (2018). The values of $a_{\mathrm{NAP}}(\lambda)$ were determined like $a_{\mathrm{p}}(\lambda)$ after an extraction of algal pigments according to hot ethanol method (SFS-EN ISO 10260 1992). Finally, $a_{\mathrm{phyto}}(\lambda)$ was determined as the difference between $a_{\mathrm{p}}(\lambda)$ and $a_{\mathrm{NAP}}(\lambda)$. The absorption spectrum by pure water ($a_{\mathrm{H2O}}(\lambda)$) was derived from Neeley and Mannino (2018). Total absorption coefficient at wavelength λ ($a_{\mathrm{tot}}(\lambda)$) was the sum of $a_{\mathrm{CDOM}}(\lambda)$, $a_{\mathrm{NAP}}(\lambda)$, $a_{\mathrm{phyto}}(\lambda)$ and $a_{\mathrm{H2O}}(\lambda)$.

3.3 Determination of spectral underwater light field

Attenuation coefficient of downward irradiance at wavelength λ ($K_d(\lambda)$, m^{-1}; I) was calculated according to Kirk (1981b, 1984):

$$K_d(\lambda) = (a_{tot}(\lambda)^2 + G a_{tot}(\lambda) b_{tot}(\lambda))^{1/2} \tag{1}$$

where $b_{tot}(\lambda)$ is the total scattering coefficient and G describes a contribution of scattering to vertical attenuation of solar radiation, using a value 0.231 (Kirk 2011). The value of $b_{tot}(\lambda)$ was calculated as a sum of scattering by pure water ($b_{H2O}(\lambda)$) provided by Buiteveld $et\ al.$ (1994), and by particles ($b_p(\lambda)$) calculated as:

$$b_p(\lambda) = (\lambda/550)^{-v} \times b_p(550) \tag{2}$$

where v is a value 0.78 (Belzile $et\ al.$ 2002) and $b_p(550)$ is the scattering of particles at wavelength 550 nm, estimated to equal turbidity of a water sample (FTU) (Di Toro 1978, Davies-Colley 1983).

Depths corresponding to the bottom and mid-point of the euphotic zone at wavelength λ were determined as $z_{1\%}(\lambda) = -\ln(0.01)\,K_d(\lambda)^{-1}$ and $z_{10\%}(\lambda) = -\ln(0.1)\,K_d(\lambda)^{-1}$, respectively (Kirk 1981a, Morel 1988, I). Maximum value of $z_{1\%}(\lambda)$ was used to determine the deepest penetrating wavelength in the PAR band ($\lambda_{z1\%,max}$).

Underwater photon flux densities were calculated with ASTM G173-03 reference solar radiation spectrum at water surface (Apell and McNeill 2019) adjusted to $Q_{z=0^-}(PAR) = 52$ mol m^{-2} d^{-1}, corresponding to a sunny summer day in South-Finland. The photon flux density of PAR ($Q_z(PAR)$) was determined at depths 0–15 m with 1 cm interval according to Kirk (1977):

$$Q_z(PAR) = \int_{\lambda=400}^{\lambda=700} Q_{z=0^-}(\lambda)\, e^{-K_d(\lambda)z}\, d\lambda \tag{3}$$

to determine empirically $z_{1\%}(PAR)$ and $z_{10\%}(PAR)$ as the depths where 1 % and 10 % of the $Q_{z=0^-}(PAR)$ is left, respectively. Attenuation coefficient of PAR (m^{-1}) was calculated as $K_d(PAR) = -\ln(0.01)\,z_{1\%}(PAR)^{-1}$.

Spectral photon flux densities at wavelength λ at $z_{1\%}(PAR)$ and $z_{10\%}(PAR)$ ($Q_{z=1\%}(\lambda)$, $Q_{z=10\%}(\lambda)$, mol m^{-2} d^{-1}; I) were calculated as:

$$Q_z(\lambda) = Q_{z=0^-}(\lambda)\, e^{-K_d(\lambda)z} \tag{4}$$

in a way that in each lake, the $Q_{z=1\%}(\lambda)$ was 0.52 mol m^{-2} d^{-1} and $Q_{z=10\%}(\lambda)$ was 5.2 mol m^{-2} d^{-1} when integrated over the PAR band.

The mean photon flux density over the PAR band in the mixed layer ($\bar{Q}_{mix}(PAR)$, mol m^{-2} d^{-1}; I) was calculated according to Minor $et\ al.$ (2016):

$$\bar{Q}_{mix}(PAR) = Q_{z=0^-}(PAR)(z_{mix}K_d(PAR))^{-1} \times (1 - e^{-z_{mix}K_d(PAR)}) \tag{5}$$

where z_{mix} is the mixed layer depth (m). The values of z_{mix} were calculated according to Snucins and Gunn (2000):

$$\log_{10}z_{mix} = 0.91 + 0.07\log_{10}\mathrm{VOL} - 0.58\log_{10}(\mathrm{DOC} + 1) \tag{6}$$

where VOL is the lake volume (Mm³).

3.4 Determination of light absorption by phytoplankton

The spectral rate of photons absorbed by phytoplankton in the water column (mol m⁻² d⁻¹) was calculated as:

$$\mathrm{PUR}_{z-\infty}(\lambda) = \frac{a_{\mathrm{phyto}}(\lambda)}{a_{\mathrm{tot}}(\lambda)} Q_z(\lambda) \tag{7}$$

in the whole water column ($\mathrm{PUR}_{z=0-\infty}(\lambda)$) based on $Q_{z=0^-}(\lambda)$ and in the lower half of the euphotic layer ($\mathrm{PUR}_{z=10\%-\infty}(\lambda)$) based on $Q_{z=10\%}(\lambda)$ (I). The PUR values were also summed over the spectral bands of 400–500 nm (blue) and 600–700 nm (red) and examined relative to the PUR over the whole PAR band (I).

The fraction of phytoplankton absorption of the total PAR entering to lake (PUR/PAR, unitless) was calculated as (II):

$$\frac{\mathrm{PUR}}{\mathrm{PAR}} = \frac{\sum \mathrm{PUR}_{z=0-\infty}(\lambda)}{\sum Q_{z=0^-}(\lambda)} \tag{8}$$

where $\mathrm{PUR}_{z=0-\infty}(\lambda)$ summed over the PAR band was termed as PUR, and $Q_{z=0^-}(\lambda)$ (mol m⁻² d⁻¹) summed over the PAR band was termed PAR.

3.5 Continuous monitoring in lake Jyväsjärvi

Within the monitoring study of lake Jyväsjärvi, meteorological parameters and water chemistry profiles of the water column were continuously monitored in an automated floating monitoring station (III). Continuous weather monitoring sensors measured air temperature (T_{air}, °C), atmospheric pressure (P_{air}, mbar), global radiation (GR, kW m⁻²) and wind speed (WS, m s⁻¹), which were averaged to daily mean values. Daily depth of euphotic layer (z_{eu}) was approximated from weekly determined vertical attenuation coefficient of light (K_d(PAR), m⁻¹). The K_d values were determined as the slope of a linear regression between depth z and ln-transformed downwelling irradiance (E_d(PAR), W m⁻²) measured with TriOS Ramses ACC-UV/VIS sensor from several depths.

An automated multiparameter sonde profiled the water column at 0.5 depth intervals once an hour, including water temperature (T_{water}, °C), and fluorescence of Chl$a$ (RFU) and CDOM (RFU). Additionally, weekly water samples from the top 2 meter were collected for the determination of Chl$a$ concentration (mg m^{-3}). The Chl$a$ fluorescence was converted to concentration (mg m^{-3}) using a calibration between the fluorescence and concentration of Chl$a$ measured from the water samples. Depths of the mixed layer (z_{mix}) and seasonal thermocline (z_{thermo}) were determined according to a temperature decrease of 0.3°C from the surface value, and a depth of the deepest density gradient found in each profile, respectively. Daily mean values in the mixed layer were determined for the water quality parameters. Global radiation in the mixed layer (GR_{mix}) was determined as eq. 5 but using values of GR (kW m^{-2}) instead of Q (mol m^{-2} d^{-1}) at water surface. Daily phytoplankton biomass in the mixed layer (Chla_{area}, mg m^{-2}) was quantified as concentration of Chl$a$ (mg m^{-3}) in mixed layer multiplied by z_{mix}.

3.6 Data analysis

Linear regression analysis was used to examine the impact of CDOM content ($a_{CDOM}(400)$) on the spectral underwater light field, photoacclimation and chromatic adaptation by phytoplankton and spectral photon absorption of phytoplankton in the 128 boreal study lakes, using non- and log-transformed data and selecting a more parsimonious model based on adjusted R^2 value (I). To visualize the spectral data, study lakes were grouped into ten deciles according to their $a_{CDOM}(400)$ value, and a median spectrum of each decile band was shown in figures (I).

Regression analysis was also applied to examine the dependence of PUR/PAR ratio on the CDOM content and Chl$a$, using competing logarithmic models in the 128 study lakes (II). The most parsimonious model according to the Akaike information criterion was applied to estimate PUR/PAR values in the 2250 reference lakes based on their water quality. The reference lakes were grouped into nine decile bands according to their $a_{CDOM}(400)$ value (5–15th, 15–25th, 25–35th, 35–45th, 45–55th, 55–65th, 65–75th, 75–85th and 85–95th), covering 90 % of the reference lakes to represent typical boreal lakes. Furthermore, the response of PUR/PAR to browning expressed as increases in $a_{CDOM}(400)$ value by 25 %, 50 %, 75 % and 100 %, examples of browning reported in last decades (Räike *et al.* 2016, Kritzberg 2017, Lepistö *et al.* 2021), was estimated in a typical boreal lake defined as a median of the reference lakes according to CDOM and Chl$a$ (II).

Pearson correlation matrix was used to address the correlations between meteorological and water quality parameters in the monitoring study of Lake Jyväsjärvi (III). Using principal component analysis (PCA), the parameters were combined and reduced into two independent principal components. Regression analysis was used to estimate the dependence of phytoplankton biomass on individual meteorological and lake water quality parameters as well as on the

PC1 and PC2 using linear and quadratic models. In all data analyses, the limit of the statistical significance was set to $p < 0.05$. Statistical testing and data processing of the doctoral thesis were performed using R software (R Core Team 2022, version 4.2.1), and results were visualized using ggplot2 package (Wickham 2016).

4 RESULTS AND DISCUSSION

4.1 Spectral underwater light field along a CDOM gradient

In the 128 boreal study lakes characterised in Table 2 (I, II), spectral euphotic layer ($z_{1\%}(\lambda)$) was shallower and flatter in lakes with higher CDOM content (I, Fig. 2). Consistently, the euphotic layer over the total PAR ($z_{1\%}$(PAR)) was also shallower in lakes with higher CDOM content (Fig. 2), indicating that CDOM content strongly controlled the euphotic layer, in consistent with earlier studies from the boreal region (Eloranta 1978, Horppila *et al.* 2023, Sherbo *et al.* 2023).

TABLE 2   Main morphometrical and water quality parameters of the 128 sampled study lakes (I, II), including minimum, maximum, mean and median of lake area (LA) and volume (VOL), mean depth (z_{mean}), concentrations of total nitrogen (TN), phosphorus (TP), chlorophyll a (Chl$a$) and dissolved organic carbon (DOC), absorption coefficient of chromophoric dissolved organic matter at wavelength 400 nm ($a_{CDOM}(400)$) and water colour value.

	LA km²	VOL Mm³	z_{mean} m	TN µg l⁻¹	TP µg l⁻¹	Chl$a$ µg l⁻¹	DOC mg l⁻¹	$a_{CDOM}(400)$ m⁻¹	colour mg Pt l⁻¹
min	0.009	0.1	0.6	115	3	1	2	1.2	13
mean	62	600	6.3	554	23	10	11	9.7	77
median	15	88	5.4	519	16	7	10	6.9	56
max	894	12000	23	1503	173	77	24	35	240

CDOM also induced a shift in the spectral penetration of light, as the deepest penetrating wavelength shifted towards the red waveband in lakes with higher CDOM content (Fig. 2, I). A shift in the underwater light field along a gradient from ocean to lakes has been demonstrated in earlier studies using modelling (Holtrop *et al.* 2021) or underwater measurements (Stomp *et al.* 2007a). In our and earlier studies, the shift was not smooth but stepwise, creating three waveband

niches around 570 nm in the most transparent lakes, ~650 nm in the moderate level of transparency, and ~700 nm in the least transparent lakes (Fig. 2).
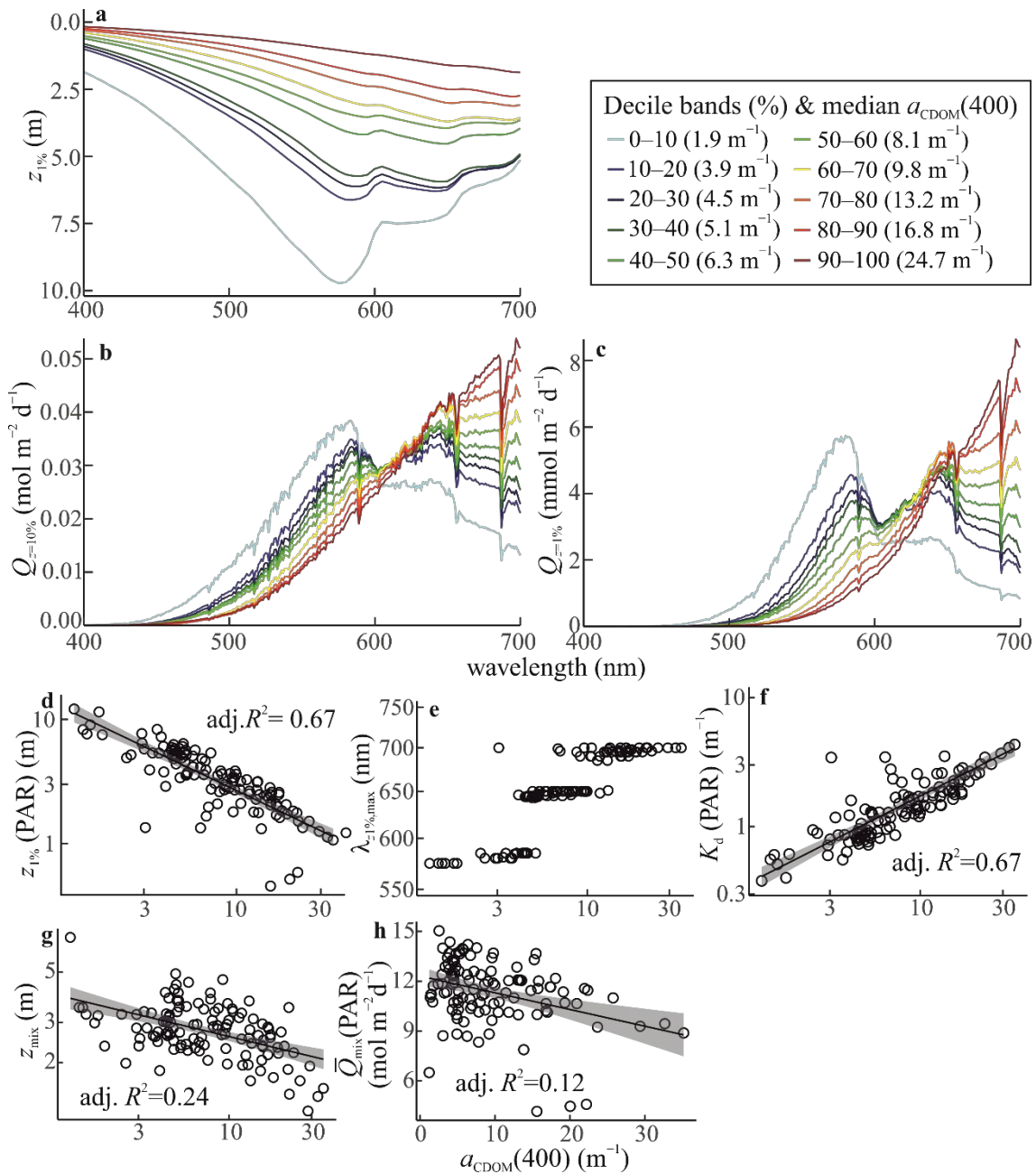

FIGURE 2   Spectral depth where radiation is attenuated to 1 % of its surface value (a), and spectral photon flux densities at $z_{1\%}$ (b) and $z_{10\%}$ (c) in the study lakes. The lakes are grouped into decile bands according to $a_{CDOM}(400)$ value and visualized with colours from low CDOM (light blue) to high CDOM (dark red) lakes. The legend shows a median $a_{CDOM}(400)$ value of each decile band. The dependence of the depth where subsurface PAR is attenuated to 1 % (d), the deepest penetrating wavelength of the spectral $z_{1\%}$ (e), the vertical attenuation coefficient of PAR (f), depth of the mixed layer (g) and daily photon flux density in the mixed layer (h) on $a_{CDOM}(400)$ value in the study lakes. Regression curves and adj. R^2 values are shown for significant ($p < 0.05$) models, and axes are log-transformed in all but panel (h).

Following the stepwise shift in the spectral $z_{1\%}$ along the CDOM gradient, the spectral photon fluxes at the bottom and mid-point of the euphotic layer ($Q_{z=1\%}(\lambda)$, $Q_{z=10\%}(\lambda)$) also showed drops at wavelength of ~600 nm, which was evident in the most transparent but not in the least transparent lakes (Fig. 2, I). These observed gaps in the spectral light field correspond with the harmonics in the absorption of pure water (Stomp *et al*. 2007a, Holtrop *et al*. 2021). The optical data of our study lakes confirms that the waveband niches around 570 nm, 650 nm and 700 nm are generally found in the PAR band in boreal lakes.

The attenuation coefficient of PAR ($K_d(PAR)$) increased but the depth of the mixed layer (z_{mix}) decreased in lakes with higher CDOM content (Fig. 2, I). The mean intensity of PAR in the mixed layer ($\bar{Q}_{mix}(PAR)$) was lower in lakes with higher CDOM content (Fig. 2). However, the $\bar{Q}_{mix}(PAR)$ changed less than $K_d(PAR)$ or $z_{1\%}$ along the CDOM gradient of the study lakes. This was likely caused by the CDOM not only steepening the light attenuation, but also shallowing z_{mix} closer to surface with highest light intensity (Fig. 2), observed also in earlier studies (Snucins and Gunn 2000, Heiskanen *et al*. 2015, Horppila *et al*. 2023). These findings also suggest that phytoplankton in the mixed layer are less affected by the CDOM or browning than benthic primary producers (Karlsson *et al*. 2009, Godwin *et al*. 2014, Rivera Vasconcelos *et al*. 2016).

4.2 Photoacclimation and light absorption by phytoplankton

In the study lakes, Chl*a* concentration (0.5–77 µg l⁻¹) and phytoplankton biomass (196–44800 µg fresh weight l⁻¹) both tended to be higher in lakes with higher CDOM content (Fig. 3; I). However, phytoplankton did not have increased cellular Chl*a* content in the mixed layer of study lakes with higher CDOM content (Fig. 3). This indicates a lack of phtoacclimation of phytoplankton in response to lower $\bar{Q}_{mix}(PAR)$ in higher-CDOM lakes (Fig. 2–3). Contrasting results were detected in eight Canadian boreal lakes, where Chl*a*/biomass was higher with increasing DOC or decreasing light intensity in the epilimnion (Sherbo *et al*. 2023). It is possible that photoacclimation is detectable among homogenous group of lakes (Sherbo *et al*. 2023, Chl*a* 1.4–2.8 µg l⁻¹) but is obscured among heterogenous lakes like in our study (Chl*a* range 0.5–76.5 µg l⁻¹). Hence, our and earlier findings suggest that photoacclimation of phytoplankton is possible but less usual in the mixed layer compared to phytoplankton below mixed layer with low light availability (deep Chl*a* maximum, Pérez *et al*. 2007, Sherbo *et al*. 2023).

In lakes without deep Chl*a* maxima, pelagic phytoplankton remain largely in the mixed layer, where the light availability fluctuates according to water movements (Spigel and Imberger 1987). In the mixed layer, phytoplankton reside at certain intervals close to surface, where light is abundant for photosynthesis. Thereby, investment to increase the cellular content of Chl*a* might not be needed despite occasional lowered light availability in deeper depths. Our findings suggest a true increase in phytoplankton biomass in lakes with higher CDOM content. In contrast, some studies conducted in the boreal region have

documented a unimodal dependence of phytoplankton biomass or productivity on DOC concentration, where the biomass decreases at high DOC levels (Solomon *et al.* 2015, Bergström and Karlsson 2019, Horppila *et al.* 2023). The different results might be caused by differences in the methodology or study lake characteristics, and hence the different conclusions are not necessarily contradictory. Nevertheless, the biomass of phytoplankton can indeed be sustained or be even higher in high-CDOM lakes like in our study, if the higher allochthonous loading associated to high-CDOM lakes also brings more nutrients to lakes, while the light level remains sufficient, to support primary production (Corman *et al.* 2018, Finér *et al.* 2021, Lepistö *et al.* 2021).
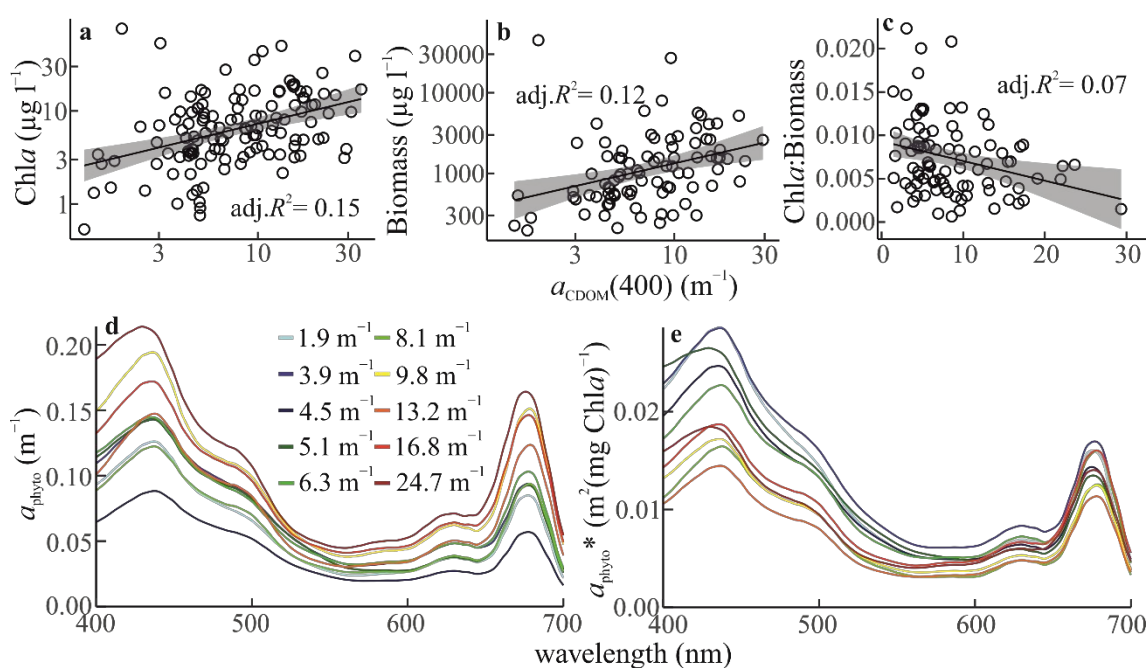

FIGURE 3   The impact of $a_{CDOM}(400)$ on chlorophyll *a* concentration (a), phytoplankton biomass (b) and their ratio (c) in the study lakes, showing regression curves and adj. R^2 values for significant ($p < 0.05$) models. Spectral absorption coefficient of phytoplankton (d) an Ch*la*-specific absorption coefficient in the study lakes grouped into ten decile bands according to their $a_{CDOM}(400)$ value from low CDOM (light blue) to high CDOM (dark red) lakes.

The spectral absorption coefficient of phytoplankton did not show any major changes in terms of shape among the lakes, but the values of $a_{phyto}(\lambda)$ tended to be higher throughout the PAR band in less transparent than in most transparent lakes, in consistence with higher Ch*la* concentration (Fig. 3; I). Also, Ch*la* specific absorption coefficient ($a_{phyto}*$) at the blue part of the spectrum was lower in less transparent lake deciles (Fig. 3). This finding indicates that phytoplankton decrease their blue-absorbing pigmentation relative to red-absorbing pigmentation in response to lower availability of the blue waveband in high-CDOM lakes. Indeed, the availability of blue light was very low at the mid-point and nearly absent at the bottom of the euphotic layer (Fig. 2), and therefore, it is not profitable for phytoplankton to invest on the blue-absorbing pigmentation in these boreal study lakes. Moreover, as CDOM effectively absorbs ultraviolet

radiation and thereby protects phytoplankton from UV exposure (Morris *et al*. 1995, Vähätalo *et al*. 2000, Choudhury and Behera 2001), the need for photoprotective pigments by phytoplankton is lower in high-CDOM lakes.

Spectral rate of absorption by phytoplankton (PUR) was examined by combining the available spectral photon flux density and spectral absorption by phytoplankton pigments and viewed in the lower half of the euphotic layer and over the entire water column (Fig. 4; I). The number of blue photons (400–500 nm) captured by phytoplankton was lower in higher-CDOM lakes (Fig. 4). Instead, the number of red (600–700 nm) photons absorbed by phytoplankton was higher in the lower half of the euphotic layer in higher-CDOM lakes, while no change was detected when examined over the whole water column (Fig. 4).
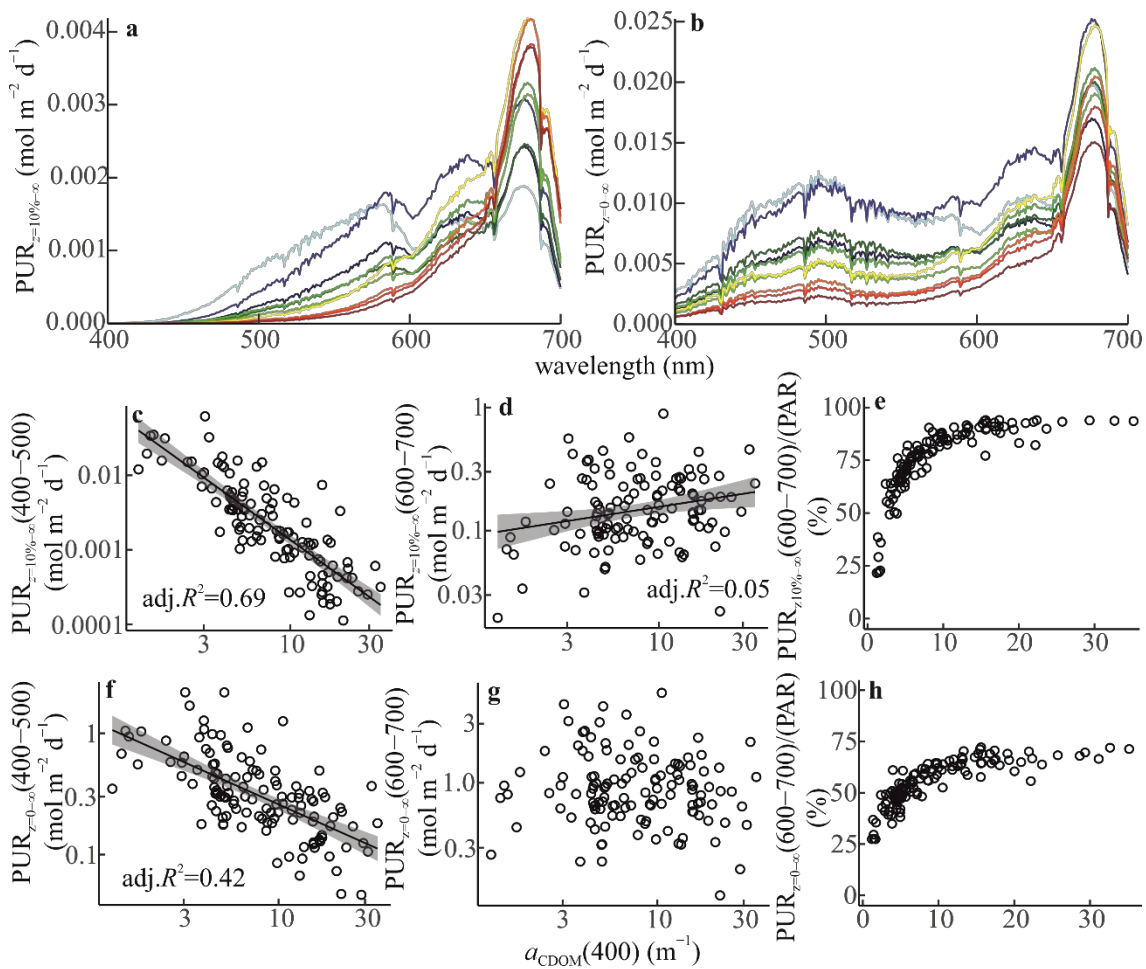

FIGURE 4   Spectral rate of photon absorption by phytoplankton (PUR) in the lower half of the euphotic layer (a) and over the entire water column (b) in the deciles of study lakes from low CDOM (light blue) to high-CDOM lakes (dark red), see the legend in Fig. 2. The impact of CDOM content on the absorption of photons by phytoplankton in the blue (400–500 nm) and red (600–700 nm) wavebands and the fraction of red light of the total absorption of PAR by phytoplankton in the lower half of the euphotic layer (c–e) and over the entire water column (f–h) in the study lakes. Regression curves and adj. R^2 values are shown in plots with significant dependence ($p < 0.05$).

The contribution of red photons of the absorption of total PAR by phytoplankton in the lower half of the euphotic layer was > 50 % in all but six most transparent lakes (Fig. 4). When examined in the whole water column, red light covered > 50 % of the PAR absorption by phytoplankton in 87 of the study lakes characterized by $a_{CDOM}(400)$ value > 5 m^{-1} (Fig. 4). The $a_{CDOM}(400)$ values in earlier studies of thousands boreal lakes have been reported to exceed 5 m^{-1} in majority of the lakes (Kallio 2006, Pace *et al.* 2012, Weyhenmeyer *et al.* 2014), suggesting that red light might dominate the light absorption by phytoplankton in most boreal lakes.

The examinations of the blue and red wavebands demonstrate a response of phytoplankton to the shift in the spectral distribution of light available from green towards red light, as the spectral photon absorption by phytoplankton shifts towards the red waveband to match the most available wavebands underwater. In many boreal lakes where z_{mix} is deeper than z_{eu} (Donis *et al.* 2021, Horppila *et al.* 2023), non-motile phytoplankton remain a significant part of the time in the lower half of the euphotic layer, where the increased availability of red light in lakes with higher CDOM content may considerably promote primary production. As the spectral light field shifts towards red waveband in the water column as shown in this and earlier studies (Reinart *et al.* 2001, Arst *et al.* 2008, Holtrop *et al.* 2021), it in fact drives photons towards the red absorption peak of Chl*a*, which is the most important pigment of phytoplankton. Therefore, the spectral shift in the underwater light can be beneficial for phytoplankton owing to their spectral light absorption properties.

4.3   PUR/PAR values and their response to browning

Phytoplankton contributed generally only little to the absorption of the incoming PAR (PUR/PAR) in the 128 studied lakes, where the PUR/PAR value ranged 0.4–17 % with a median of 3 % (Fig. 5; II). Instead, CDOM was the highest light absorbing component in all but one lake (Fig. 5). The PUR/PAR values in the 128 study lakes are lower compared to values of a close variable a_{phyto}/a_{tot} reported for Scandinavian lakes (median 7 %; Thrane *et al.* 2014) and for a Canadian reservoir (mean 5 %; Watanabe *et al.* 2015). This difference is likely caused by the higher upper ranges of CDOM (1.2–35 m^{-1}) and DOC (1.8–24 mg l^{-1}) in our study lakes than those reported elsewhere, such as by Thrane *et al.* (2014; $a_{CDOM}(400)$ 0.1–15 m^{-1} and DOC 0.3–12.3 mg l^{-1}), or by Kutser *et al.* (2005; $a_{CDOM}(400)$ 1.2–7.7 m^{-1} and DOC 7–12 mg l^{-1}). Nevertheless, it appears that the importance of phytoplankton in the absorption of PAR is generally minor in boreal lakes, where CDOM dominates light absorption (Thrane *et al.* 2014).

Among the study lakes, a logarithmic model containing CDOM content and Chl*a* concentration was the most parsimonious for predicting PUR/PAR values (adj. $R^2 = 0.52$). The model was converted to a linear scale as:

$$\text{PUR/PAR} = a_{CDOM}(400)^{-0.645} \times \text{Chl}a^{0.552} \times e^{-3.288} \tag{9}$$

In the model, CDOM had a negative and Chl$a$ (and nutrients) a positive effect on the PUR/PAR (Fig. 5 c–d). Similar associations were found in a model applied to Scandinavian lakes, where phosphorus concentration increased, and DOC decreased the light absorption by phytoplankton pigments (Thrane $et\ al.$ 2014). An increase in CDOM content or the chromophores of DOC in lake water reduce the part of PAR absorbed by phytoplankton, as phytoplankton cannot capture the photons absorbed by the CDOM (Solomon $et\ al.$ 2015). In contrary, increased nutrient supplies can promote higher phytoplankton biomass and thereby enhance light absorption by phytoplankton (Marzetz $et\ al.$ 2020).

PUR/PAR values were predicted for the over 2000 reference boreal lake dataset based on their Chl$a$ along a CDOM gradient from 5–15th to the 85–95th decile band of $a_{CDOM}(400)$, where PUR/PAR values ranged 2.5–3.8 % (Fig. 5 d–e). Chl$a$ for each centred $a_{CDOM}(400)$ decile band was calculated based on their logarithmic dependence in the reference lakes (Chl$a = 1.80a_{CDOM}(400)^{0.75}$, adj.$R^2$ = 0.29; Fig. 5 f). Along 90 % of the reference lakes, $a_{CDOM}(400)$ ranged 3.8–21 m^{-1}, while Chl$a$ concurrently more than tripled (Fig. 5 e–g). Concomitant increases in nutrients and DOC or CDOM have been often reported in lakes (Thrane $et\ al.$ 2014, Seekell $et\ al.$ 2015, Hamdan $et\ al.$ 2021), which support our assumption of concurrently increasing CDOM and Chl$a$. DOC can also be used as energy source by mixotrophic phytoplankton, promoting their higher biomass and light absorption in high-CDOM lakes (Calderini $et\ al.$ 2022). Furthermore, phytoplankton can increase their cellular Chl$a$ content in response to lowered light intensity in high-CDOM lakes, which could increase their light absorption without a concurrent increase in biomass (Fennel and Boss 2003, Sherbo $et\ al.$ 2023). However, there was no sign of a photoacclimation among the study lakes (Fig. 3, I). All in all, higher concentration of nutrients and carbon can partly compensate the shading effect of CDOM in high-CDOM lakes (Thrane $et\ al.$ 2014).

In a typical boreal lake, defined as the median reference lake ($a_{CDOM}(400)$ of 8.9 m^{-1} and Chl$a$ of 9.2 µg l^{-1}), a browning scenario of 25–100 % increase in the $a_{CDOM}(400)$ value decreased PUR/PAR values 5–15 %. The browning scenario assumed a concurrent increase in Chl$a$ concentration, based on an average development of Chl$a$ (30–67 %) in the reference lakes along with CDOM. Hence, while CDOM reduced the PUR/PAR values according to the eq. 9, the steepness of the decrease was partly counteracted by a presumed increase of Chl$a$ (Fig. 5). Owing to this compensatory effect, PUR/PAR values were predicted to decrease only moderately for an average rate of browning (25 %) reported in the recent decades (Räike $et\ al.$ 2016, Lepistö $et\ al.$ 2021). The browning scenario is supported by earlier studies, where similar co-occurring increases in both CDOM or DOC and Chl$a$ have been reported (Corman $et\ al.$ 2018, Lepistö $et\ al.$ 2021).
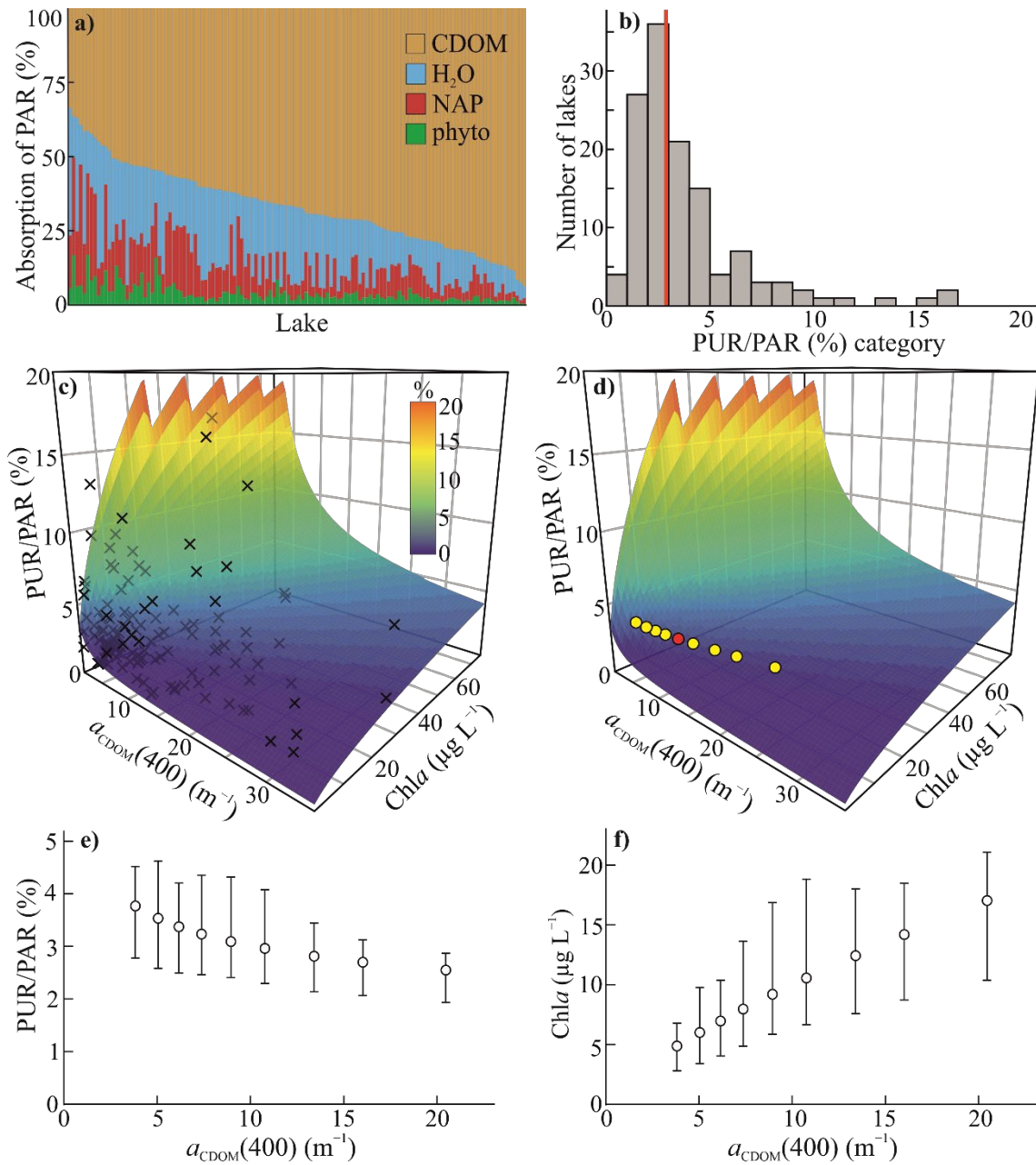
FIGURE 5   The fraction of incoming PAR absorbed by CDOM, H₂O, NAP and phytoplankton (a) and the PUR/PAR values (b) in the 128 sampled lakes, vertical red line indicating the median value. Crosses (c) show the PUR/PAR values of the sampled lakes according to their $a_{CDOM}(400)$ and Chl$a$. 3D surfaces (c–d) show predicted PUR/PAR values based on eq. 9, a colour scale indicating the PUR/PAR value. Yellow circles (d) are the predicted PUR/PAR values and red circle a median value according to the nine centred decile bands of $a_{CDOM}(400)$ covering 90 % of the reference lakes. The circles (e–f) show the calculated PUR/PAR (eq. 9) values and Chl$a$ concentrations based on measured values with the centred decile bands of $a_{CDOM}(400)$ in the reference lakes, the error bars indicating the first and third quartiles of PUR/PAR and Chl$a$ in each decile band.

The browning scenario here bases on spatial differences between lakes and their catchments along a CDOM gradient, and not on temporal responses of PUR/PAR to an increased input of CDOM into a lake. The purpose of our scenario was to predict the average responses in PUR/PAR values along typical boreal catchments. However, a temporal response in a particular lake depends most importantly on the lake-specific characteristics of the catchment and the causes of the browning, such as the changes in the acid deposition, land use or vegetation (Corman *et al.* 2018, Lepistö *et al.* 2021, Stetler *et al.* 2021a). One of the main factors affecting the PUR/PAR values in a lake experiencing browning is the ratio of nutrients and CDOM in the increased allochthonous loading (Kelly *et al.* 2018). In the current study, the changes in the water quality along the browning scenario were characterized by ratios 1.8 µg TP/mg DOC, 1.4 µg TP/m^{-1} a_{CDOM}(400) and 0.15 µg TP/mg Pt colour, according to the average associations found in the reference lakes with increasing CDOM. In earlier studies, both lower and higher ratios of TP/DOC in the allochthonous loading and soil leachates have been reported in forested boreal and temperate catchments, respectively (Jansson *et al.* 2012, Corman *et al.* 2018, Finér *et al.* 2021), compared to the ratio in the browning scenario of this study, respectively. Moreover, lower TP/colour ratio of the loading in Swedish forest streams was reported (Meili 1992). Hence, browning of lakes may decrease PUR/PAR values more than what was described by the browning scenario here if the nutrient to CDOM ratio within the increased loading of allochthonous material is lower than in the reference lakes. However, the responses of phytoplankton to the increased allochthonous loading take place in the affected lakes, and therefore the responses of PUR/PAR should not be predicted only based on the characteristics of the allochthonous material. For example, allochthonous nutrients have complex cycles in aquatic systems, and CDOM can be quickly photobleached by solar radiation (Del Vecchio and Blough 2002, Vähätalo and Wetzel 2004), resulting in lower competition of photons between phytoplankton and CDOM. Also, phytoplankton can adapt to environmental changes e.g. via mixotrophy or photoacclimation (Dubinsky and Stambler 2009, Hansson *et al.* 2019).

4.4   The impact of mixed layer on daily phytoplankton biomass

In a mesotrophic humic lake Jyväsjärvi during the first half of the summer stratification (III), the depth of the mixed layer (z_{mix}) ranged 2–7 m and was deeper or equal to the euphotic layer almost always (Fig. 6, 7). The mixed layer was mostly shallower than the seasonal thermocline, and the Chl*a* concentration (Chl$a_{vol,z,t}$) and the CDOM content (CDOM$_{z,t}$) were approximately homogenous within the mixed layer, following its dynamics (Fig. 6). In the study lake, wind speed and the difference of temperature in air and in z_{mix} were most strongly associated with the depth of z_{mix}, which was deep on days characterised by high wind speed, low air pressure and colder air relative to water, favouring convective mixing (Fig. 6). The areal chlorophyll *a* concentration over the mixed

layer (Chl*a*area, hereafter referred as phytoplankton biomass) ranged 21–115 mg m⁻², and was primarily depended on the depth of z_{mix}, which explained 69 % of the variability in the biomass (Fig. 6, 7). In the study lake, biomass tended to be higher on days with deeper z_{mix}. In addition, the biomass was positively dependent on the PC1 of the principal component analysis, which explained 43 % of the variation in the phytoplankton biomass according to a nonlinear model, indicating high biomass on days with deep mixing, high wind, and colder air than mixed layer (Fig. 7).
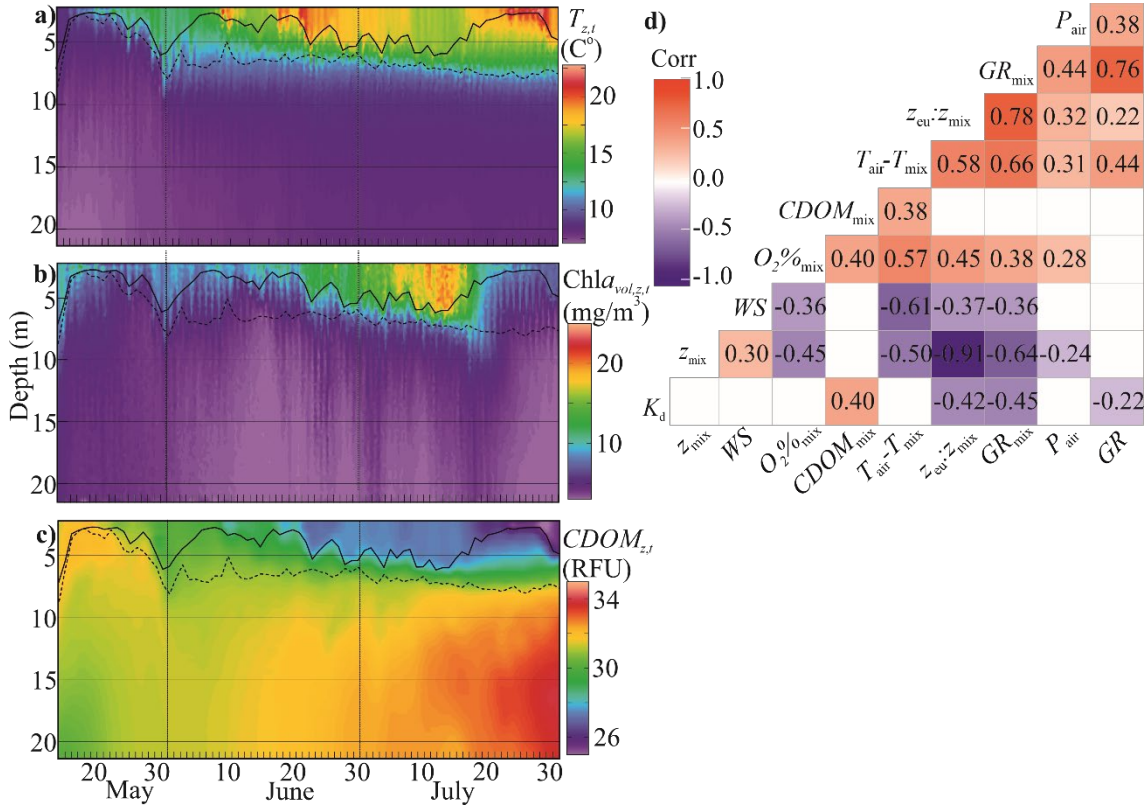

FIGURE 6   Temperature (a), Chl*a* concentration (b), and CDOM fluorescence (c) in the water column of lake Jyväsjärvi from mid-May to end-July 2019 plotted with mixed layer depth (solid curve) and seasonal thermocline (dashed). Correlation matric shows the association between meteorological and water chemistry parameters (d). Blue and red colours and their intensity refer to the significant ($p < 0.05$) negative and positive correlation coefficients, respectively.

The positive dependence of phytoplankton biomass on z_{mix} found in Lake Jyväsjärvi is largely consistent with older studies of modelling (Diehl 2002, Berger *et al*. 2006, Mesman *et al*. 2022), experiments (Diehl *et al*. 2002, Cantin *et al*. 2011, Giling *et al*. 2017) and lake comparisons (Berger *et al*. 2006). The positive association between the biomass and z_{mix} may be explained by improved nutrient availability from deeper layers as the z_{mix} deepens (Weithoff *et al*. 2000, Diehl 2002, Giling *et al*. 2017), which would benefit phytoplankton requiring nutrients to gain biomass. Higher biomass in deep z_{mix} can be also caused by lower sinking losses of phytoplankton out of the deeper mixed layer (Ptacnik *et al*. 2003, Cantin *et al*. 2011). Moreover, deep z_{mix} can decrease encounter rates between

phytoplankton and grazer as the phytoplankton are diluted in a larger volume of water, thereby reducing grazing losses of phytoplankton (Berger *et al.* 2006).
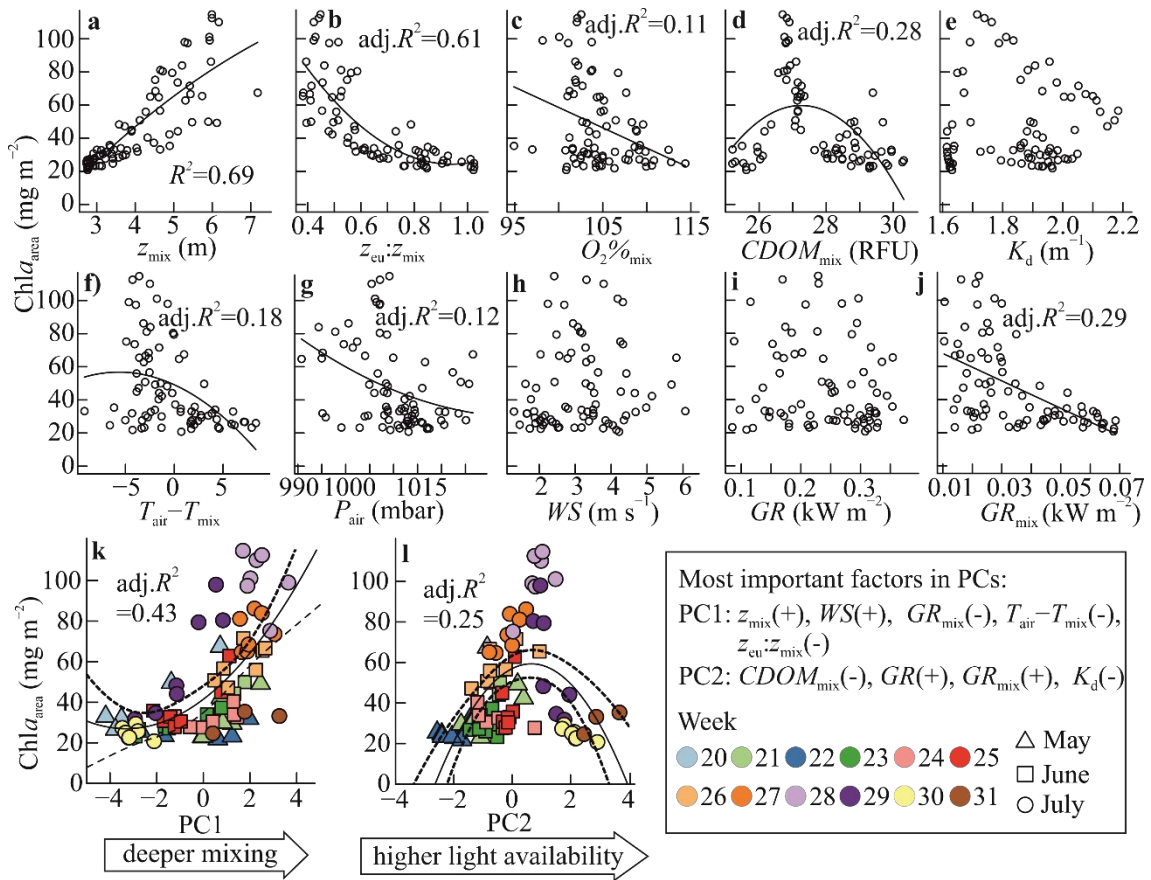

FIGURE 7   The dependency of daily $Chla_{area}$ on mixed layer depth (a), the ratio of euphotic and mixed layer depths (b), oxygen saturation (c), CDOM fluorescence (d), vertical attenuation coefficient (e), difference between air and mixed layer temperature (f), air pressure (g), wind speed (h), global radiation in air and in the mixed layer (i, j), and on PC1 (k) and PC2 (l) axes of PCA. The legend shows the most important factors and their directions (+/−) in the principal components. Linear or non-linear regression curves and adj. R^2 values are plotted for significant ($p < 0.05$) regression models.

In terms of light availability, the phytoplankton biomass had a negative dependence on $z_{eu}{:}z_{mix}$ and global radiation in the mixed layer (Fig. 7). Moreover, the second principal component PC2 explained 25 % of the variation in the biomass by a non-linear model, indicating a higher biomass with improving light availability when light levels are low but lower biomass under the highest light availability. The depth of euphotic layer relative to mixed layer is of importance in characterising the underwater light conditions experienced by phytoplankton in the mixed layer. During the study period, the range of $z_{eu}{:}z_{mix}$ (0.4–1.0) was larger than 0.2, which is considered a critical value, above which net growth of the biomass can be supported according to Cloern (1987). Thus, our findings indicate that an increase in z_{mix} may primarily increase phytoplankton biomass in aquatic systems where the $z_{eu}{:}z_{mix}$ is ≥ ca. 0.4 like in our study lake. Overall, these findings suggest that light is not the major limiting factor of phytoplankton

biomass in non-eutrophic lakes like the study lake during the first half of the summer stratification period.

In the study lake, wind speed and the difference between air and mixed layer temperature, the main climatic impact-drivers, had a major impact on the depth of z_{mix}, which was further strongly associated with phytoplankton biomass (Fig. 6). Increased surface water temperature, an indicator of stratification strength, has been documented to affect negatively on phytoplankton biomass in global ocean and lakes, which are non-eutrophic like lake Jyväsjärvi (Behrenfeld *et al.* 2006, Kraemer *et al.* 2017, Mesman *et al.* 2021, Siemer *et al.* 2021, Mishra *et al.* 2022). This commonly found response indicates that a stronger stratification and shallower z_{mix} can reduce nutrient supplies to phytoplankton in non-eutrophic lakes. Atmospheric stilling and heatwaves can further reduce the z_{mix} and the upward flux of nutrients to the mixed layer, resulting in lower phytoplankton biomass based on our results and findings elsewhere (Coumou and Rahmstorf 2012, Perkins-Kirkpatrick and Lewis 2020, Deng *et al.* 2021, Woolway *et al.* 2022). These together suggest that warmer air temperature and lower wind speed driven by climate change can reduce the z_{mix} depth and phytoplankton biomass in non-eutrophic lakes during the first half of the summer stratification. During the second half of the stratification season, however, the effects of these climatic drivers may be different, when the seasonal cooling of air and lower solar radiation deepen z_{mix} until the autumn turnover. For example, climate change driven warmer air can prolong the growing season of phytoplankton and support their higher biomass during the second half of the stratification season (Yang *et al.* 2016, Kraemer *et al.* 2017, Wasmund *et al.* 2019).

5   CONCLUSIONS

This thesis showed that CDOM exerts a strong control over the quantity and spectral quality of light in boreal lakes. Firstly, CDOM reduced the penetration of light into the water column, and consequently restricted the euphotic layer into shallower water in lakes with higher CDOM content. Moreover, increasing content of CDOM in lakes influenced the spectral availability of underwater light field, inducing a stepwise shift in the wavelength composition towards red wavelength region of PAR, owing to the increasing light absorption by CDOM towards the shorter wavelength region of the visible light. Correspondingly, the attenuation of PAR was higher in lakes with higher CDOM content. However, higher CDOM content in lake water also pushed mixed layer shallower, and therefore the light intensity in the mixed layer was less affected by the higher CDOM content than what was euphotic layer and attenuation of PAR in the lakes. All in all, these findings suggest that increased input of CDOM within the elevated loading of allochthonous material causing browning in lakes is reflected in the underwater light field as changes similar to those documented in the study lakes with varying CDOM content. In addition, while higher CDOM content decreases the overall light availability in lakes, the light intensity experienced by the pelagic phytoplankton in mixed layer is perhaps less affected, owing to the steeper light attenuation but also a shallower mixed layer. The shift in the spectral composition of underwater light from the dominance of green light towards red light nevertheless changes the spectral light field available for phytoplankton to use in photosynthesis.

Phytoplankton responded to the shifted spectrum of available light from most to least transparent lakes by decreasing the blue-absorbing pigmentation. The photon absorption of red light by phytoplankton in the lower half of the euphotic layer was higher in lakes with higher CDOM content. Indeed, red light covered over 50 % of PAR absorption by phytoplankton over the whole water column in most lakes, and hence it appears that autochthonous production of phytoplankton is mainly fuelled by red light in most boreal lakes. Instead, the absorption of incoming total PAR by phytoplankton in the whole water column decreased in lakes with higher CDOM content, although the decrease was only

moderate. Chl*a* concentration tended to concurrently increase with CDOM content of a lake, and this tendency partly compensated for the negative effect of CDOM on the fraction of total PAR absorbed by phytoplankton. Despite the lowered light intensity and absorption of total PAR by phytoplankton in lakes with higher CDOM content, there were no signs of an increase in phytoplankton pigment content in high-CDOM lakes. Instead, phytoplankton biomass tended to be higher in lakes with higher CDOM content. According to these findings, phytoplankton communities appear to be able to sustain or even increase their biomass in higher-CDOM lakes despite the decreased light availability. This is perhaps caused by combined effects of sufficient light availability, increased supplies of nutrients and/or shifts in community composition in lakes with higher CDOM content. However, these findings are based on data collected during summertime stratification, whereas the responses of phytoplankton biomass to the changes in CDOM might be different at other times of the year, when daily doses of solar radiation are lower.

The browning scenario in a typical boreal lake caused only a moderate decrease in the absorption of PAR by phytoplankton in this study, owing to the assumed increases in both CDOM and nutrients contents of a lake. The predictions were made for typical boreal lakes in terms of CDOM and nutrient contents, and thus individual lakes may exhibit different responses to the browning of lakes. The browning scenario assumed that light is absorbed within the mixed layer, and thus the response may not be the same in lakes with high transparency and where light reaches the bottom. Moreover, the cause of browning and the catchment characteristics alter the content of the increased allochthonous loading to the lake, and hence also the consequently impacted phytoplankton absorption. Especially, the relative composition of CDOM and nutrients in the allochthonous loading appears to be important in determining the negative versus positive effects of browning on the phytoplankton communities in the receiving lakes. Hence, if browning increases CDOM content but not nutrient supplies in the receiving lakes, the light absorption by phytoplankton is likely more affected by the shading of CDOM than what was modelled in this study.

The daily phytoplankton biomass in the mixed layer of Lake Jyväsjärvi during the first half of the stratification period was higher on days with deeper of mixed layer, despite a concurrent decrease in the light conditions. Overall, the improved light availability elevated biomass only when light level was low. This, supported by the results from the 128 study lakes, suggests that during the summer stratification period, other factors than light, such as nutrients, might be the main drivers of daily phytoplankton biomass in non-eutrophic boreal lakes like most of the study lakes. During the summer stratification period, mixed layer was deeper on days characterised by colder air relative to water and higher wind speed, when also phytoplankton biomass tended to be higher. In contrast, lower biomass was observed on days with warmer air than water and low wind speed. These meteorological conditions prevail during heatwaves, that are predicted to increase in frequency and severity along the ongoing climate change. These findings demonstrate as an example, how warming climate together with

declining wind speed, the drivers of climate change, can induce oligotrophication in boreal lakes during the summertime stratification. These findings were reported during the first half of the stratification, when daily doses of sunlight, air temperature and stratification strength are usually increasing. In terms of climate change, this period is of importance as especially the ice-out days and the onset of stratification have advanced due to global warming, causing earlier spring blooms but also earlier nutrient depletion in the stratified water columns. The main drivers of the phytoplankton biomass might, however, be different during the second half of the stratification period, when daily doses of sunlight start to decrease and the tendency to deeper and more regular mixing increases.

Overall, the findings of this thesis suggest that during the summer stratification period, light is perhaps not the main limiting factor of phytoplankton biomass in the mixed layer across a range of boreal lakes with varying CDOM contents, despite the major role of CDOM in controlling the optical properties in these lakes. Instead, phytoplankton biomass can be high even in high-CDOM lakes, where biomass may be fuelled by increased supplies of nutrients, while light levels stay sufficient to provide energy for photosynthesis. Also, as mixed layer will be likely reduced by stronger stratification caused by the combined effects of climate warming and browning, so is the depth within which phytoplankton are turbulently mixed and thus the light availability experienced by the phytoplankton might not be as dramatically affected. In addition, shifts in the phytoplankton community composition towards species that grow efficiently at low light, are motile or utilize energy via heterotrophic pathways, may contribute to the higher biomass in lakes with higher CDOM content. However, more research is needed to examine possible changes in the community composition as response to increasing CDOM content in lakes. All in all, I want to emphasize that factors influencing the aquatic food webs in lakes are highly complex and locally variable, making it difficult to predict common responses of phytoplankton to the ongoing environmental stressors. Further research is needed to understand the mechanisms that cause parallel environmental changes to lead to opposite responses in phytoplankton biomass in different lakes. High-frequency and temporal monitoring of lake water column would also help to identify the main drivers and mechanisms behind the various responses of phytoplankton documented in this and earlier studies.

Acknowledgements

I wish to thank a large group of people, without whom this work would not have been possible. Firstly, I would like to thank my supervisors Anssi Vähätalo and Jukka Seppälä for excellent guidance. I thank Anssi for giving me the opportunity to start the PhD project, despite the minor knowledge I had about aquatic optics when I started. You always found time for my questions, you taught me a great deal about the optics, among others, and guided me when I had lost my focus or trust in what I was doing. Jukka, thank you for willing to participate the PhD project as a supervisor and sharing your knowledge of phytoplankton communities and important technical details, which have had a key role in improving this work. I thank you both for the positive and encouraging support.

I wish to thank the co-authors for their valuable contribution in this project. This thesis would not have been possible without the datasets you provided from previous projects. I thank you for your input towards the manuscripts, sharing your expertise and giving me constructive comments. A special thanks to Roger Jones for the valuable contribution in the quality improvement of the research articles and the positive and encouraging feedback. I thank my follow-up group, Marko Järvinen and Anna Kuparinen, for their encouraging support during the project and helping me to make a realistic research plan with respect to the time limit.

I am deeply grateful to Jonna Kuha and Harri Kovanen for the maintenance of the monitoring research platform Aino and all the help you both gave me at all stages of the data collection in Lake Jyväsjärvi. With your excellent guidance, I managed get through unpredictable obstacles. I also wish to thank Mervi, Emma, Nina, Juha and Ahti for helping me with laboratory and technical issues.

I wish to thank colleagues for the inspiring conversations in the D2 coffee room and in lunch breaks. A special thanks to Minna for sharing the office with me for several years and listening to my concerns. You have been like a mentor to me, and I am highly grateful for all your support and guidance. Ole, thank you for the numerous coffee breaks and support during the years in the D2 corridor. I thank the fellow doctoral researchers for the peer support and kind help when wandering through the jungle of manifold instructions.

I thank my family for supporting me whenever needed. I wish to thank my friends for the support as well as understanding in times when all I could think of was research. Ossi, no words are enough to express my gratitude for the love, support and care you have given me every day. Thank you Ossi also for helping me to improve my R language skills. Uula, thank you for keeping me busy and my mind outside of science during the weekends and holiday seasons, you have brought balance between the work and free time.

The doctoral program of the University of Jyväskylä funded my salary during my PhD time. Funds to co-authors enabled the creation of the large datasets used within this project. Travel grants were provided by the doctoral program and Maa- ja vesitekniikan tuki ry.

YHTEENVETO (RÉSUMÉ IN FINNISH)

Veden valo-ominaisuuksien vaikutukset kasviplanktonin spektraaliseen valosaatavuuteen ja biomassaan boreaalisissa järvissä

Kasviplanktonlevät ovat mikroskooppisia yhteyttäviä organismeja, jotka sitovat ilmakehän hiiltä orgaanisiksi yhdisteiksi, ja jotka ovat vesistöissä ravintoverkkojen pääasiallinen energialähde. Kasviplankton tarvitsee biomassan tuottamiseen sekä ravinteita että valoenergiaa säteilyn fotosynteettisesti aktiivisella aallonpituusalueella (PAR, 400–700 nm), mutta niitä on usein epätasaisesti saatavilla vesipatsaassa. Valoa on parhaiten saatavilla lähellä vedenpintaa, kun taas ravinnesaatavuus on usein parempi syvemmällä vesipatsaassa. Valon vaimenemisnopeus vesipatsaassa riippuu veden ja siihen sekoittuneiden aineiden, eli värillisen liuenneen orgaanisen aineksen (CDOM), kasviplanktonin ja muiden kuin leväpartikkelien (NAP) absorptio- ja sirontaominaisuuksista. Monissa boreaalisissa järvissä on runsaasti CDOM:ia, joka absorboi näkyvää valoa voimakkaasti erityisesti PAR-alueen lyhyillä aallonpituuksilla, värjäten veden ruskeaksi. CDOM voi rajoittaa järven valoisaa eli eufoottista kerrosta, jonka alarajana pidetään syvyyttä, jossa veden pinnassa olevasta valosta on 1 % jäljellä. Eufoottisen kerroksen syvyyttä käytetään arvioimaan sitä osaa vesipatsaasta, jossa valo on riittävää perustuottajien nettofotosynteesiin. Boreaaliset järvet kerrostuvat kesäisin, muodostaen toisistaan erillään olevia kerroksia. Lähimpänä veden pintaa olevaa kerrosta kutsutaan sekoittuvaksi kerrokseksi, jossa liikuntakyvyttömät kasviplanktonsolut kulkeutuvat veden liikkeiden mukaisesti. Sekoittuvan ja eufoottisen kerroksen syvyyksien suhde määrittelee kasviplanktonsolujen keskimääräisen valosaatavuuden sekoittuvassa kerroksessa.

Ympäristönmuutokset, kuten ilmaston lämpeneminen ja pohjoisella pallonpuoliskolla havaittu järvien tummuminen, vaikuttavat fysikaalisiin, kemiallisiin ja biologisiin prosesseihin järvissä. Ilmaston lämpeneminen aikaistaa jäiden lähtöä ja kerrostuneisuuden alkua sekä pidentää ja voimistaa kesäaikaista kerrostuneisuutta järvissä. Järvien tummuminen johtuu lisääntyneestä maalta peräisin olevasta CDOM-kuormasta ja rajoittaa suoraan järvien eufoottista kerrosta, mutta voi myös voimistaa kesäaikaista kerrostuneisuutta CDOM:in voimakkaan valoabsorption vuoksi. CDOM:in ajatellaan rajoittavan kasviplanktonin määrää boreaalisissa järvissä, mutta sen vaikutuksista kasviplanktonin valoabsorptioon ja biomassaan tiedetään vielä vähän.

Väitöskirjatyössäni tutkin boreaalisten järvien valo-olosuhteita ja niiden merkitystä kasviplanktonin valoabsorption ja biomassan vaihtelussa. Tutkimukseni koostui kahdesta eri aineistosta. Niistä ensimmäinen koostui vuosien 2014–2018 aikana kerätyistä vesinäytteistä 128 järvestä ympäri Suomea. Vesinäytteistä määritettiin veden, CDOM:in, kasviplanktonin ja NAP:n absorptiospektrit, klorofyllipitoisuus, mikroskopoitu kasviplanktonbiomassa, ja muita yleisiä vedenlaatumuuttujia. Absorptiospektreistä määritettiin valon tunkeutumiskerros eri aallonpituuksilla ja arvioitiin eufoottisen kerroksen syvyys näytejärvissä.

CDOM:in absorptiokerrointa aallonpituudella 400 nm (a_{CDOM}(400)) käytettiin kuvaamaan CDOM:in määrää järvessä. Kasviplanktonin absorptiospektrejä käytettiin arvioimaan kasviplanktonin absorboimien fotonien määrää järvissä. Toinen aineisto koostui vesipatsaan ja säätilan jatkuvatoimisesta seurannasta sekä viikoittaisista vesinäytteistä ja vedenalaisen valospektrin mittaamisesta Jyväsjärvellä kesän kerrostuneisuuden aikana. Vesipatsaan lämpötilaprofiileista määritettiin päivittäinen sekoittuvan kerroksen syvyys ja kasviplanktonbiomassa.

Lähes kaikissa tutkimusjärvissä suurin absorboiva tekijä oli CDOM, jonka suurempi määrä järvessä oli yhteydessä matalampaan eufoottiseen kerrokseen. CDOM:in suurempi määrä sai myös aikaan syvimmälle tunkeutuvan valon siirtymisen vihreästä kohti punaista aallonpituusaluetta. Samalla kasviplanktonin absorboimasta valosta punaisen valon osuus kasvoi ja vastaavasti sinisen valon osuus väheni. Kaiken kaikkiaan suurimmassa osassa tutkimusjärvistä punainen valo kattoi yli 50 % kasviplanktonin absorboimasta valosta. Klorofyllipitoisuus ja kasviplanktonbiomassa olivat korkeampia enemmän CDOM:ia sisältävissä järvissä. Kasviplanktonilla ei kuitenkaan havaittu kasvanutta solun sisäistä klorofylli *a*:n määrää tummimmissa järvissä, heikentyneestä valosaatavuudesta huolimatta. Mallinnettu tummuminen tyypillisessä boreaalisessa järvessä, olettaen, että CDOM ja ravinnesaatavuus kasvavat samanaikaisesti, vähensi kasviplanktonin absorboimaa osuutta järveen tulevasta valosta, mutta vain vähän, sillä parantunut ravinnesaatavuus kompensoi CDOM:in negatiivista vaikutusta.

Kesän kerrostuneisuuden alkupuoliskolla kasviplanktonbiomassa oli tyypillisesti suurempi tuulisina ja kylminä päivinä, kun sekoittuva kerros oli syvemmällä. Kaikista matalimmillaan kasviplanktonbiomassa oli tyynenä hellejaksona, jolloin sekoittuva kerros oli matala. Parempi valosaatavuus oli yhteydessä korkeampaan biomassaan vain silloin, kun valosaatavuus oli alhainen. Tulosten perusteella valo ei välttämättä ole tärkein kasviplanktonin biomassaa säätelevä tekijä ei-rehevissä järvissä kesän kerrostuneisuuden alkupuoliskolla. Sen sijaan syvemmän sekoittuvan kerroksen yhteys suurempaan biomassaan johtuu kenties ravinnesaatavuuden paranemisesta. Kaiken kaikkiaan tulokset viittaavat kasviplanktonin pystyvän ylläpitämään tai jopa lisäämään biomassaansa siitä huolimatta, että CDOM rajoittaa järvien valosaatavuutta tummissa järvissä. Tulokset ovat tärkeitä ympäristönmuutosten vaikutusten arvioinnin kannalta, sillä hellejaksojen ennustetaan lisääntyvän ja voimistuvan entisestään. Sekoittuvan kerroksen madaltuminen kesän hellejaksojen aikana voi rajoittaa kasviplanktonbiomassaa heikentyneen ravinnesaatavuuden vuoksi kerrostuneissa järvissä.

REFERENCES

Adrian R., O'Reilly C.M., Zagarese H., Baines S.B., Hessen D.O., Keller W., Livingstone D.M., Sommaruga R., Straile D., Donk E.V., Weyhenmeyer G.A. & Winder M. 2009. Lakes as sentinels of climate change. *Limnol. Oceanogr.* 54: 2283–2297.

Álvarez E., Lazzari P. & Cossarini G. 2022. Phytoplankton diversity emerging from chromatic adaptation and competition for light. *Prog. Oceanogr.* 204, 102789.

Anas M.U.M., Scott K.A. & Wissel B. 2015. Carbon budgets of boreal lakes: State of knowledge, challenges, and implications. *Environmental Reviews* 23: 275–287.

Apell J.N. & McNeill K. 2019. Updated and validated solar irradiance reference spectra for estimating environmental photodegradation rates. *Environ. Sci. Process Impacts* 21: 427–437.

Arst H., Erm A., Herlevi A., Kutser T., Leppäranta M., Reinart A. & Virta J. 2008. Optical properties of boreal lake waters in Finland and Estonia. *Boreal Environ. Res.* 13: 133–158.

Ask J., Karlsson J. & Jansson M. 2012. Net ecosystem production in clear-water and brown-water lakes. *Global Biogeochem. Cy.* 26, GB1017.

Banse K. 2004. Should we continue to use the 1% light depth convention for estimating the compensation depth of phytoplankton for another 70 years? *Limnol. Oceanogr. Bull.* 13: 49–52.

Behrenfeld M.J., O'Malley R.T., Siegel D.A., McClain C.R., Sarmiento J.L., Feldman G.C., Milligan A.J., Falkowski P.G., Letelier R.M. & Boss E.S. 2006. Climate-driven trends in contemporary ocean productivity. *Nature* 444: 752–755.

Belzile C., Vincent W.F. & Kumagai M. 2002. Contribution of absorption and scattering to the attenuation of UV and photosynthetically available radiation in Lake Biwa. *Limnol. Oceanogr.* 47: 95–107.

Benoy G., Cash K., McCauley E. & Wrona F. 2007. Carbon dynamics in lakes of the boreal forest under a changing climate. *Environ. Rev.* 15: 175–189.

Berger S.A., Diehl S., Kunz T.J., Albrecht D., Oucible A.M. & Ritzer S. 2006. Light supply, plankton biomass, and seston stoichiometry in a gradient of lake mixing depths. *Limnol. Oceanogr.* 51: 1898–1905.

Berger S.A., Diehl S., Stibor H., Trommer G., Ruhenstroth M., Wild A., Weigert A., Jäger C.G. & Striebel M. 2007. Water temperature and mixing depth affect timing and magnitude of events during spring succession of the plankton. *Oecologia* 150: 643–654.

Bergström A.K. & Karlsson J. 2019. Light and nutrient control phytoplankton biomass responses to global change in northern lakes. *Glob. Chang. Biol.* 25: 2021–2029.

Binding C.E., Jerome J.H., Bukata R.P. & Booty W.G. 2008. Spectral absorption properties of dissolved and particulate matter in Lake Erie. *Remote Sens. Environ.* 112: 1702–1711.

Boehrer B. & Schultze M. 2008. Stratification of lakes. *Rev. Geophys.* 46, RG2005.

Bricaud A., Morel A. & Prieur L. 1981. Absorption by dissolved organic matter of the sea (yellow substance) in the UV and visible domains. *Limnol. Oceanogr.* 26: 43–53.

BS EN 15204 2006. Water quality. Guidance standard on the enumeration of phytoplankton using inverted microscopy (Utermoehl technique).

Buiteveld H., Hakvoort J.H.M. & Donze M. 1994. The optical properties of pure water. *Ocean Optics XIII* 2258: 174–183.

Calderini M.L., Salmi P., Rigaud C., Peltomaa E. & Taipale S.J. 2022. Metabolic plasticity of mixotrophic algae is key for their persistence in browning environments. *Mol. Ecol.* 31: 4726–4738.

Camill P. 2005. Permafrost thaw accelerates in boreal peatlands during late-20th century climate warming. *Clim. Change.* 68: 135–152.

Cantin A., Beisner B.E., Gunn J.M., Prairie Y.T. & Winter J.G. 2011. Effects of thermocline deepening on lake plankton communities. *Can. J. Fish. Aquat. Sci.* 68: 260–276.

Caplanne S. & Laurion I. 2008. Effect of chromophoric dissolved organic matter on epilimnetic stratification in lakes. *Aquat. Sci.* 70: 123–133.

Chambers P.A. & Kalff J. 1985. Depth distribution and biomass of submersed aquatic macrophyte communities in relation to secchi depth. *Can. J. Fish. Aquat. Sci.* 42: 701–709.

Choudhury N.K. & Behera R.K. 2001. Photoinhibition of photosynthesis: Role of carotenoids in photoprotection of chloroplast constituents. *Photosynthetica* 39: 481–488.

Cloern J.E. 1987. Turbidity as a control on phytoplankton biomass and productivity in estuaries. *Cont. Shelf. Res.* 7: 1367–1381.

Corman J.R., Bertolet B.L., Casson N.J., Sebestyen S.D., Kolka R.K. & Stanley E.H. 2018. Nitrogen and phosphorus loads to temperate seepage lakes associated with allochthonous dissolved organic carbon loads. *Geophys. Res. Lett.* 45: 5481–5490.

Cornec M., Laxenaire R., Speich S. & Claustre H. 2021. Impact of mesoscale eddies on deep chlorophyll maxima. *Geophys. Res. Lett.* 48, e2021GL093470.

Coumou D. & Rahmstorf S. 2012. A decade of weather extremes. *Nat. Clim. Chang.* 2: 491–496.

Creed I.F., Bergström A.K., Trick C.G., Grimm N.B., Hessen D.O., Karlsson J., … Weyhenmeyer G.A. 2018. Global change-driven effects on dissolved organic matter composition: Implications for food webs of northern lakes. *Glob. Chang. Biol.* 24: 3692–3714.

Croce R. & Van Amerongen H. 2014. Natural strategies for photosynthetic light harvesting. *Nat. Chem. Biol.* 10: 492–501.

Davies-Colley R.J. 1983. Optical properties and reflectance spectra of 3 shallow lakes obtained from a spectrophotometric study. *New Zeal. J. Mar. Fresh.* 17: 445–459.

de Wit H.A., Valinia S., Weyhenmeyer G.A., Futter M.N., Kortelainen P., Austnes K., Hessen D.O., Räike A., Laudon H. & Vuorenmaa J. 2016. Current browning of surface waters will Be further promoted by wetter climate. *Environ. Sci. Technol. Let.* 3: 430–435.

Del Vecchio R. & Blough N. V. 2002. Photobleaching of chromophoric dissolved organic matter in natural waters: Kinetics and modeling. *Mar. Chem.* 78: 231–253.

DeLuca T.H. & Boisvenue C. 2012. Boreal forest soil carbon: Distribution, function and modelling. *Forestry* 85: 161–184.

Deng K., Azorin-Molina C., Minola L., Zhang G. & Chen D. 2021. Global near-surface wind speed changes over the last decades revealed by reanalyses and CMIP6 model simulations. *J. Clim.* 34: 2219–2234.

Di Toro D.M. 1978. Optics of turbid estuarine waters: approximations and applications. *Water. Res.* 12: 1059–1068.

Diehl S. 2002. Phytoplankton, light, and nutrients in a gradient of mixing depths: theory. *Ecology* 83: 386–398.

Diehl S., Berger S., Ptacnik R. & Wild A. 2002. Phytoplankton, light, and nutrients in a gradient of mixing depths: Field experiments. *Ecology* 83: 399–411.

Dimier C., Brunet C., Geider R. & Raven J. 2009. Growth and photoregulation dynamics of the picoeukaryote Pelagomonas calceolata in fluctuating light. *Limnol. Oceanogr.* 54: 823–836.

Dokulil M.T., de Eyto E., Maberly S.C., May L., Weyhenmeyer G.A. & Woolway R.I. 2021. Increasing maximum lake surface temperature under climate change. *Clim. Change* 165: 1–17.

Donis D., Mantzouki E., McGinnis D.F., Vachon D., Gallego I., Grossart H., … Ibelings B. 2021. Stratification strength and light climate explain variation in chlorophyll a at the continental scale in a European multilake survey in a heatwave summer. *Limnol. Oceanogr.* 66: 4314-4333.

Dubinsky Z. & Stambler N. 2009. Photoacclimation processes in phytoplankton: Mechanisms, consequences, and applications. *Aquat. Microb. Ecol.* 56: 163–176.

Einola E., Rantakari M., Kankaala P., Kortelainen P., Ojala A., Pajunen H., Mäkelä S. & Arvola L. 2011. Carbon pools and fluxes in a chain of five boreal lakes: A dry and wet year comparison. *J. Geophys. Res. Biogeosci.* 116, G03009.

Eloranta P. 1978. Light penetration in different types of lakes in Central Finland. *Holarctic Ecology* 1: 362–366.

Evans C.D., Monteith D.T. & Cooper D.M. 2005. Long-term increases in surface water dissolved organic carbon: Observations, possible causes and environmental impacts. *Environ. Pollut.* 137: 55–71.

Evans C.D., Chapman P.J., Clark J.M., Monteith D.T. & Cresser M.S. 2006. Alternative explanations for rising dissolved organic carbon export from organic soils. *Glob. Chang. Biol.* 12: 2044–2053.

Falkowski P.G. 1994. The role of phytoplankton photosynthesis in global biogeochemical cycles. *Photosynth. Res.* 39: 235–258.

Falkowski P.G. & LaRoche J. 1991. Acclimation to spectral irradiance in algae. *J. Phycol.* 27: 8–14.

Falkowski P.G. & Raven J.A. 2014. *Aquatic photosynthesis.* Princeton University Press. Princeton, New Jersey.

Fee E.J., Hecky R.E., Kasian S.E.M. & Cruikshank D.R. 1996. Effects of lake size, water clarity, and climatic variability on mixing depths in Canadian Shield lakes. *Limnol. Oceanogr.* 41: 912–920.

Fennel K. & Boss E. 2003. Subsurface maxima of phytoplankton and chlorophyll: Steady-state solutions from a simple model. *Limnol. Oceanogr.* 48: 1521–1534.

Field C.B., Behrenfeld M.J., Randerson J.T. & Falkowski P. 1998. Primary production of the biosphere: Integrating terrestrial and oceanic components. *Science* 281: 237–240.

Findlay D.L., Kasian S.E.M., Stainton M.P., Beaty K. & Lyng M. 2001. Climatic influences on algal populations of boreal forest lakes in the Experimental Lakes Area. *Limnol. Oceanogr.* 46: 1784–1793.

Finér L., Lepistö A., Karlsson K., Räike A., Härkönen L., Huttunen M., … Ukonmaanaho L. 2021. Drainage for forestry increases N, P and TOC export to boreal surface waters. *Sci. Tot. Environ.* 762, 144098.

Giling D.P., Nejstgaard J.C., Berger S.A., Grossart H.P., Kirillin G., Penske A., Lentz M., Casper P., Sareyka J. & Gessner M.O. 2017. Thermocline deepening boosts ecosystem metabolism: evidence from a large-scale lake enclosure experiment simulating a summer storm. *Glob. Chang. Biol.* 23: 1448–1462.

Godwin S.C., Jones S.E., Weidel B.C. & Solomon C.T. 2014. Dissolved organic carbon concentration controls benthic primary production: Results from in situ chambers in north-temperate lakes. *Limnol. Oceanogr.* 59: 2112–2120.

Gray E., Elliott J.A., Mackay E.B., Folkard A.M., Keenan P.O. & Jones I.D. 2019. Modelling lake cyanobacterial blooms: Disentangling the climate-driven impacts of changing mixed depth and water temperature. *Freshw. Biol.* 64: 2141–2155.

Grossman A.R., Schaefer M.R., Chiang G.G. & Collier J.L. 1993. The phycobilisome, a light-harvesting complex responsive to environmental conditions. *Microbiol Rev.* 57: 725–749.

Hamdan M., Byström P., Hotchkiss E.R., Al-Haidarey M.J. & Karlsson J. 2021. An experimental test of climate change effects in northern lakes: Increasing allochthonous organic matter and warming alters autumn primary production. *Freshw. Biol.* 66: 815–825.

Hansson T.H., Grossart H.P., del Giorgio P.A., St-Gelais N.F. & Beisner B.E. 2019. Environmental drivers of mixotrophs in boreal lakes. *Limnol. Oceanogr.* 64: 1688–1705.

Heiskanen J.J., Mammarella I., Ojala A., Stepanenko V., Järvinen H., Vesala T. & Nordbo A. 2015. Effects of water clarity on lake stratification and lake-atmosphere heat exchange. *J. Geophys. Res. Atmos.* 120: 7412–7428.

Holtrop T., Huisman J., Stomp M., Biersteker L., Aerts J., Grébert T., Partensky F., Garczarek L. & van der Woerd H. 2021. Vibrational modes of water predict spectral niches for photosynthesis in lakes and oceans. *Nat. Ecol. Evol.* 5: 55–66.

Horppila J., Keskinen S., Nurmesniemi M., Nurminen L., Pippingsköld E., Rajala S., Sainio K. & Estlander S. 2023. Factors behind the threshold-like changes

in lake ecosystems along a water colour gradient: The effects of dissolved organic carbon and iron on euphotic depth, mixing depth and phytoplankton biomass. *Freshw. Biol.* 68: 1031-1040.

Huisman J., Van Oostveen P. & Weissing F.J. 1999. Critical depth and critical turbulence: Two different mechanisms for the development of phytoplankton blooms. *Limnol. Oceanogr.* 44: 1781–1787.

Huisman J., Sharples J., Stroom J.M., Visser P.M., Kardinaal W.E.A., Verspagen J.M.H. & Sommeijer B. 2004. Changes in turbulent mixing shift competition for light between phytoplankton species. *Ecology* 85: 2960–2970.

Hutchinson G.E. & Löffler H. 1956. The thermal classification of lakes. *Proc. Natl. Acad. Sci. U.S.A.* 42: 84–86.

Ilvesniemi H., Levula J., Ojansuu R., Kolari P., Kulmala L., Pumpanen J., Launiainen S., Vesala T. & Nikinmaa E. 2009. Long-term measurements of the carbon balance of a boreal Scots pine dominated forest ecosystem. *Boreal Environ. Res.* 14: 731–753.

Imberger J. 1985. The diurnal mixed layer. *Limnol. Oceanogr.* 30: 737–770.

Imberger J. & Parker G. 1985. Mixed layer dynamics in a lake exposed to a spatially variable wind field. *Limnol. Oceanogr.* 30: 473–488.

Imboden D.M. & Wuest A. 1995. Mixing mechanisms in lakes. In: A. Lerman, D.M. Imboden & J.R. Gat (Eds.), *Physics and chemistry of lakes*, Springer-Verlag. Berlin, Germany. pp. 83–138.

Neeley A.R. & Mannino A. (Eds.) 2018. *Inherent Optical Property Measurements and Protocols: Absorption Coefficient.* IOCCG Protocol Series, Darthmouth, NS, Canada.

IPCC 2021. *Climate change 2021: The physical science basis.* Contribution of working group I to the sixth assessment report of the intergovernmental panel on climate change. Cambridge University Press. UK.

Jansson M., Berggren M., Laudon H. & Jonsson A. 2012. Bioavailable phosphorus in humic headwater streams in boreal Sweden. *Limnol. Oceanogr.* 57: 1161–1170.

Jentsch A., Kreyling J. & Beierkuhnlein C. 2007. A new generation of climate-change experiments: Events, not trends. *Front. Ecol. Environ.* 5: 365–374.

Jöhnk K.D., Huisman J., Sharples J., Sommeijer B., Visser P.M. & Stroom J.M. 2008. Summer heatwaves promote blooms of harmful cyanobacteria. *Glob. Chang. Biol.* 14: 495–512.

Jones R.I. 2000. Mixotrophy in planktonic protists: An overview. *Freshw. Biol.* 45: 219–226.

Kallio K. 2006. Optical properties of Finnish lakes estimated with simple bio-optical models and water quality monitoring data. *Nord. Hydrol.* 37: 183–204.

Karlsson J. & Byström P. 2005. Littoral energy mobilization dominates energy supply for top consumers in subarctic lakes. *Limnol. Oceanogr.* 50: 538–543.

Karlsson J., Byström P., Ask J., Ask P., Persson L. & Jansson M. 2009. Light limitation of nutrient-poor lake ecosystems. *Nature* 460: 506–509.

Kelly P.T., Solomon C.T., Zwart J.A. & Jones S.E. 2018. A framework for understanding variation in pelagic gross primary production of lake ecosystems. *Ecosystems* 21: 1364–1376.

Kirillin G. & Shatwell T. 2016. Generalized scaling of seasonal thermal stratification in lakes. *Earth Sci. Rev.* 161: 179–190.

Kirk J.T.O. 1977. Attenuation of light in natural waters. *Aust. J. Mar. Fresh. Res.* 28: 497–508.

Kirk J.T.O. 1981a. Monte Carlo study of the nature of the underwater light field in, and the relationships between optical properties of, turbid yellow waters. *Aust. J. Mar. Fresh. Res.* 32: 517–549.

Kirk J.T.O. 1981b. Estimation of the scattering coefficient of natural waters using underwater irradiance measurements. *Aust. J. Mar. Fresh. Res.* 32: 533–542.

Kirk J.T.O. 1984. Dependence of relationship between inherent and apparent optical properties of water on solar altitude. *Limnol. Oceanogr.* 29: 350–356.

Kirk J.T.O. 2011. *Light and Photosynthesis in Aquatic Ecosystems*. Cambridge University Press, Cambridge, England.

Kivinen S., Rasmus S., Jylhä K. & Laapas M. 2017. Long-term climate trends and extreme events in northern Fennoscandia (1914-2013). *Climate* 5, cli5010016.

Kortelainen P. 1993. Content of total organic carbon in Finnish lakes and its relationship to catchment characteristics. *Can. J. Fish. Aquat. Sci.* 50: 1477–1483.

Kortelainen P. & Saukkonen S. 1998. Leaching of nutrients, organic carbon and iron from Finnish forestry land. *Water Air Soil Poll.* 105: 239–250.

Kraemer B.M., Mehner T. & Adrian R. 2017. Reconciling the opposing effects of warming on phytoplankton biomass in 188 large lakes. *Sci. Rep.* 7: 1–7.

Kritzberg E.S. 2017. Centennial-long trends of lake browning show major effect of afforestation. *Limmol. Oceanogr. Lett.* 2: 105–112.

Kritzberg E.S. & Ekström S.M. 2012. Increasing iron concentrations in surface waters - A factor behind brownification? *Biogeosciences* 9: 1465–1478.

Kutser T., Pierson D.C., Kallio K.Y., Reinart A. & Sobek S. 2005. Mapping lake CDOM by satellite remote sensing. *Remote Sens. Environ.* 94: 535–540.

Lenard T. & Ejankowski W. 2017. Natural water brownification as a shift in the phytoplankton community in a deep hard water lake. *Hydrobiologia* 787: 153–166.

Lepistö A., Räike A., Sallantaus T. & Finér L. 2021. Increases in organic carbon and nitrogen concentrations in boreal forested catchments — Changes driven by climate and deposition. *Sci. Tot. Environ.* 780, 146627.

Lepori F., Roberts J.J. & Schmidt T.S. 2018. A paradox of warming in a deep peri-Alpine lake (Lake Lugano, Switzerland and Italy). *Hydrobiologia* 824: 215–228.

Litchman E. & Klausmeier C.A. 2008. Trait-based community ecology of phytoplankton. *Ann. Rev. Ecol. Evol. S.* 39: 615–639.

Litchman E., Klausmeier C.A., Schofield O.M. & Falkowski P.G. 2007. The role of functional traits and trade-offs in structuring phytoplankton communities: Scaling from cellular to ecosystem level. *Ecol. Lett.* 10: 1170–1181.

Livingstone D.M. 2003. Thermal Structure of a Large Temperate Central European Lake. *Clim. Change* 57: 205–225.

MacIntyre S. 1993. Vertical mixing in a shallow, eutrophic lake: Possible consequences for the light climate of phytoplankton. *Limnol. Oceanogr.* 38: 798–817.

Magee M.R. & Wu C.H. 2017. Response of water temperatures and stratification to changing climate in three lakes with different morphometry. *Hydrol. Earth Syst. Sci.* 21: 6253–6274.

Majasalmi T., Rautiainen M. & Stenberg P. 2014. Modeled and measured fPAR in a boreal forest: Validation and application of a new model. *Agric. For. Meteorol.* 189–190: 118–124.

Marzetz V., Spijkerman E., Striebel M. & Wacker A. 2020. Phytoplankton community responses to interactions between light Intensity, light variations, and phosphorus supply. *Front. Environ. Sci.* 8, 539733.

Mcfarland W.N. 1986. Light in the Sea - Correlations with behaviors of fishes and invertebrates. *Am. Zool.* 26: 389–401.

Meili M. 1992. Sources, concentrations and characteristics of organic matter in softwater lakes and streams of the Swedish forest region. *Hydrobiologia* 229: 23–41.

Mesman J.P., Stelzer J.A.A., Dakos V., Goyette S., Jones I.D., Kasparian J., McGinnis D.F. & Ibelings B.W. 2021. The role of internal feedbacks in shifting deep lake mixing regimes under a warming climate. *Freshw. Biol.* 66: 1021–1035.

Mesman J.P., Ayala A.I., Goyette S., Kasparian J., Marcé R., Markensten H., Stelzer J.A.A., Thayne M.W., Thomas M.K., Pierson D.C. & Ibelings B.W. 2022. Drivers of phytoplankton responses to summer wind events in a stratified lake: A modeling study. *Limnol. Oceanogr.* 67: 85–873.

Minor E.C., Austin J.A., Sun L., Gauer L., Zimmerman R.C. & Mopper K. 2016. Mixing effects on light exposure in a large-lake epilimnion: A preliminary dual-dye study. *Limnol. Oceanogr. Methods* 14: 542–554.

Mishra R.K., Jena B., Venkataramana V., Sreerag A., Soares M.A. & AnilKumar N. 2022. Decadal changes in global phytoplankton compositions influenced by biogeochemical variables. *Environ. Res.* 206, 112546.

Modenutti B.E., Balseiro E.G., Callieri C. & Bertoni R. 2008. Light versus food supply as factors modulating niche partitioning in two pelagic mixotrophic ciliates. *Limnol. Oceanogr.* 53: 446–455.

Monismith S.G. & MacIntyre S. 2009. The surface mixed layer in lakes and reservoirs. In: Likens G.E. (Ed.), *Encyclopedia of Inland Waters*, Elsevier/Academic Press. Oxford, UK. pp. 636–650.

Monteith D.T., Stoddard J.L., Evans C.D., de Wit H.A., Forsius M., Høgåsen T., Wilander A., Skjelkvåle B.L., Jeffries D.S. & Vuorenmaa J. 2007. Dissolved organic carbon trends resulting from changes in atmospheric deposition chemistry. *Nature* 450: 537–540.

Morel A. 1978. Available, usable, and stored radiant energy in relation to marine photosynthesis. *Deep-Sea Res.* 25: 673–688.

Morris D.P., Zagarese H., Williamson C.E., Balseiro E.G., Hargreaves B.R., Modenutti B., Moeller R. & Quelimalinos C. 1995. The attenuation of solar

UV radiation in lakes and the role of dissolved organic carbon. *Limnol Oceanogr* 40: 1381–1391.

Moss B. 2012. Cogs in the endless machine: Lakes, climate change and nutrient cycles: A review. *Sci. Tot. Environ.* 434: 130–142.

Moss B., Hering D., Green A.J., Aidoud A., Becares E., Beklioglu M., … Weyhenmeyer G.A. 2009. Climate change and the future of freshwater biodiversity in Europe: a primer for policy-makers. *Freshwater Reviews* 2: 103–130.

Murray C., Markager S., Stedmon C.A., Juul-Pedersen T., Sejr M.K. & Bruhn A. 2015. The influence of glacial melt water on bio-optical properties in two contrasting Greenlandic fjords. *Estuar. Coast. Shelf Sci.* 163: 72–83.

Nieminen M., Koskinen M., Sarkkola S., Laurén A., Kaila A., Kiikkilä O., Nieminen T.M. & Ukonmaanaho L. 2015. Dissolved organic carbon export from harvested peatland forests with differing site characteristics. *Water Air Soil Pollut.* 226, 181.

Pace M.L., Reche I., Cole J.J., Fernández-Barbero A., Mazuecos I.P. & Prairie Y.T. 2012. pH change induces shifts in the size and light absorption of dissolved organic matter. *Biogeochemistry* 108: 109–118.

Pérez G.I., Queimalinõs C.P. & Modenutti B.E. 2002. Light climate and plankton in the deep chlorophyll maxima in North Patagonian Andean lakes. *J. Plankton Res.* 24: 591–599.

Pérez G.I., Queimaliños C., Balseiro E. & Modenutti B. 2007. Phytoplankton absorption spectra along the water column in deep North Patagonian Andean lakes (Argentina). *Limnologica* 37: 3–16.

Perkins-Kirkpatrick S.E. & Lewis S.C. 2020. Increasing trends in regional heatwaves. *Nat. Commun.* 11: 1–8.

Persson I. & Jones I.D. 2008. The effect of water colour on lake hydrodynamics: A modelling study. *Freshw. Biol.* 53: 2345–2355.

Prowse T.D., Furgal C., Wrona F.J. & Reist J.D. 2009. Implications of Climate Change for Northern Canada: Freshwater, Marine, and Terrestrial Ecosystems. *Ambio* 38: 282–289.

Ptacnik R., Diehl S. & Berger S. 2003. Performance of sinking and nonsinking phytoplankton taxa in a gradient of mixing depths. *Limnol. Oceanogr.* 48: 1903–1912.

Räike A., Kortelainen P., Mattsson T. & Thomas D.N. 2016. Long-term trends (1975–2014) in the concentrations and export of carbon from Finnish rivers to the Baltic Sea: organic and inorganic components compared. *Aquat. Sci.* 78: 505–523.

Reinart A., Arst H., Nõges P. & Nõges T. 2000. Comparison of euphotic layer criteria in lakes. *Geophysica* 36: 141–159.

Richardson K., Beardall J. & Raven J.A. 1983. Adaptation of unicellular algae to irradiance: An analysis of strategies. *New Phytol.* 93: 157–191.

Rivera Vasconcelos F., Diehl S., Rodríguez P., Karlsson J., Byström P. & Hedström P. 2016. Asymmetrical competition between aquatic primary producers in a warmer and browner world. *Ecology* 97: 2580–2592.

54

Schwaderer A.S., Yoshiyama K., De Tezanos Pinto P., Swenson N.G., Klausmeier C.A. & Litchman E. 2011. Eco-evolutionary differences in light utilization traits and distributions of freshwater phytoplankton. *Limnol. Oceanogr.* 56: 589–598.

Seekell D.A., Lapierre J.-F. & Karlsson J. 2015. Trade-offs between light and nutrient availability across gradients of dissolved organic carbon concentration in Swedish lakes: implications for patterns in primary production. *Canadian Journal of Fisheries and Aquat. Sci.* 72: 1663–1671.

SFS-EN ISO 11905-1. 1997. *Water quality. Determination of nitrogen.* Part 1: Method using oxidative digestion with peroxodisulfate. International Organization for Standardization.

SFS-EN ISO 10260. 1992. *Water quality – Measurement of biochemical parameters – Spectrometric determination of the chlorophyll-a concentration.* International Organization for Standardization.

SFS-EN ISO 7887. 2011. *Water quality. In Examination and determination of colour.* International Organization for Standardization.

SFS-EN ISO 15681-2 2018. Water quality. *Determination of orthophosphate and total phosphorus contents by flow analysis (FIA and CFA).* Part 2: Method by continuous flow analysis (CFA). International Organization for Standardization.

Shatwell T., Thiery W. & Kirillin G. 2019. Future projections of temperature and mixing regime of European temperate lakes. *Hydrol. Earth Syst. Sci.* 23: 1533–1551.

Sherbo B.A.H., Tonin J., Paterson M.J., Hann B.J., Kozak J. & Higgins S.N. 2023. The effects of terrestrial dissolved organic matter on phytoplankton biomass and productivity in boreal lakes. *Freshw. Biol.* 68: 2109–2119.

Siemer J.P., Machin F., González-Vega A., Arrieta J.M., Gutiérrez-Guerra M.A., Pérez-Hernández M.D., Vélez-Belchí P., Hernández-Guerra A. & Fraile-Nuez E. 2021. Recent trends in SST, Chl-a, productivity and wind stress in upwelling and open ocean areas in the upper Eastern North Atlantic subtropical gyre. *J. Geophys. Res. Oceans* 126, e2021JC017268.

Škerlep M., Steiner E., Axelsson A.L. & Kritzberg E.S. 2020. Afforestation driving long-term surface water browning. *Glob. Chang. Biol.* 26: 1390–1399.

Smith R.C., Marra J., Perry M.J., Baker K.S., Swift E., Buskey E., & Kiefer D.A. 1989. Estimation of a photon budget for the upper ocean in the Sargasso Sea. *Limnol. Oceanogr.* 34: 1673–1693.

Snucins E. & Gunn J. 2000. Interannual variation in the thermal structure of clear and colored lakes. *Limnol. Oceanogr.* 45: 1639–1646.

Solomon C.T., Jones S.E., Weidel B.C., Buffam I., Fork M.L., Karlsson J., Larsen S., Lennon J.T., Read J.S., Sadro S. & Saros J.E. 2015. Ecosystem consequences of changing inputs of terrestrial dissolved organic matter to lakes: current knowledge and future challenges. *Ecosystems* 18: 376–389.

Sommer U., Gliwicz M.Z., Lampert W. & Duncan A. 1986. The PEG-model of seasonal succession of planktonic events in fresh waters. *Arch. Hydrobiol.* 106: 433–471.

Spigel R.H. & Imberger J. 1987. Mixing processes relevant to phytoplankton dynamics in lakes. *New Zeal. J. Mar. Fresh. Res.* 21: 361–377.

Stetler J.T., Knoll L.B., Driscoll C.T. & Rose K.C. 2021a. Lake browning generates a spatiotemporal mismatch between dissolved organic carbon and limiting nutrients. *Limnol. Oceanogr. Lett.*, 6: 182–191.

Stetler J.T., Girdner S., Mack J., Winslow L.A., Leach T.H. & Rose K.C. 2021b. Atmospheric stilling and warming air temperatures drive long-term changes in lake stratification in a large oligotrophic lake. *Limnol. Oceanogr.* 66: 954–964.

Stockwell J.D., Doubek J.P., Adrian R., Anneville O., Carey C.C., Carvalho L., … Wilson H.L. 2020. Storm impacts on phytoplankton community dynamics in lakes. *Glob. Chang. Biol.* 26: 2756–2784.

Stomp M., Huisman J., De Jongh F., Veraart A.J., Gerla D., Rijkeboer M., Ibelings B.W., Wollenzien U.I.A. & Stal L.J. 2004. Adaptive divergence in pigment composition promotes phytoplankton biodiversity. *Nature* 432: 104–107.

Stomp M., Huisman J., Stal L.J. & Matthijs H.C.P. 2007a. Colorful niches of phototrophic microorganisms shaped by vibrations of the water molecule. *ISME J.* 1: 271–282.

Stomp M., Huisman J., Vörös L., Pick F.R., Laamanen M., Haverkamp T. & Stal L.J. 2007b. Colourful coexistence of red and green picocyanobacteria in lakes and seas. *Ecol. Lett.* 10: 290–298.

Straile D., Jöhnk K. & Rossknecht H. 2003. Complex effects of winter warming on the physicochemical characteristics of a deep lake. *Limnol. Oceanogr.* 48: 1432–1438.

Strock K.E., Nelson S.J., Kahl J.S., Saros J.E. & McDowell W.H. 2014. Decadal trends reveal recent acceleration in the rate of recovery from acidification in the northeastern U.S. *Environ. Sci. Technol.* 48: 4681–4689.

Thrane J.-E., Hessen D.O. & Andersen T. 2014. The absorption of light in lakes: Negative impact of dissolved organic carbon on primary productivity. *Ecosystems* 17: 1040–1052.

Thrane J.E., Hessen D.O. & Andersen T. 2016. The impact of irradiance on optimal and cellular nitrogen to phosphorus ratios in phytoplankton. *Ecol. Lett.* 19: 880–888.

Tranvik L.J., Downing J.A., Cotner J.B., Loiselle S.A., Striegl R.G., Ballatore T.J., … Weyhenmeyer G.A. 2009. Lakes and reservoirs as regulators of carbon cycling and climate. *Limnol. Oceanogr.* 54: 2298–2314.

Utermöhl H. 1958. Methods of collecting plankton for various purposes are discussed. *Int. Ver. The.* 9: 1-38.

Vähätalo A. V., Salkinoja-Salonen M., Taalas P. & Salonen K. 2000. Spectrum of the quantum yield for photochemical mineralization of dissolved organic carbon in a humic lake. *Limnol. Oceanogr.* 45: 664–676.

Vähätalo A. V. & Wetzel R.G. 2004. Photochemical and microbial decomposition of chromophoric dissolved organic matter during long (months-years) exposures. *Mar. Chem.* 89: 313–326.

56

Wagner C. & Adrian R. 2011. Consequences of changes in thermal regime for plankton diversity and trait composition in a polymictic lake: A matter of temporal scale. *Freshw. Biol.* 56: 1949–1961.

Wang F. & Chen M. 2022. Chromatic acclimation processes and their relationships with phycobiliprotein complexes. *Microorganisms* 10, 1562.

Wasmund N., Nausch G., Gerth M., Busch S., Burmeister C., Hansen R. & Sadkowiak B. 2019. Extension of the growing season of phytoplankton in the western Baltic Sea in response to climate change. *Mar. Ecol. Prog. Ser.* 622: 1–16.

Watanabe S., Laurion I., Markager S. & Vincent W.F. 2015. Abiotic control of underwater light in a drinking water reservoir: Photon budget analysis and implications for water quality monitoring. *Water Resour. Res.* 51: 6290–6310.

Weithoff G., Lorke A. & Walz N. 2000. Effects of water-column mixing on bacteria, phytoplankton, and rotifers under different levels of herbivory in a shallow eutrophic lake. *Oecologia* 125: 91–100.

Weyhenmeyer G.A., Prairie Y.T. & Tranvik L.J. 2014. Browning of boreal freshwaters coupled to carbon-iron interactions along the aquatic continuum. *PLoS One* 9, e88104.

Winder M. & Cloern J.E. 2010. The annual cycles of phytoplankton biomass. *Philos. T. R. Soc. B.* 365: 3215–3226.

Winder M. & Sommer U. 2012. Phytoplankton response to a changing climate. *Hydrobiologia* 698: 5–16.

Woolway R.I. & Merchant C.J. 2019. Worldwide alteration of lake mixing regimes in response to climate change. *Nat. Geosci.* 12: 271–276.

Woolway R.I., Meinson P., Nõges P., Jones I.D. & Laas A. 2017. Atmospheric stilling leads to prolonged thermal stratification in a large shallow polymictic lake. *Clim Change* 141: 759–773.

Woolway R.I., Sharma S., Weyhenmeyer G.A., Debolskiy A., Golub M., Mercado-Bettín D., … Jennings E. 2021a. Phenological shifts in lake stratification under climate change. *Nat. Commun.* 12: 1–11.

Woolway R.I., Jennings E., Shatwell T., Golub M., Pierson D.C. & Maberly S.C. 2021b. Lake heatwaves under climate change. *Nature* 589: 402–407.

Woolway R.I., Sharma S. & Smol J.P. 2022. Lakes in hot water: The impacts of a changing climate on aquatic ecosystems. *Bioscience* 72: 1050–1061.

Wrona F.J., Prowse T.D., Reist J.D., Hobbie J.E., Lévesque L.M.J. & Vincent W.F. 2006. Climate impacts on arctic freshwater ecosystems and fisheries: background, rationale and approach of the Arctic Climate Impact Assessment (ACIA). *Ambio* 35: 326–329.

Wu J., Lee Z., Xie Y., Goes J., Shang S., Marra J.F., Lin G., Yang L. & Huang B. 2021. Reconciling between optical and biological determinants of the euphotic zone depth. *J. Geophys. Res. Oceans* 126, e2020JC016874.

Xiao Y.H., Sara-Aho T., Hartikainen H. & Vähätalo A.V. 2013. Contribution of ferric iron to light absorption by chromophoric dissolved organic matter. *Limnol. Oceanogr.* 58: 653–662.

Xiao Z., Liang S., Sun R., Wang J. & Jiang B. 2015. Estimating the fraction of absorbed photosynthetically active radiation from the MODIS data based GLASS leaf area index product. *Remote Sens. Environ.* 171: 105–117.

Yang Y., Colom W., Pierson D. & Pettersson K. 2016. Water column stability and summer phytoplankton dynamics in a temperate lake (Lake Erken, Sweden). *Inland Waters* 6: 499–508.

Yang X., O'Reilly C.M., Gardner J.R., Ross M.R.V., Topp S.N., Wang J. & Pavelsky T.M. 2022. The Color of Earth's Lakes. *Geophys. Res. Let.* 49, e2022GL098925.

Ylöstalo P., Kallio K. & Seppälä J. 2014. Absorption properties of in-water constituents and their variation among various lake types in the boreal region. *Remote Sens. Environ.* 148: 190–205.

Yoshiyama K., Mellard J.P., Litchman E. & Klausmeier C.A. 2009. Phytoplankton competition for nutrients and light in a stratified water column. *Am. Nat.* 174: 190–203.

ORIGINAL PAPERS

I

PHYTOPLANKTON IN BOREAL LAKES
MAINLY ABSORB RED LIGHT

by

Salla A. Ahonen, Roger I. Jones, Jukka Seppälä, Kristiina M. Vuorio,
Marja Tiirola & Anssi V. Vähätalo

II

ASSESSING AND PREDICTING THE INFLUENCE OF CHROMOPHORIC DISSOLVED ORGANIC MATTER ON LIGHT ABSORPTION BY PHYTOPLANKTON IN BOREAL LAKES

by

Salla A. Ahonen, Kristiina M. Vuorio, Roger I. Jones, Heikki Hämäläinen, Krista Rantamo, Marja Tiirola & Anssi V. Vähätalo 2024

LIMNOLOGY and OCEANOGRAPHY

Assessing and predicting the influence of chromophoric dissolved organic matter on light absorption by phytoplankton in boreal lakes

Salla A. Ahonen [1*] **Kristiina M. Vuorio** [2] **Roger I. Jones** [1] **Heikki Hämäläinen** [1] **Krista Rantamo,** [1]
Marja Tiirola [1] **Anssi V. Vähätalo** [1]
[1]Department of Biological and Environmental Science, University of Jyväskylä, Jyväskylä, Finland
[2]Finnish Environment Institute, Helsinki, Finland

Abstract

Many boreal lakes are colored brown due to strong light absorption by chromophoric dissolved organic matter (CDOM), which reduces light penetration into the water column. However, the influence of CDOM on the fraction of photosynthetically utilizable radiation (PUR) absorbed by phytoplankton from the photosynthetically active radiation (PAR) entering the lake (i.e., PUR/PAR) remains largely unknown. Here, we (1) quantified PUR/PAR values and examined the major water quality parameters determining PUR/PAR from 128 sampled boreal lakes, (2) predicted PUR/PAR values for 2250 reference boreal lakes, and (3) estimated the response of PUR/PAR to typical browning trends reported in earlier studies. The PUR/PAR values ranged from 0.4% to 17% in the sampled lakes, and a logarithmic model including CDOM and chlorophyll *a* (Chl *a*) concentration was the most parsimonious for predicting PUR/PAR values. Applying the model to the reference lakes, PUR/PAR values ranged from 0.5% to 20% (median 3%). In the model, an increase in CDOM content decreases the PUR/PAR value, but a concurrent increase in Chl *a* concentration with the CDOM partly compensates the negative effect of CDOM on the PUR/PAR values. Assuming that browning increases both CDOM and Chl *a* contents, as found for our reference lakes, our model suggests that the decrease in light absorption by phytoplankton in response to a typical degree of browning is only moderate. The moderate response of the PUR/PAR to browning may be explained by photoacclimation of phytoplankton to lowered light availability, and/or an increased loading of nutrients to lakes both leading to higher Chl *a* concentration.

Chromophoric dissolved organic matter (CDOM) has optical properties which, along with those of suspended particulate matter and H_2O, determine the availability of light in aquatic environment (Kirk 2011). In many lakes, CDOM is the most important light-absorbing component, which stains water brown and reduces the depth of the euphotic zone (Jones and Arvola 1984; Kallio 2006; Thrane et al. 2014; Ylöstalo et al. 2014). When CDOM reduces the euphotic depth, it restricts the distribution of benthic primary producers and their

photosynthesis to shallow water (Chambers and Kalff 1985; Daniels et al. 2015). In lakes with high CDOM, reduced availability of light for benthic producers can decrease the overall primary as well as secondary production of the entire lake ecosystem (Karlsson et al. 2009; Ask et al. 2012). The impact of CDOM on the light availability for phytoplankton, which is largely responsible for pelagic photosynthesis, is less known but often considered negative (e.g., Karlsson et al. 2009; Thrane et al. 2014). Naumann (1929) categorized brown-colored lakes as dystrophic and concluded that production of phytoplankton is generally low in dystrophic lakes. Phytoplankton cannot capture those photons absorbed by CDOM, but turbulent mixing even in high-CDOM lakes transports phytoplankton to and from the well-lit surface layer and hence alleviates potential light limitation (e.g., Reynolds et al. 1990).

Lakes with high CDOM content have typically elevated concentrations of dissolved organic and inorganic nutrients, which are imported to lake water along with other allochthonous matter from the terrestrial catchment (Thrane et al. 2014; Hamdan et al. 2021; Lepistö et al. 2021). The CDOM content in lakes varies naturally by two orders of magnitude (e.g., between 0.6 and 74 m^{-1} in 3549 Finnish lakes) when quantified as the

absorption coefficient at the wavelength of 400 nm ($a_{CDOM}(400)$; Kallio 2006). In CDOM-rich lakes, the elevated concentration of nutrients has the potential to increase Chl *a* concentration and phytoplankton biomass, which can help to compensate for the reduced availability of light caused by CDOM (Bergström and Karlsson 2019; Sherbo et al. 2023). Due to this compensatory effect, the extent to which phytoplankton actually experiences reduced light availability in lakes with different CDOM contents remains poorly known.

In recent decades, the CDOM content of surface waters across the boreal zone has increased and made water darker and browner (Evans et al. 2006; Monteith et al. 2007; Kritzberg and Ekström 2012; de Wit et al. 2016). This browning is caused by increased inputs of dissolved organic and inorganic (iron) chromophores (i.e., CDOM) from the terrestrial catchments to surface waters (Xiao et al. 2013; Škerlep et al. 2020). Along with an increased loading of CDOM, browning is often monitored as an increase in dissolved (DOC) or total organic carbon (TOC) and water color (e.g., Tranvik 1990; Thrane et al. 2014; Ylöstalo et al. 2014), while the chromophoric content of DOC/TOC is variable (e.g., Siegel et al. 2002). In the past three decades, the increase in water color value or concentrations of DOC or TOC (i.e., browning) in lakes has been variable (from 8% to over 100%) but typically about 25% (Williamson et al. 2015; Räike et al. 2016; Kritzberg 2017; Lepistö et al. 2021). The increased inputs of allochthonous matter seen as browning are caused by several factors, such as (1) the recovery from anthropogenic acidification (Evans et al. 2006; Monteith et al. 2007; Strock et al. 2014), (2) climate change associated increases in air temperature and precipitation (de Wit et al. 2016; Lenard and Ejankowski 2017), and (3) intensifying land use and forestry practices (Kritzberg 2017; Škerlep et al. 2020; Finér et al. 2021; Nieminen et al. 2021). While the browning increases water color and can reduce light availability, the increased input of allochthonous matter also provides nutrients, which can promote phytoplankton biomass and thus help to compensate for the light limitation (Corman et al. 2018). As brown lakes are projected to become more common in the future (Yang et al. 2022), it will be useful to understand the effect of browning on the light availability to phytoplankton.

Light availability to phytoplankton can be evaluated from water samples by measuring the spectral absorption coefficient of phytoplankton pigments ($a_{phyto}(\lambda)$) over the range of photosynthetically available radiation (PAR) and comparing it to the corresponding values of non-algal particles ($a_{NAP}(\lambda)$), H_2O ($aH_2O(\lambda)$), and CDOM ($a_{CDOM}(\lambda)$) or the sum of all components ($a_{tot}(\lambda)$). The contribution of phytoplankton to the total absorption of PAR (a_{phyto}/a_{tot}) has been reported to vary from 12% to 39% in the Sargasso Sea (Smith et al. 1989) and 5–32% in Greenland fjords (Murray et al. 2015) to 2–28% in Scandinavian lakes (Thrane et al. 2014) and 3–10% in a Canadian reservoir (Watanabe et al. 2015). For the same sites, the fraction of PAR absorbed by CDOM was 0–13%, 6–18%, 37–76%, and 32–55%, respectively. The lower contributions of phytoplankton to light

absorption in freshwater systems compared to marine systems suggest that the higher content of CDOM in lakes than in seas can reduce light availability to phytoplankton (Kirk 2011).

Another way to evaluate the light availability involves the calculation of photosynthetically usable radiation (PUR_z; Morel 1978). PUR_z refers to the absorption of photons within PAR by phytoplankton and accounts for the spectral variability of both solar radiation and $a_{phyto}(\lambda)$ (Morel 1978). Morel (1978) introduced a term PUR_z for a specific depth *z* in the ocean, where the distribution of phytoplankton varies with depth and often includes a maximum below the mixed layer owing to high transparency of oceanic water (e.g., $a_{CDOM}(400)$ often < 0.03 m^{-1}). For the boreal lakes examined in this study, we approximated PUR over the entire water column. Our approximation of PUR assumes that PAR is absorbed within the epilimnion, where phytoplankton is homogenously mixed among the other absorbing components as shown for one of our study lakes (Ahonen et al. 2023). When PUR is divided by the PAR entering to the lake, the unitless ratio PUR/PAR quantifies the light availability as a fraction of PAR absorbed by phytoplankton. Our PUR/PAR ratio in lakes is also comparable to the fraction of absorbed PAR by the photosynthesizing tissue of the canopy in the forest next to lakes. For example, in needle-leaf forests characteristic of boreal catchments, the fraction of absorbed PAR is 40–80% and hence higher than in aquatic environments, where non-algal particles, H_2O and CDOM absorb a major fraction of PAR (Majasalmi et al. 2014; Xiao et al. 2015).

In this study, we examined the fraction of PAR absorbed by phytoplankton (PUR/PAR values) in boreal lakes along a gradient of CDOM. We hypothesized that in lakes with increasing CDOM, both decreased light availability due to increased CDOM and the compensation by increased nutrient availability would act on the PUR/PAR values. We sampled 128 boreal lakes along a CDOM gradient and quantified their PUR/PAR values. Competing models were applied to predict the PUR/PAR values with commonly measured water quality parameters in the sampled lakes. The most parsimonious model was used to estimate PUR/PAR values in 2250 reference lakes based on their water quality, focusing on typical boreal lakes, i.e., on 90% of the lakes from 5th to 95th percentile along the CDOM gradient. Finally, using the most parsimonious model, we estimated how browning changes PUR/PAR values in scenarios following possible browning trends (i.e., increase in CDOM content) reported in earlier studies (e.g., Williamson et al. 2015; Räike et al. 2016; Kritzberg 2017; Lepistö et al. 2021). Since PUR/PAR values are relatively time-consuming to determine directly, our models provide a convenient tool to estimate the PUR/PAR values for lakes using widely available water quality parameters.

Materials and methods
Study lakes and sampling
Our study used two lake datasets. The first consists of 128 mostly boreal and a few subarctic dimictic lakes in

Finland (Fig. 1) that were sampled for optical properties and water quality (hereafter referred to as sampled lakes). The lakes were sampled in 2014–2018 during the summer stratification period (May–August), when a significant part of the primary production in boreal dimictic lakes occurs. The sampling period excludes the period of spring turnover when the availability of nutrients can be high, and DOM is less important as a source of nutrients. Later in the summer, when inorganic nutrients have been consumed from the epilimnion, the organic nutrients associated to DOM (and CDOM) may become more important. Water samples were taken with a 30 or 50 cm long water sampler (Limnos Ltd, Finland) as a composite sample from the homogenous surface mixed layer into 1 L high density polyethylene bottles.

The second dataset consists of 2250 regularly monitored Finnish boreal dimictic lakes and data were retrieved from the open access Hertta database portal (Open data service) maintained by the Finnish Environment Institute (https://www.syke.fi/en-US/Open_information). These lakes were used as a reference dataset of boreal lakes (hereafter referred to as reference lakes). 28% of the sampled lakes are included in the reference lake dataset. The data for the reference lakes were restricted

to the same season (May–August) as for the sampled lakes and a mean value of each parameter was determined from the data reported between 2010 and 2022. The Hertta database was also the source for lake morphometry characteristics for both the sampled and reference lakes. The parameters gathered for the reference lakes included lake area and volume, mean and maximum depths, concentrations of total phosphorus (tot-P, μg L^{-1}), total nitrogen (tot-N, μg L^{-1}), and chlorophyll *a* (Chl *a*, μg L^{-1}), and water color value (mg Pt L^{-1}). DOC concentrations for the reference lakes were converted from color values with an equation DOC $= 0.0872$color$+ 3.55$ by Kortelainen (1993).

Water chemistry measurements

Samples for tot-P and tot-N were frozen ($-20°$C) and analyzed according to methods in standards ISO/DIS 15681–2 (2005) and SFS-EN ISO 11905-1 (1997) and measured with Gallery™ Plus Automated Photometric Analyzer (Thermo Fisher Scientific, USA). Samples for DOC (mg L^{-1}) were filtered through a polyethylene sulfone syringe filter (Sarstedt, nominal pore size 0.20 μm), stored in acid washed and precombusted glass vials at $+ 4°$C and in the dark. DOC concentration was measured according to high-temperature catalytic oxidation method with a total organic carbon analyzer (TOC-L, Shimadzu, Japan) calibrated with standard solutions of potassium hydrogen phthalate. Chl *a* samples were filtered onto glass fiber filters (Whatman GF/C nominal pore size 1.2 μm, diameter 47 mm) and the concentration (μg L^{-1}) was spectrophotometrically measured with a Shimadzu UV-1800 spectrophotometer (Shimadzu, Kyoto, Japan) after ethanol extraction at 75°C for 5 min (SFS-ISO 10260 1992). Water color (mg Pt L^{-1}) was estimated using an optical comparator (Hellige, Germany) for comparison with hexachloroplatinate reference disks (SFS-EN ISO 7887 2011). In those cases where the lake was sampled more than once, an average value was calculated for each water quality and optical property parameter. For $\sim$ 10% of the sampled lakes from which tot-P, tot-N, Chl *a*, and water color were not measured, the values were retrieved from the Hertta database as average values from the data collected in May–August between 2010 and 2022.

Absorption measurements

The water samples for optical properties were filtered through glass fiber filters (Whatman GF/F, nominal pore size 0.7 μm, diameter 25 mm). The filtrate was stored in a 50 mL centrifuge tube at $+ 4°$C and in the dark prior to determination of the spectral absorption coefficient of CDOM ($a_{\mathrm{CDOM}}(\lambda)$), which was made within 2 weeks of sampling. The values of $a_{\mathrm{CDOM}}(\lambda)$ (m^{-1}) were calculated as:

$$a_{\mathrm{CDOM}}(\lambda) = \ln(10)\frac{A_{\mathrm{CDOM}}(\lambda)}{L} \tag{1}$$

where L is the optical length of the cuvette (0.01 or 0.05 m), $A_{\mathrm{CDOM}}(\lambda)$ is the absorbance of lake water at wavelength λ (nm) corrected with a blank (Ultrapure water from Ultra Clear
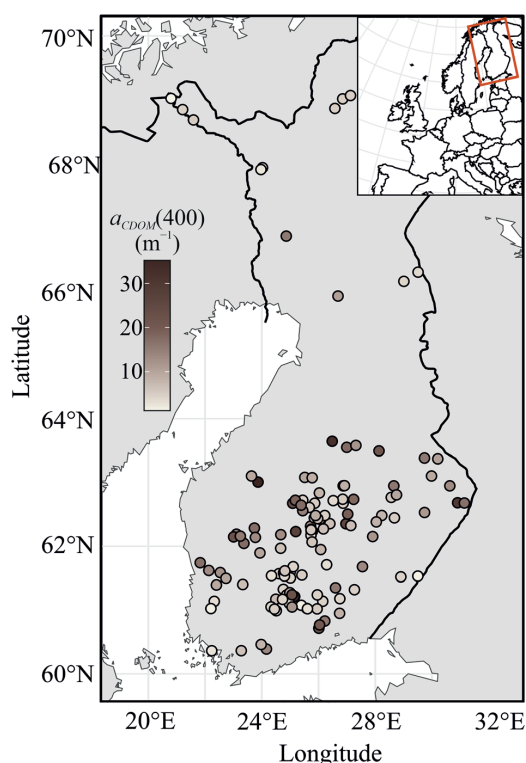
Fig. 1. A map showing the location of the 128 sampled lakes. The color scale indicates the value of $a_{\mathrm{CDOM}}(400)$.

UV UF TM system; Evoqua Water Technologies) and measured with a Shimadzu UV-1800 or PerkinElmer Lambda™ 650 UV/Vis spectrophotometer. The absorption coefficient of CDOM at wavelength of 400 nm ($a_{CDOM}(400)$) was selected to quantify the CDOM content of lake water, as has been done in previous studies (e.g., Kallio 2006; Thrane et al. 2014). The values of $a_{CDOM}(400)$ of the reference lakes were converted from water color values with an equation $a_{CDOM}(400) = 1.14 + 0.11 color$ (Supporting Information Fig. S1) derived from the sampled lakes.

The absorption coefficients of total particles ($a_p(\lambda)$) were determined from filters with particles according to "Measurement of filter pad absorption inside an integrating sphere"-method (IOCCG 2018). The filters were stored in separate petri dishes and kept frozen ($-80°C$) until the analyses of $a_p(\lambda)$. The storage time of the filters varied from a few weeks up to 5 years. The effect of storage time of filters on the absorption of particles was non-significant according to an assessment explained in Data S1. The filters with particles and the blank filters were water-saturated for the measurements of optical density inside a 150-mm integrating sphere connected to a PerkinElmer Lambda™ 650 UV/Vis spectrophotometer using 2-nm slits at 1 nm-intervals. The absorption coefficient of phytoplankton pigments ($a_{phyto}(\lambda)$) (m^{-1}) was calculated as the difference between $a_p(\lambda)$ and the absorption coefficient of non-algal particles ($a_{NAP}(\lambda)$; m^{-1}):

$$a_{phyto}(\lambda) = a_p(\lambda) - a_{NAP}(\lambda) \qquad (2)$$

The values of $a_{NAP}(\lambda)$ were determined like $a_p(\lambda)$ after extracting algal pigments from particles on filter with hot ethanol method (SFS 5772).

The spectral absorption coefficient for pure water ($aH_2O(\lambda)$) was derived from Neeley and Mannino (IOCCG, 2018) and interpolated to 1 nm spectral resolution with a spline function in Matlab. Total absorption coefficient spectrum was calculated as a sum of the absorption coefficients of CDOM, NAP, H$_2$O, and phytoplankton:

$$a_{tot}(\lambda) = a_{CDOM}(\lambda) + a_{NAP}(\lambda) + a_{phyto}(\lambda) + a_{H2O}(\lambda) \qquad (3)$$

Determination of PUR/PAR

The fraction of PUR absorbed by phytoplankton over the entire water column from the PAR entering the lake (i.e., PUR/PAR) was determined as:

$$\frac{PUR}{PAR} = \frac{\sum Q_{abs,phyto,z=0-\infty}(\lambda)}{\sum Q_{d,z=0-}(\lambda)} \qquad (4)$$

where $\sum Q_{abs,phyto,z=0-\infty}(\lambda)$ is the absorption of photons by phytoplankton in the whole water column (mol m^{-2} d^{-1} nm^{-1}) summed over the PAR spectrum (termed PUR) and $\sum Q_{d,z=0-}(\lambda)$ is the daily spectral downward photon flux density right below

the water surface (mol m^{-2} d^{-1} nm^{-1}) summed over the PAR spectrum (termed PAR). $Q_{d,z=0-}(\lambda)$ was the ASTM G173-03 irradiance reference spectrum (Apell and McNeill 2019; SMARTS 2020). The absorption of photons by phytoplankton over the whole water column was calculated as:

$$Q_{abs,phyto,z=0-\infty}(\lambda) = Q_{d,z=0-}(\lambda) \frac{a_{phyto}(\lambda)}{a_{tot}(\lambda)} \qquad (5)$$

The rationale and assumptions for the determination of PUR/PAR are explained in Data S1. Note that the determination of PUR/PAR is independent on the intensity of $Q_{d,z=0-}(\lambda)$.

Statistical methods

Statistical analyses were used for three purposes: (1) to assess the major water quality parameters affecting PUR/PAR in the sampled lakes, (2) to estimate the variability of PUR/PAR in the reference lakes based on their water quality, and (3) to estimate the impact of browning on PUR/PAR in a typical boreal lake.

We applied a regression analysis to examine the major determinants of PUR/PAR ratio in the sampled lakes along a CDOM-gradient. The dependency of the PUR/PAR value on $a_{CDOM}(400)$ and Chl a, tot-P, or tot-N concentrations was tested with competing logarithmic models (details in Data S1). We selected logarithmic models because the selected variables commonly display non-linear relationships (Nürnberg and Shaw 1998; Webster et al. 2008; Thrane et al. 2014). The eight competing models included explanatory variables separately, together, or through their interaction (Data S1). The most parsimonious model was selected based on the Akaike information criterion.

The most parsimonious model was applied to estimate PUR/PAR values in the 2250 reference lakes based on their water quality measures. To estimate a change in PUR/PAR values along a CDOM gradient in typical boreal lakes, we predicted PUR/PAR-values based on the average water quality at nine percentile bands of $a_{CDOM}(400)$: 5–15th, 15–25th, 25–35th, 35–45th, 45–55th, 55–65th, 65–75th, 75–85th, and 85–95th percentile, covering 90% of the reference lakes.

Finally, we estimated the response of PUR/PAR to browning expressed as an increase of $a_{CDOM}(400)$ value by 25%, 50%, 75% and 100%, which are examples of browning detected in the past decades and what could also happen in the future (Williamson et al. 2015; Räike et al. 2016; Kritzberg 2017; Lepistö et al. 2021). For the estimations, we selected a typical boreal lake according to a median value of $a_{CDOM}(400)$ in the reference lakes. The impact of browning was assessed as a typical development of PUR/PAR-values in the reference lakes described by the most parsimonious model. All statistical analyses and data processing were performed using R software (R Core Team 2022, version 4.2.1).

Table 1. Min, max, mean, and median values as well as 5th, 25th, 75th, and 95th percentiles of the lake morphometry and water quality among the 128 sampled lakes. Lakes are characterized by lake area (km^2), lake volume (million m^3, Mm^3), max and mean depths (m), concentrations of total nitrogen and phosphorus ($\mu g\ L^{-1}$), Chl a concentration ($\mu g\ L^{-1}$), color value (mg Pt L^{-1}), $a_{CDOM}(400)$ value (m^{-1}), and DOC concentration (mg L^{-1}).

Parameter	Min–max	Mean	Median	5th	25th	75th	95th
Lake area (km^2)	0.009–894	61	15.2	1.0	6.1	48	229
Lake vol (Mm^3)	2–12195	636	88	6	26	451	2201
Max depth (m)	2.3–94	31	25	6.0	12	44	85
Mean depth (m)	0.6–23	6.4	5.4	1.9	3.3	8.5	16
The tot-N ($\mu g\ L^{-1}$)	115–1503	560	519	290	416	630	1010
The tot-P ($\mu g\ L^{-1}$)	3–173	23	16	5	8	26	78
Chl a ($\mu g\ L^{-1}$)	1–77	11	7	2	4	14	34
$a_{CDOM}(400)$ (m^{-1})	1.2–35.2	9.7	6.9	2.2	4.5	13.3	24.7
Color (mg Pt L^{-1})	13–240	77	56	20	38	103	188
DOC (mg L^{-1})	1.8–24.4	10.5	10.1	4.9	8.3	12.5	17.0

Results

Water quality and morphometry of the study lakes

Regarding water quality, 90% of the 128 sampled lakes from 5th to 95th percentile covered tot-N range 290–1010 $\mu g\ L^{-1}$, tot-P range 5–78 $\mu g\ L^{-1}$, Chl a range 2–34 $\mu g\ L^{-1}$, and $a_{CDOM}(400)$ range 2–25 m^{-1} (Table 1; Fig. 1). In addition, DOC concentration ranged from 5 to 17 mg L^{-1} among 90% of the sampled lakes. In comparison, 90% of the 2250 reference lakes covered ranges in tot-N of 255–1032 $\mu g\ L^{-1}$, tot-P of 5–66 $\mu g\ L^{-1}$, Chl a of 2–40 $\mu g\ L^{-1}$, $a_{CDOM}(400)$ of 2–26 m^{-1}, and DOC of 5 to 22 mg L^{-1} (Table 2). Concerning lake morphometry, 90% of the sampled lakes represented ranges in lake area of 1–229 km^2, lake volume of 6–2200 million m^3 (Mm^3) and mean depth of 2–16 m (Table 1). Respectively, 90% of the reference lakes covered lake area range 0.4–30.8 km^2, lake volume range 0.9–287 Mm^3 and mean depth range 1–9 m (Table 2). Large lakes were overrepresented among the sampled lakes compared to the reference lakes. However, the water quality of the sampled lakes represented well that of the reference lakes, and hence boreal lakes in general.

Absorption of PAR in the sampled lakes

For each sampled lake, we determined the spectral absorption coefficient for CDOM, H_2O, non-algal particles and phytoplankton as illustrated for Lake Jyväsjärvi in Fig. 2a. Each absorption coefficient was divided by the total absorption coefficient as illustrated for a_{phyto}/a_{tot} in Fig. 2b. These ratios were multiplied with the spectral PAR entering the lake (Fig. 2c) to calculate the spectral PAR absorbed by each absorbing component in the entire water column, as illustrated for phytoplankton in Fig. 2d. Finally, the photons absorbed by each absorption component over the wavelength range 400–700 nm were divided by the PAR entering the lake for the fraction of PAR absorbed by each absorbing component like shown for phytoplankton as a

Table 2. Min, max, mean, and median values as well as 5th, 25th, 75th, and 95th percentiles of the lake morphometry and water quality among the 2250 reference boreal lakes. Lakes are characterized by lake area (km^2), lake volume (million m^3, Mm^3), max and mean depths (m), concentrations of total nitrogen and phosphorus ($\mu g\ L^{-1}$), Chl a concentration ($\mu g\ L^{-1}$), color value (mg Pt L^{-1}), $a_{CDOM}(400)$ value (m^{-1}), and DOC concentration (mg L^{-1}).

| Parameter	Min–max	Mean	Median	5th	25th	75th	95th
Lake area (km^2)	0.02–1377	10	1.5	0.4	0.8	4	31
Lake vol (Mm^3)	0.04–14822	98	6	0.9	3	21	287
Max depth (m)	0.7–94	16	12	2	7	21	42
Mean depth (m)	0.2–23	4	4	1	2	5	9
The tot-N ($\mu g\ L^{-1}$)	97–2725	542	477	255	369	642	1032
The tot-P ($\mu g\ L^{-1}$)	1–209	24	18	5	11	29	66
Chl a ($\mu g\ L^{-1}$)	0.5–310	14	8	2	5	16	40
Color (mg Pt L^{-1})	2–375	87	70	17	40	120	208
$a_{CDOM}(400)$ (m^{-1})	0.3–46.5	10.8	8.9	2.1	5.0	14.9	25.8
DOC (mg L^{-1})	3.7–36.3	11.1	9.7	5.0	7.1	14.0	21.7
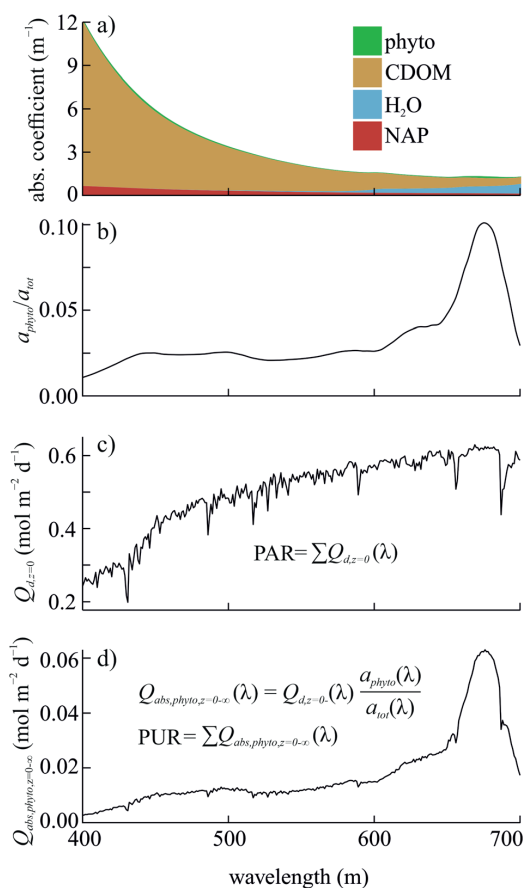
Fig. 2. A graphical visualization of determining PUR from the PAR in Lake Jyväsjärvi. Panel (**a**) shows the spectral absorption coefficients of phytoplankton, CDOM, H_2O, and NAP. Panel (**b**) shows the ratio of spectral absorption coefficients, phytoplankton ($a_{phyto}(\lambda)$) to the total absorption ($a_{tot}(\lambda)$). Panel (**c**) shows the spectral photon flux density of PAR just below the water surface. Panel (**d**) shows spectral PUR determined over the whole water column. The PUR summed over the wavelengths of 400–700 nm was used to calculate PUR/PAR (Eq. 4).

PUR/PAR ratio (Eq. 4). The fraction of PAR absorbed by phytoplankton over the whole water column (i.e., PUR/PAR) was 0.4–17% (median 3%) in the sampled lakes (Figs. 3, 4a). In most of the sampled lakes, CDOM was the largest absorbing component, absorbing 33–94% of the incident PAR (Fig. 3a). The fractions of PAR absorbed by non-algal particles and H_2O absorption were 1–40% and 3–43%, respectively (Fig. 3a).

The major water quality predictors of PUR/PAR in the sampled lakes

We used regression analyses to explore how the PUR/PAR values depended on CDOM and Chl *a*, tot-P or
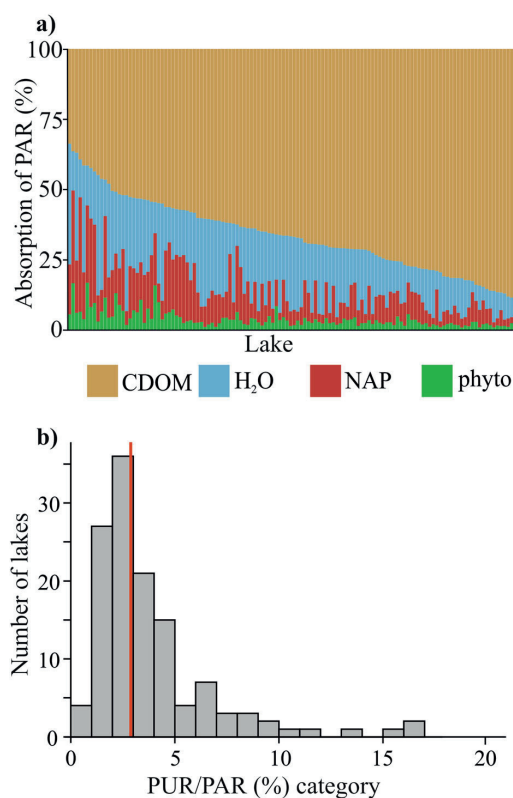
Fig. 3. The percentage of incoming PAR absorbed by (**a**) the four components and (**b**) phytoplankton in the 128 sampled lakes. In (a) the barplot shows the relative absorption of PAR by CDOM, H_2O, NAP, and phytoplankton (phyto, i.e., PUR/PAR) in each sampled lake. In (b) the histogram shows the variation in PUR/PAR values, with the vertical red line indicating the median value.

tot-N in competing logarithmic models (Supporting Information Tables S2–S4). Among the competing models, three models were equally good and each explained 52% of the variability in logarithmic PUR/PAR values: (1) a model including $a_{CDOM}(400)$ and Chl *a* as individual predictors (model 5 in Supporting Information Table S2; Fig. 4a,b); (2) a full model including $a_{CDOM}(400)$, Chl *a* and their interaction term (model 8 in Supporting Information Table S2); and (3) a model including tot-P and an interaction term of tot-P and $a_{CDOM}(400)$ (model 7 in Table S3; model equations in Data S1). In the three best models, the regression coefficient of $a_{CDOM}(400)$ was negative and the regression coefficient of Chl *a* or tot-P was positive (Supporting Information Table S2, S3). Model 8 (Supporting Information Table S2) had one non-significant parameter and thus was set aside. Among the two remaining, equally good models, model 5 (Supporting Information Table S2)

was selected for further examination due to its simpler structure compared to model 7 (Supporting Information Table S3).

Estimation of PUR/PAR values in the reference lakes

The model 5 (Supporting Information Table S2) was selected to predict PUR/PAR values in the reference lakes based on their $a_{CDOM}(400)$ and Chl *a* concentration (Supporting Information Table S2; Fig. 4a,b). The logarithmic model 5 was converted to a linear scale:

$$\frac{PUR}{PAR} = a_{CDOM}(400)^{-0.645} \times Chl\,a^{0.552} \times e^{-3.288} \quad (6)$$

and illustrated as surfaces in Fig. 4a,b. According to Eq. 6, the values of PUR/PAR varied from 0.5% to 20% with a median of 3% in the reference lakes (Fig. 5).

To estimate a typical range of PUR/PAR values in most boreal lakes, PUR/PAR values were calculated (Eq. 6) for the reference lakes based on their concentration of Chl *a* along a CDOM gradient from 5 to 15th and 85 to 95th percentile bands of $a_{CDOM}(400)$. Chl *a* concentration for each centered $a_{CDOM}(400)$ percentile band was determined based on a logarithmic dependence between the variables in the reference lakes (Chl $a = 1.80\,a_{CDOM}(400)^{0.75}$, adj. $R^2 = 0.29$; Fig. 4d; Supporting Information Fig. S2). The PUR/PAR value was on average 3.8% for the 5–15th percentile band of $a_{CDOM}(400)$ centered at $3.8\,m^{-1}$ and decreased to on average 2.5% for the 85–95th percentile band of $a_{CDOM}(400)$ centered at $20\,m^{-1}$ (Fig. 4b,c; Supporting Information Table S5). Along the same gradient, the mean concentration of Chl *a* more than tripled, as the values increased from 5 to $17\,\mu g\,L^{-1}$ (Supporting Information Table S5; Fig. S2; Fig. 4b,d). Both total nitrogen and phosphorus concentrations increased with CDOM content in the reference lakes (Supporting Information Fig. S3). In addition, an increase in the CDOM content decreased PUR/PAR values more in low-CDOM than in high-CDOM lakes (Fig. 4a–c).
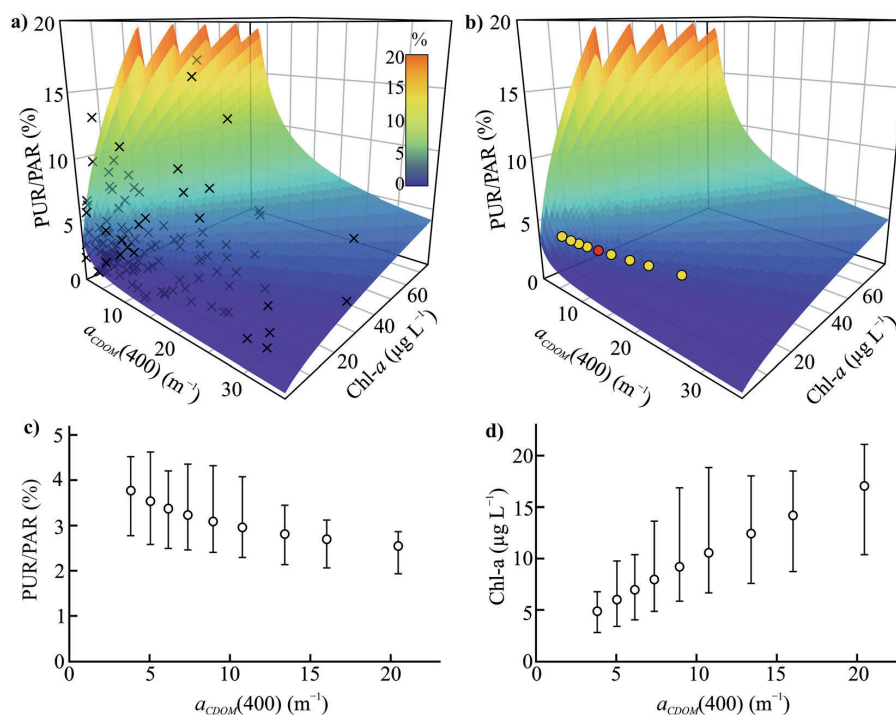
Fig. 4. Graphs showing the dependency of the fraction of PAR absorbed by phytoplankton (PUR/PAR, %) on $a_{CDOM}(400)$ and Chl *a* (**a–c**), and Chl *a* (**d**) on $a_{CDOM}(400)$ value. The 3D surfaces in (a and b) show calculated PUR/PAR (model 5 in Supporting Information Table S2) based on $a_{CDOM}(400)$ and Chl *a*, a color scale indicating the PUR/PAR value. Ticks (a) show the datapoints in the sampled lakes, and yellow dots (b) show the predicted PUR/PAR according to the nine centered percentile bands of $a_{CDOM}(400)$ from 5 to 15th to 85 to 95th percentile and corresponding Chl *a* values in the reference lakes (Supporting Information Table S5; Fig. S2). The red point (b) shows a median boreal lake according to $a_{CDOM}(400)$. The dots in (c and d) show the calculated PUR/PAR values (model 5 in Supporting Information Table S2) and Chl *a* concentrations based on measured values (Supporting Information Fig. S2), respectively, with the centered percentile bands of $a_{CDOM}(400)$ in the reference lakes. The error bars in (c and d) indicate the first and third quartiles of PUR/PAR and Chl *a* in each percentile band.
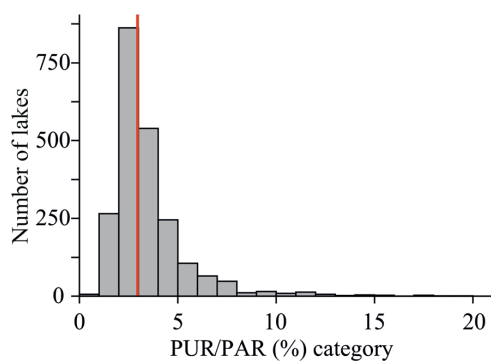
Fig. 5. A histogram of the variation in the percentage of photosynthetically active radiation absorbed by phytoplankton (PUR/PAR) calculated using model 5 in Supporting Information Table S2 in the 2250 reference boreal lakes. The vertical red line indicates the median value.

Predicting the impact of browning on PUR/PAR values

The impact of browning on PUR/PAR values was estimated for the median reference lake (PUR/PAR = 3.1%, $a_{CDOM}(400) = 8.9$ m^{-1} and Chl $a = 9.2$ μg L^{-1}, Fig. 4b–d, Supporting Information Table S6). Our browning scenario assumed not only an increase in the CDOM content but also an increase in the Chl a concentrations as found in the reference lakes along the CDOM gradient (Supporting Information Figs. S2, S3; Supporting Information Table S7). In terms of nutrients, the browning scenario assumed that water quality of the median lake will change according to the ratios 1.4 μg tot-P/m^{-1} $a_{CDOM}(400)$, 1.8 μg tot-P/mg DOC and 0.15 μg tot-P/mg Pt with increasing allochthonous input (Supporting Information Table S7). Browning causing a 25% increase in the $a_{CDOM}(400)$ value and an increase in Chl a concentration to 10.9 μg L^{-1} of the median boreal lake was predicted to decrease PUR/PAR to 2.9% (Fig. 4c,d; Supporting Information Table S6). PUR/PAR-values were predicted to decrease to 2.8%, 2.7% and 2.6% but Chl a concentrations to increase to 12.4, 14.0 and 15.4 μg L^{-1} with 50%, 75% and 100% increases, respectively, in $a_{CDOM}(400)$. Thus, although CDOM decreases PUR/PAR values according to the model 5, the severity of the decrease was partly compensated by an assumed increase of Chl a concentration. Due to this compensation, the predicted decrease in PUR/PAR values was only moderate for a typical range of browning reported in the recent decades.

Discussion

This study quantifies the decrease in the fraction of PAR absorbed by phytoplankton over the whole water column (i.e., PUR/PAR) as a function of increasing CDOM content in boreal lakes. We show that phytoplankton generally makes a low contribution to the absorption of PAR in boreal lakes, whereas CDOM absorbs most of the PAR in the water column.

The PUR/PAR value in the sampled lakes is best predicted by a logarithmic model including CDOM content (quantified as $a_{CDOM}(400)$) and Chl a concentration as explanatory variables. Based on the model, an increase of CDOM content decreases PUR/PAR but a concurrent increase in the Chl a concentration with the CDOM partly compensates for the decline of the PUR/PAR in boreal lakes along a CDOM gradient. Assuming that browning increases both CDOM content and Chl a concentration as in the reference lakes, our model suggests that the reported degree of browning decreases the PUR/PAR values in typical boreal lakes only moderately.

The fraction of PAR absorbed by phytoplankton

The range (0.4–17%) and median (3%) of PUR/PAR values in our sampled boreal lakes are lower than values of a similar parameter a_{phyto}/a_{tot} reported previously for Scandinavian lakes (range 2.2–28.2% and median 6.6%; Thrane et al. 2014) and for a Canadian reservoir (range 2–8% and mean 5%; Watanabe et al. 2015). In our study lakes, the upper ranges of CDOM content ($a_{CDOM}(400)$ 1.2–32.5 m^{-1}) and DOC (1.8–24.4 mg L^{-1}) exceed those reported for boreal lakes in earlier studies, such as by Thrane et al. (2014) ($a_{CDOM}(400)$ 0.1–15 m^{-1} and DOC 0.3–12.3 mg L^{-1}), by Kutser et al. (2005) ($a_{CDOM}(420)$ 1.2–7.7 m^{-1} and DOC 7–12 mg L^{-1}), or by Ylöstalo et al. (2014) ($a_{CDOM}(420) \sim$ 1–7 m^{-1} and DOC 5.1–11.2 mg L^{-1}). Thus, the high content of CDOM and DOC in our study lakes likely explain the low values of PUR/PAR, owing to the strong absorption of PAR by CDOM. In general, PUR/PAR values are low in boreal lakes, where CDOM is the dominant absorbing component in most lakes (Thrane et al. 2014; our study).

The impact of CDOM, nutrients, and Chl a on PUR/PAR in lakes along a CDOM gradient

Our regression models indicate that CDOM affects the PUR/PAR value negatively, while nutrients and Chl a have a positive impact on PUR/PAR. In a similar model applied to Scandinavian lakes, tot-P and DOC increased and decreased the light absorption by phytoplankton pigments, respectively (Thrane et al. 2014). Several factors can explain the findings of the models (this study; Thrane et al. 2014). An increase in CDOM content or the chromophores of DOC decrease the fraction of PAR absorbed by phytoplankton because they compete for available photons with phytoplankton (Kirk 2011; Solomon et al. 2015). On the other hand, nutrients, such as tot-P, can increase the biomass of phytoplankton, Chl a concentrations, and hence the light absorption by phytoplankton (Marzetz et al. 2020). Nutrients and DOC often increase concurrently with CDOM in lakes (Thrane et al. 2014; Seekell et al. 2015; Hamdan et al. 2021; this study). The carbon in DOC can supply energy and the carbon metabolites for mixotrophic phytoplankton, increasing their biomass and light absorption in high-CDOM lakes (Calderini et al. 2022). Further, phytoplankton can increase

their cellular Chl *a* content as a response to lowered light availability and this photoacclimation can increase the light absorption without a similar increase in biovolume (Fennel and Boss 2003; Sherbo et al. 2023). All in all, in lakes along a CDOM gradient, the shading effect of chromophores of DOM can be partly compensated by higher concentration of phytoplankton pigments related to better availability of nutrients (tot-P) and carbon (DOC) or photoacclimation (this study; Thrane et al. 2014; Calderini et al. 2022; Sherbo et al. 2023).

The effect of browning on the PUR/PAR values

Our study suggests that an increase of $a_{CDOM}(400)$ by 25–100% in lake water does reduce PUR/PAR values, but only rather modestly (5–15%) when accounting for the typical development of Chl *a* in 2250 boreal lakes with increasing CDOM captured in our models. Our browning scenario assumes that browning increases not only the CDOM content but also elevates the nutrient and Chl *a* concentrations in lakes. Our scenario is consistent with the reported concomitant increase of nutrient concentrations and CDOM or DOC content associated with browning (e.g., Corman et al. 2018; Lepistö et al. 2021). A key feature of our scenario is that it involves the possible adaptations of phytoplankton (e.g., photoacclimation) to elevated CDOM as found on average in the 2250 reference lakes. However, our scenario is based on spatial differences among lakes and their catchments along a CDOM-gradient (a space-for-time assumption), rather than on actual temporal responses of PUR/PAR to an increasing allochthonous loading in individual lakes because of the lack of such data (Stetler et al. 2021). Our browning scenario describes a typical response in PUR/PAR values on average across boreal catchments, whereas the response of an individual lake may be different depending on the characteristics of the catchment and the factors causing browning (e.g., recovery of acidification, changes in land use or vegetation).

Individual lake responses of PUR/PAR values to browning may differ from the average modeled response based on our browning scenario. One factor that influences PUR/PAR-values in lakes experiencing browning is the nutrient to CDOM ratio of the increased allochthonous loading (Kelly et al. 2018). In this study, we assumed that browning in lakes takes place with the water quality changes characterized by the ratios 1.8 μg tot-P/mg DOC, 1.4 μg tot-P/m^{-1} $a_{CDOM}(400)$, and 0.15 μg tot-P/mg Pt color as found on average in the 2250 reference lakes along a CDOM gradient. In our reference lakes, the tot-P/DOC ratio is higher than that reported elsewhere for allochthonous loading from terrestrial boreal forest catchments (0.5–1.2 μg tot-P/mg DOC; Jansson et al. 2012; Finér et al. 2021) but lower than soil leachates in the catchments of browned lakes in the temperate region (6–15 μg tot-P/mg DOC; Corman et al. 2018). The loading from Swedish forest streams has been characterized by 0.05 μg tot-P/mg Pt-color (Meili 1992), which is lower than the corresponding mean ratio in our reference lakes. In boreal lakes,

browning may decrease PUR/PAR values more than estimated in this study if their elevated allochthonous loading has lower nutrient to CDOM ratios than in our reference lakes. However, it is not simple to predict the responses of PUR/PAR to browning based solely on the characteristics of allochthonous loading because the responses happen within the receiving lakes. For example, the cycling of allochthonous tot-P is complicated in lakes; solar radiation can quickly break down a part of CDOM (photobleaching) and phytoplankton can adapt (mixotrophy and photoacclimation) to changing environmental conditions (Del Vecchio and Blough 2002; Vähätalo and Wetzel 2004). In this study, we evaluated the response of PUR/PAR to browning based on changes found in large number of lakes along a CDOM gradient, but we encourage future research into the quality of increased allochthonous matter as an explainer of PUR/PAR values in browning lakes.

Conclusions

Owing to the high content of CDOM in many boreal lakes, the contribution of phytoplankton to the absorption of incident PAR in boreal lakes is low, while CDOM absorbs most of the light over the whole water column. Our results show that the light absorption by phytoplankton decreases with increasing CDOM content, whereas Chl *a* concentration tends to concurrently increase with CDOM, partly compensating the negative effect of the CDOM on the PUR/PAR values. Assuming that browning increases both CDOM and Chl *a* contents of a lake, our model suggests that the decrease in the light absorption by phytoplankton in response to typical browning of most boreal lakes is only moderate, owing to either/or a combination of photoacclimation of phytoplankton to lowered light supply and increased nutrient concentrations associated with allochthonous matter in high-CDOM lakes.

Data availability statement

The data that support the findings of this study are available from the corresponding author upon reasonable request.

References

Ahonen, S. A., J. Seppälä, J. S. Karjalainen, J. Kuha, and A. V. Vähätalo. 2023. Increasing air temperature relative to water temperature makes the mixed layer shallower, reducing phytoplankton biomass in a stratified lake. Freshwater Biol. **68**: 1–11. doi:10.1111/fwb.14048

Apell, J. N., and K. McNeill. 2019. Updated and validated solar irradiance reference spectra for estimating environmental photodegradation rates. Environ. Sci. Proc. Imp. **21**: 427–437. doi:10.1039/c8em00478a

Ask, J., J. Karlsson, and M. Jansson. 2012. Net ecosystem production in clear-water and brown-water lakes. Global Biogeochem. Cycles **26**: GB1017. doi:10.1029/2010GB003951

Bergström, A. K., and J. Karlsson. 2019. Light and nutrient control phytoplankton biomass responses to global change

in northern lakes. Glob. Change Biol. **25**: 2021–2029. doi:10.1111/gcb.14623

Calderini, M. L., P. Salmi, C. Rigaud, E. Peltomaa, and S. J. Taipale. 2022. Metabolic plasticity of mixotrophic algae is key for their persistence in browning environments. Mol. Ecol. **31**: 4726–4738. doi:10.1111/mec.16619

Chambers, P. A., and J. Kalff. 1985. Depth distribution and biomass of submersed aquatic macrophyte communities in relation to secchi depth. Can. J. Fish. Aquat. Sci. **42**: 701–709. doi:10.1139/f85-090

Corman, J. R., B. L. Bertolet, N. J. Casson, S. D. Sebestyen, R. K. Kolka, and E. H. Stanley. 2018. Nitrogen and phosphorus loads to temperate seepage lakes associated with allochthonous dissolved organic carbon loads. Geophys. Res. Lett. **45**: 5481–5490. doi:10.1029/2018GL077219

Daniels, W. C., G. W. Kling, and E. E. Giblin. 2015. Benthic community metabolism in deep and shallow Arctic lakes during 13 years of whole-lake fertilization. Limnol. Oceanogr. **60**: 1604–1618. doi:10.1002/lno.10120

de Wit, H. A., and others. 2016. Current browning of surface waters will be further promoted by wetter climate. Environ. Sci. Tech. Let. **3**: 430–435. doi:10.1021/acs.estlett.6b00396

Del Vecchio, R., and N. V. Blough. 2002. Photobleaching of chromophoric dissolved organic matter in natural waters: Kinetics and modelling. Mar. Chem. **78**: 231–253. doi:10.1016/S0304-4203(02)00036-1

Evans, C. D., P. J. Chapman, J. M. Clark, D. T. Monteith, and M. S. Cresser. 2006. Alternative explanations for rising dissolved organic carbon export from organic soils. Glob. Change Biol. **12**: 2044–2053. doi:10.1111/j.1365-2486.2006.01241.x

Fennel, K., and E. Boss. 2003. Subsurface maxima of phytoplankton and chlorophyll: Steady-state solutions from a simple model. Limnol. Oceanogr. **48**: 1521–1534. doi:10.4319/lo.2003.48.4.1521

Finér, L., and others. 2021. Drainage for forestry increases N, P and TOC export to boreal surface waters. Sci. Total Environ. **762**: 144098. doi:10.1016/J.SCITOTENV.2020.144098

Hamdan, M., P. Byström, E. R. Hotchkiss, M. J. Al-Haidarey, and J. Karlsson. 2021. An experimental test of climate change effects in northern lakes: Increasing allochthonous organic matter and warming alters autumn primary production. Freshwater Biol. **66**: 815–825. doi:10.1111/fwb.13679

IOCCG. 2018. IOCCG Ocean optics and biogeochemistry protocols for Satellite Ocean colour sensor validation, p. 78. *In* A. R. Neeley and A. Mannino [eds.], Inherent optical property measurements and protocols: Absorption coefficient, v. **1.0**. International Ocean-Colour Coordinating Group (IOCCG). doi:10.25607/OBP-119

ISO/DIS 15681–2. 2005. Water quality–Determination of orthophosphate and total phosphorus by flow analysis (FIA and CFA)-Part2: Method by continuous flow analysis (CFA).

Jansson, M., M. Breggren, H. Laudon, and A. Jonsson. 2012. Bioavailable phosphorus in humic headwater streams in boreal Sweden. Limnol. Oceanogr. **57**: 1161–1170. doi:10.4319/lo.2012.57.4.1161

Jones, R. I., and L. Arvola. 1984. Light penetration and some related characteristics in small forest lakes in southern Finland. Verh. Internat. Verein. Limnol. **22**: 811–816. doi:10.1080/03680770.1983.11897390

Kallio, K. 2006. Optical properties of Finnish lakes estimated with simple bio-optical models and water quality monitoring data. Nord. Hydrol. **37**: 183–204. doi:10.2166/nh.2006.0014

Karlsson, J., P. Byström, J. Ask, P. Ask, L. Persson, and M. Jansson. 2009. Light limitation of nutrient-poor lake ecosystems. Nature **460**: 506–509. doi:10.1038/nature08179

Kelly, P. T., C. T. Solomon, J. A. Zwart, and S. E. Jones. 2018. A framework for understanding variation in pelagic gross primary production of lake ecosystems. Ecosystems **21**: 1364–1376. doi:10.1007/s10021-018-0226-4

Kirk, J. T. O. 2011. Light and photosynthesis in aquatic ecosystems, 3rd ed. Cambridge Univ. Press, p. 61–90.

Kortelainen, P. 1993. Content of total organic carbon in Finnish lakes and its relationship to catchment characteristics. Can. J. Fish. Aquat. Sci. **50**: 1477–1483. doi:10.1139/f93-168

Kritzberg, E. S. 2017. Centennial-long trends of lake browning show major effect of afforestation. Limnol. Oceanogr. Lett **2**: 105–112. doi:10.1002/lol2.10041

Kritzberg, E. S., and S. M. Ekström. 2012. Increasing iron concentrations in surface waters–a factor behind brownification? Biogeosciences **9**: 1465–1478. doi:10.5194/bg-9-1465-2012

Kutser, T., D. C. Pierson, L. Tranvik, A. Reinart, S. Sobek, and K. Kallio. 2005. Using satellite remote sensing to estimate the colored dissolved organic matter absorption coefficient in lakes. Ecosystems **8**: 709–720. doi:10.1007/s10021-003-0148-6

Lenard, T., and W. Ejankowski. 2017. Natural water brownification as a shift in the phytoplankton community in a deep hard water lake. Hydrobiologia **787**: 153–166. doi:10.1007/s10750-016-2954-9

Lepistö, A., A. Räike, T. Sallantaus, and L. Finér. 2021. Increases in organic carbon and nitrogen concentrations in boreal forested catchments—Changes driven by climate and deposition. Sci. Total Environ. **780**: 146627. doi:10.1016/j.scitotenv.2021.146627

Majasalmi, T., M. Rautiainen, and P. Stenberg. 2014. Modelled and measured fPAR in a boreal forest: Validation and application of a new model. Agric. For. Meteorol. **189–190**: 118–124. doi:10.1016/j.agrformet.2014.01.015

Marzetz, V., E. Spijkerman, M. Striebel, and A. Wacker. 2020. Phytoplankton community responses to interactions between light intensity, light variations, and phosphorus supply. Front. Environ. Sci. **8**: 539733. doi:10.3389/fenvs.2020.539733

Meili, M. 1992. Sources, concentrations and characteristics of organic matter in softwater lakes and streams of the

Swedish forest region. Hydrobiologia **229**: 23–41. doi:10.1007/BF00006988

Monteith, D. T., and others. 2007. Dissolved organic carbon trends resulting from changes in atmospheric deposition chemistry. Nature **450**: 537–540. doi:10.1038/nature06316

Morel, A. 1978. Available, usable, and stored radiant energy in relation to marine photosynthesis. Deep-Sea Res. **25**: 673–688. doi:10.1016/0146-6291(78)90623-9

Murray, C., S. Markager, C. A. Stedmon, T. Juul-Pedersen, M. K. Sejr, and A. Bruhn. 2015. The influence of glacial melt water on bio-optical properties in two contrasting Greenlandic fjords. Estuar. Coast. Shelf Sci. **163**: 72–83. doi:10.1016/j.ecss.2015.05.041

Naumann, E. 1929. The scope and chief problems of regional limnology. Int. Rev. Hydrobiol. **22**: 423–444. doi:10.1002/iroh.19290220128

Nieminen, M., S. Sarkkola, T. Sallantaus, E. M. Hasselquist, and H. Laudon. 2021. Peatland drainage–a missing link behind increasing TOC concentrations in waters from high latitude forest catchments? Sci. Total Environ. **774**: 145150. doi:10.1016/j.scitotenv.2021.145150

Nürnberg, G. K., and M. Shaw. 1998. Productivity of clear and humic lakes: Nutrients, phytoplankton, bacteria. Hydrobiologia **382**: 97–112. doi:10.1023/A:1003445406964

R Core Team. 2022. R: A language and environment for statistical computing. R Foundation for Statistical Computing, https://www.R-project.org/

Reynolds, C. S., M. L. White, R. T. Clarke, and A. F. Marker. 1990. Suspension and settlement of particles in flowing water: Comparison of the effects of varying water depth and velocity in circulating channels. Freshwater Biol. **24**: 23–34. doi:10.1111/j.1365-2427.1990.tb00304.x

Räike, A., P. Kortelainen, T. Mattsson, and D. N. Thomas. 2016. Long-term trends (1975–2014) in the concentrations and export of carbon from Finnish rivers to the Baltic Sea: Organic and inorganic components compared. Aquat. Sci. **78**: 505–523. doi:10.1007/s00027-015-0451-2

Seekell, D. A., J.-F. Lapierre, and J. Karlsson. 2015. Trade-offs between light and nutrient availability across gradients of dissolved organic carbon concentration in Swedish lakes: Implications for patterns in primary production. Can. J. Fish. Aquat. Sci. **72**: 1663–1671. doi:10.1139/cjfas-2015-0187

SFS-EN ISO 11905-1. 1997. Water quality. Determination of nitrogen. Part 1: Method using oxidative digestion with peroxodisulfate.

SFS-ISO 10260. 1992. Water quality—Measurement of biochemical parameters—Spectrometric determination of the chlorophyll-a concentration. International Organization for Standardization.

SFS-EN ISO 7887. 2011. Water quality. *In* Examination and determination of colour. International Organization for Standardization.

Sherbo, B. A. H., J. Tonin, M. J. Paterson, B. J. Hann, J. Kozak, and S. N. Higgins. 2023. The effects of terrestrial dissolved organic matter on phytoplankton biomass and productivity in boreal lakes. Freshwater Biol. **68**: 1–11. doi:10.1111/fwb.14178

Siegel, D. A., S. Maritorena, N. B. Nelson, D. A. Hansell, and M. Lorenzi-Kayser. 2002. Global distribution and dynamics of colored dissolved and detrital organic materials. J. Geophys. Res. **107**: 1–14. doi:10.1029/2001JC000965

Škerlep, M., E. Steiner, A. L. Axelsson, and E. S. Kritzberg. 2020. Afforestation driving long-term surface water browning. Glob. Change Biol. **26**: 1390–1399. doi:10.1111/gcb.14891

SMARTS. 2020. ASTM G173-03 irradiance reference spectrum calculated using the Simple Model of the Atmospheric Radiative Transfer of Sunshine (SMARTS). https://www.nrel.gov/grid/solar-resource/spectra.html

Smith, R. C., J. Marra, M. J. Perry, K. S. Baker, E. Swift, E. Buskey, and D. A. Kiefer. 1989. Estimation of a photon budget for the upper ocean in the Sargasso Sea. Limnol. Oceanogr. **34**: 1673–1693. doi:10.4319/lo.1989.34.8.1673

Solomon, C. T., and others. 2015. Ecosystem consequences of changing inputs of terrestrial dissolved organic matter to lakes: Current knowledge and future challenges. Ecosystems **18**: 376–389. doi:10.1007/s10021-015-9848-y

Stetler, J. T., L. B. Knoll, C. T. Driscoll, and K. C. Rose. 2021. Lake browning generates a spatiotemporal mismatch between dissolved organic carbon and limiting nutrients. Limnol. Oceanogr. Lett. **6**: 182–191. doi:10.1002/lol2.10194

Strock, K. E., S. J. Nelson, J. S. Kahl, J. E. Saros, and W. H. McDowell. 2014. Decadal trends reveal recent acceleration in the rate of recovery from acidification in the northeastern U.S. Environ. Sci. Technol. **48**: 4681–4689. doi:10.1021/es404772n

Thrane, J.-E., D. O. Hessen, and T. Andersen. 2014. The absorption of light in lakes: Negative impact of dissolved organic carbon on primary productivity. Ecosystems **17**: 1040–1052. doi:10.1007/s10021-014-9776-2

Tranvik, L. J. 1990. Bacterioplankton growth on fractions of dissolved organic carbon of different molecular weights from humic and clear waters. Appl. Environ. Microbiol. **56**: 1672–1677. doi:10.1128/aem.56.6.1672-1677.1990

Vähätalo, A. V., and R. G. Wetzel. 2004. Photochemical and microbial decomposition of chromophoric dissolved organic matter during long (months–years) exposures. Mar. Chem. **89**: 313–326. doi:10.1016/j.marchem.2004.03.010

Watanabe, S., I. Laurion, S. Markager, and W. F. Vincent. 2015. Abiotic control of underwater light in a drinking water reservoir: Photon budget analysis and implications for water quality monitoring. Water Resour. Res. **51**: 6290–6310. doi:10.1002/2014WR015617

Webster, K. E., and others. 2008. An empirical evaluation of the nutrient-color paradigm for lakes. Limnol. Oceanogr. **53**: 1137–1148. doi:10.4319/lo.2008.53.3.1137

Williamson, C. E., E. P. Overholt, R. M. Pilla, T. H. Leach, J. A. Brentrup, L. B. Knoll, E. M. Mette, and R. E. Moeller. 2015. Ecological consequences of long-term browning in lakes. Sci. Rep. **5**: 18666. doi:10.1038/srep18666

Xiao, Y., T. Sara-Aho, H. Hartikainen, and A. V. Vähätalo. 2013. Contribution of ferric iron to light absorption by chromophoric dissolved organic matter. Limnol. Oceanogr. **58**: 653–662. doi:10.4319/lo.2013.58.2.0653

Xiao, Z., S. Liang, R. Sun, J. Wang, and B. Jiang. 2015. Estimating the fraction of absorbed photosynthetically active radiation from the MODIS data based GLASS leaf area index product. Remote Sens. Environ. **171**: 105–117. doi:10.1016/j.rse.2015.10.016

Yang, X., C. M. O'Reilly, J. R. Gardner, M. R. V. Ross, S. N. Topp, J. Wang, and T. M. Pavelsky. 2022. The color of Earth's lakes. Geophys. Res. Lett. **49**: e2022GL098925. doi:10.1029/2022GL098925

Ylöstalo, P., K. Kallio, and J. Seppälä. 2014. Absorption properties of in-water constituents and their variation among various lake types in the boreal region. Remote Sens. Environ. **148**: 190–205. doi:10.1016/j.rse.2014.03.023

Acknowledgments

Conflict of Interest

None declared.

III

INCREASING AIR TEMPERATURE RELATIVE TO WATER TEMPERATURE MAKES THE MIXED LAYER SHALLOWER, REDUCING PHYTOPLANKTON BIOMASS IN A STRATIFIED LAKE

by

Salla A. Ahonen, Jukka Seppälä, Juha S. Karjalainen, Jonna Kuha & Anssi V. Vähätalo 2023

Freshwater Biology 68: 577–587.

ORIGINAL ARTICLE

Increasing air temperature relative to water temperature makes the mixed layer shallower, reducing phytoplankton biomass in a stratified lake

Salla A. Ahonen[1] | Jukka Seppälä[2] | Juha S. Karjalainen[1] | Jonna Kuha[1] |
Anssi V. Vähätalo[1]

[1]Department of Biological and Environmental Science, University of Jyväskylä, Jyväskylä, Finland

[2]Research infrastructure unit, Finnish Environment Institute, Helsinki, Finland

Correspondence
Salla A. Ahonen, Department of Biological and Environmental Science, University of Jyväskylä, P.O. Box 35, FI-40014 University of Jyväskylä, Finland.
Email: salla.a.ahonen@jyu.fi

Funding information
Academy of Finland, Grant/Award Number: 304466; Doctoral Training, Department of Biological and Environmental Science, University of Jyväskylä

Abstract

1. The depth of the mixed layer is a major determinant of nutrient and light availability for phytoplankton in stratified waterbodies. Ongoing climate change influences surface waters through meteorological forcing, which modifies the physical structure of fresh waters including the mixed layer, but effects on phytoplankton biomass are poorly known.

2. To determine the responses of phytoplankton biomass to the depth of the mixed layer, light availability and associated meteorological forcing, we followed daily changes in weather and water column properties in a boreal lake over the first half of a summer stratification period.

3. Phytoplankton biomass increased with the deepening of the mixed layer associated with high wind speeds and low air temperature relative to the temperature of the mixed layer ($T_{air}-T_{mix}<0$), whereas heatwave conditions—shallow mixed layer driven by high $T_{air}-T_{mix}$ value and low wind speed—reduced the biomass.

4. Improving light availability from low to moderate light conditions increased the phytoplankton biomass, while the highest light availability was associated with low phytoplankton biomass.

5. Our study demonstrates that the climatic impact-drivers wind speed and $T_{air}-T_{mix}$ are major drivers of mixed layer depth, which controlled phytoplankton biomass during the early summer stratification period. Our study suggests that increasing air temperature relative to water temperature and declining wind speeds have potential to lead to reduced phytoplankton biomass due to a shallower mixed layer during the first half of the stratification period in non-eutrophic lakes with sufficient light availability.

KEYWORDS
algal biomass, climate warming, heatwave, lake mixing, thermal stratification

1 | INTRODUCTION

Phytoplankton are essential for primary production and secondary production in aquatic food webs (Field et al., 1998). In stratified water bodies, actively photosynthesising phytoplankton often reside in the surface mixed layer, which refers to a turbulently mixed and relatively homogenous layer above a diurnal thermocline (Imberger, 1985; MacIntyre, 1993; Monismith & MacIntyre, 2009; Figure 1). Climatic and weather conditions as well as lake morphometry and water transparency are the major controllers of the lake mixing regimes (Hutchinson & Löffler, 1956; Imberger, 1985; Kirillin & Shatwell, 2016). The depth of the mixed layer (Z_{mix}) is determined by the balance between the rate at which turbulence is produced due to wind action and convection, and the buoyancy created by surface heat flux towards the waterbody (Imberger, 1985; Imboden & Wuest, 1995; Spigel & Imberger, 1987).

The depth of the mixed layer affects light availability, nutrient supply, grazing pressure and sedimentation losses of phytoplankton (Diehl, 2002; Huisman et al., 1999; Winder & Sommer, 2012). The shallowing of Z_{mix} relative to the depth of the euphotic layer (Z_{eu})—the depth at which the photosynthetically active radiation (PAR) attenuates to 1% of the surface values (Wetzel, 2001)—enhances light conditions for phytoplankton in the mixed layer (Huisman et al., 1999). At the same time, the reservoir of nutrients in the mixed layer decreases and the sinking losses of phytoplankton out of the mixed layer increases (Berger et al., 2006; Ptacnik et al., 2003; Weithoff et al., 2000; Yang et al., 2016). In contrast, deepening of Z_{mix} reduces light availability for phytoplankton but leads to entrainment of colder, typically nutrient rich water into the mixed layer. Moreover, deepening of Z_{mix} dilutes phytoplankton and zooplankton densities and reduces their encounter rates, whereas a shallow mixed layer may allow effective grazing by zooplankton (Berger et al., 2006).

The physical structure of a water column depends on external meteorological forcing such as solar radiation, wind speed, and air temperature (T_{air}) acting on the surface of the water body (Imberger & Parker, 1985; Macintyre et al., 1999; Persson & Jones, 2008). After the onset of spring turnover in lakes, an increase in solar radiation and air temperature relative to water temperature (T_{mix}) enhances the strength of stratification in the water column up to late summer when surface water reaches its maximum seasonal temperature (Boehrer & Schultze, 2008; Persson & Jones, 2008). The climate change-driven increase in summertime T_{air} further enhances the strength of stratification and reduces Z_{mix} (e.g., during heatwaves, which have become more frequent and severe; Coumou & Rahmstorf, 2012; Stetler et al., 2021; Woolway, Jennings, et al., 2021). Climate change has also reduced average wind speeds over continents (Woolway et al., 2019). This, also called as atmospheric stilling, tends to strengthen thermal stratification (Magee & Wu, 2017; Stetler et al., 2021; Woolway et al., 2019). Furthermore, climatic warming has advanced the timing of the onset of thermal stratification and prolonged the stratification season (Shatwell et al., 2019; Stetler et al., 2021; Woolway, Sharma, et al., 2021). The advanced onset of summer stratification increases a temporal
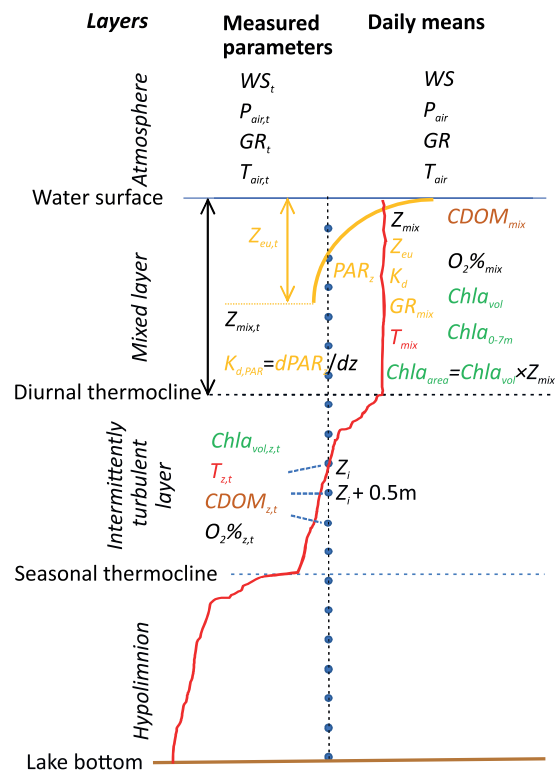

FIGURE 1 A schematic figure of the layers examined (left), the measured parameters (middle) and their daily means (right). Meteorological parameters were wind speed (WS_t, m/s), atmospheric pressure ($P_{air,t}$, mbar), global radiation (GR_t, kW m^{-2}), and air temperature ($T_{air,t}$, °C) recorded at 1-min intervals on Lake Jyväsjärvi. The corresponding daily means were WS, P_{air}, GR, and T_{air}. Vertical light attenuation coefficient ($K_{d,t}$, m^{-1}) and euphotic layer ($Z_{eu,t}$, m) refer to weekly measurements, which were interpolated to daily values (K_d, Z_{eu}). Water temperature ($T_{z,t}$, °C), CDOM fluorescence ($CDOM_{z,t}$, RFU), Chl-a concentration ($Chla_{vol,z,t}$, mg/m^3) converted from in situ Chl-a fluorescence (RFU), and oxygen saturation ($O_2\%_{z,t}$) were measured at 0.5 m depth (z) intervals from water-column profiles once in 1 hr. Mixed-layer depth ($Z_{mix,t}$) was determined from each temperature profiles and the daily means were reported as Z_{mix}. Daily mean water qualities within the mixed layer were reported as T_{mix}, $CDOM_{mix}$, $O_2\%_{mix}$, GR_{mix}, $Chla_{vol}$, $Chla_{area}$, and $Chla_{0-7m}$.

mismatch between spring phytoplankton blooms (during high nutrient availability after spring overturn) and the highest seasonal light availability, which occurs around the solstice (Gronchi et al., 2021).

The climate change-driven increase in stratification strength has reduced the transport of nutrients from the deeper layers to the ocean surface and reduced phytoplankton biomass in the global ocean (Behrenfeld et al., 2006; Mishra et al., 2022; Siemer et al., 2021). Evidence for similar trends in lakes is not as clear, and both positive and negative responses by phytoplankton biomass to warming and reduced mixing have been reported, highlighting the system-specificity of lakes (Gray et al., 2019; Lepori et al., 2018;

Straile et al., 2003). Phytoplankton biomass can nevertheless correlate negatively with the surface water temperature in non-eutrophic lakes, where an increase in stratification possibly reduces phytoplankton biomass (as in the ocean) (Kraemer et al., 2017). In eutrophic lakes, the response of phytoplankton might be the opposite (Kraemer et al., 2017). The latter can be explained by improved light availability, nutrient supplies from the catchment and N_2-fixing cyanobacteria, which favour higher temperature and can retrieve nutrients from hypolimnion via vertical migrations (Kraemer et al., 2017; O'Neil et al., 2012).

In this study, we hypothesise that climate change-driven shallowing of the mixed layer would have a negative impact on freshwater phytoplankton biomass in a stratified mesotrophic lake, where compensatory nutrient supplies from external sources are low. More precisely, an increase in summertime T_{air} relative to T_{mix} and reduced wind speeds are expected to reduce the depth of Z_{mix} during the first half of the summer stratification period when the water column is becoming more stable. A shallower Z_{mix} increases grazing and sedimentary losses of phytoplankton and reduces nutrient transport from the bottom of the mixed layer. To test these predictions, we monitored day-to-day variability in the meteorological forcing on the lake surface, the water column profiles and phytoplankton biomass in the mixed layer in a boreal lake over 2.5 months during the first half of the summer stratification period. Our study period included several cold spells and warm periods, one associated with a record-breaking heatwave in Europe (Vautard et al., 2020).

2 | MATERIAL AND METHODS

2.1 | Study lake

Our study lake is a boreal dimictic Lake Jyväsjärvi (area 3.3 km²; mean depth 7.0 m; maximum depth 25 m; mean total phosphorus concentration 20 mg/m³), ice-covered in winter and thermally stratified typically from May to October (Kuha, Arvola, et al., 2016; Kuha, Palomäki, et al., 2016). We examined the lake during the first half of the stratification period from May 15 to July 31 2019 (Supporting Information 1.1.1). An automated floating monitoring station profiled the water column and measured weather parameters continuously at the deepest point of the lake at 62°14′11.671″N 25°46′2.868″E (Kuha, Arvola, et al., 2016; Kuha, Palomäki, et al., 2016; Figure S1). Manual measurements and water samples were collected from the monitoring station.

2.2 | Water quality and meteorological variables

Our aim was to analyse day-to-day variability in phytoplankton biomass in the mixed layer and explain its variability using the corresponding variability in lake physics and meteorological forcing acting on the lake. The cell division of phytoplankton occurs typically once a day (Nelson & Brand, 1979), and thus our analyses focused on daily

changes (Supporting Information 1.1.2). The primary measurements of phytoplankton biomass, lake physics, and weather conditions were averaged over 1 day and water quality was averaged over the mixed layer for statistical analyses (as explained below).

A weather station (Campbell Scientific Research Grade Weather Station) measured continuously air temperature ($T_{air,t}$, °C), atmospheric pressure ($P_{air,t}$, mbar), global radiation (GR_t, kW m⁻²) and wind speed (WS_t, m s⁻¹) 2 m above the lake surface and recorded the data at 1-min intervals (Figure 1). The daily means of the meteorological variables were calculated as the averages of 1,440 measurements from midnight to the following midnight (T_{air}, P_{air}, GR, and WS; Figure 1).

The water quality monitoring covered four conceptual layers: euphotic, mixed, and an intermittently turbulent layer as well as the hypolimnion below the seasonal thermocline (Figure 1, details in Supporting Information 1.2). Daily depths of euphotic layer (Z_{eu}) were linearly interpolated from the manual weekly determinations of a vertical light attenuation coefficient (K_d [PAR], m⁻¹). The K_d values were determined as the slope of a line fitted on the relationship between depth z and $\log_e$ transformed downwelling irradiance, E_d (PAR, W m⁻²), measured with TriOS Ramses ACC-UV/VIS sensors (Rastede, Germany) from approximately 15 depths (Figure 1, Supporting Information 1.3 for details).

An automated EXO2 Multiparameter Sonde (YSI Inc. Yellow Springs, OH, USA) profiled the water column at 0.5 m depth z intervals about once in 1 hr (t) and measured water temperature ($T_{z,t}$, °C), fluorescence of chromophoric dissolved organic matter (CDOM; $CDOM_{z,t}$, RFU), oxygen saturation ($O_2\%_{z,t}$), and in vivo chlorophyll-a (Chl-a) fluorescence (RFU; Figure 1; the monitoring station in Figure S1). The relative fluorescence units of Chl-a were converted to concentration ($Chla_{vol,z,t}$, mg m⁻³, Figure 1) based on a calibration of the fluorometer with concentration of Chl-a measured in laboratory from water samples collected manually (see details in Supporting Information 1.4). The depth of the mixed layer (i.e., diurnal thermocline, $Z_{mix,t}$, m) was defined as the depth at which $T_{z,t}$ decreased 0.3°C from the surface temperature (details in Supporting Information 1.2). The depth of a seasonal thermocline was defined as the deepest density gradient found in the profile according to the R package rLakeAnalyzer (Winslow et al., 2019). Daily mean water quality in the mixed layer (Z_{mix}, T_{mix}, $Chla_{vol}$, $O_2\%_{mix}$, and $CDOM_{mix}$) was calculated as the averages from the measurements across the depths z from the surface to $Z_{mix,t}$ and over the c. 24 profiles per day (Figure 1). Daily mean global radiation in the mixed layer (GR_{mix}) was determined by combining daily values of Z_{mix}, K_d and GR as (Minor et al., 2016):

$$GR_{mix} = \left(Z_{mix} K_d\right)^{-1} \times \left(1 - e^{-Z_{mix} K_d}\right)$$

2.3 | Phytoplankton biomass in the mixed-layer and its specific rate of change

On each day, phytoplankton biomass was quantified in the mixed layer as the concentration of Chl-a expressed per volume ($Chla_{vol}$,

mg m^{-3}) and per area integrated from the surface to the diurnal thermocline ($Chla_{area}$, mg m^{-2}). A lake bathymetry correction was also tested for the $Chla_{area}$ values (equations 3 and 6 in Johansson et al., 2007) but omitted due to its minor effect on the statistical tests (see Supporting Information 1.4.1). Additionally, phytoplankton biomass was expressed per area integrated over the mixed and the intermittently turbulent layer ($Chla_{0-7m}$, mg m^{-2}). $Chla_{area}$ was chosen as the main response variable in the statistical analyses. $Chla_{vol}$ describes the volumetric phytoplankton biomass in the mixed layer and is proportional to the primary production rate in the euphotic layer but sensitive to dilution by deepening Z_{mix} (Behrenfeld & Boss, 2014; Kuha, Arvola, et al., 2016; Kuha, Palomäki, et al., 2016). $Chla_{area}$ expresses collectively the biomass of phytoplankton, which is responsible for the primary production over the entire water column (Behrenfeld & Boss, 2014). Additionally, $Chla_{area}$ is sensitive to the changes in Z_{mix} and acts as the ultimate source of phytoplankton biomass to the secondary consumers in the water column and in the sediment surface too (details in Supporting Information 1.4).

The daily values of $Chla_{vol}$ were calculated from a calibration equation between a spectrophotometrically measured Chl-a concentration (Shimadzu UV-1800 spectrophotometer, Shimadzu Co., Kyoto, Japan) from weekly collected composite water samples between 0–2 m and a mean in situ Chl-a fluorescence measurements (RFU) in the mixed layer at corresponding times (see the calibration curve in Figure S2, details in Supporting Information 1.4). $Chla_{area}$ was calculated as a multiplication of the daily mean volumetric Chl-a concentration ($Chla_{vol}$, mg m^{-3}) and the Z_{mix} (Figure 1, see details in Supporting Information 1.4). $Chla_{0-7m}$ was an integral of $Chla_{vol,z}$ from water surface to 7 m depth (methodological details in Supporting Information 1.4).

A daily specific rate of change in $Chla_{area}$ (r_d, d^{-1}) was determined as

$$r_d = \ln\left(\frac{Chla_{area,di+1}}{Chla_{area,di}}\right)$$

where $Chla_{area,di}$ and $Chla_{area,di+1}$ refer to $Chla_{area}$ on day i and the following day $i+1$, respectively (Behrenfeld & Boss, 2014). A positive value of r_d indicates an increase and negative value a decrease in phytoplankton biomass.

2.4 | Data analysis

Statistical analyses assessed how the phytoplankton biomass ($Chla_{area}$, $Chla_{vol}$, and $Chla_{0-7m}$) and its change (r_d) depended on water quality parameters (Z_{mix}, Z_{eu}, K_d, T_{mix}, $O_2\%_{mix}$, $CDOM_{mix}$, and GR_{mix}, Figure 1) and associated external meteorological forcing parameters (T_{air}, P_{air}, GR, and WS, Figure 1). Z_{eu} was also related to Z_{mix} (Z_{eu}:Z_{mix}) to further characterise underwater light availability. Air temperature minus water temperature in the mixed layer ($T_{air} - T_{mix}$) acted also as an explanatory variable because climatic warming (i.e., an increase in T_{air}) affects Z_{mix} through this difference (see details in Supporting Information 1.3.2).

We used several statistical approaches to investigate the dependence of phytoplankton biomass on environmental variables. Firstly, a Pearson correlation matrix addressed the relationships between the meteorological and water quality parameters. Secondly, the dependence of phytoplankton biomass (on day i) and its change (from day i to $i+1$) on individual meteorological and lake physical parameters (on day i) were assessed with regression analysis using two competing models (a linear model y $= \beta_1 x + \beta_0$; a quadratic model y $= \beta_2 x^2 + \beta_1 x + \beta_0$). The quadratic model approximated non-linear dependencies common to phytoplankton such as the dependence of photosynthesis on light. The most parsimonious model was selected based on an adjusted R^2 value. Thirdly, we used principal component analysis (PCA) to reduce the dimensionality of the external meteorological and lake physical parameters into two independent principal components. The interpretation of the principal components is based on the loadings of explanatory variables on the components. Finally, the dependence of phytoplankton biomass (on day i) and its change (from day i to $i+1$) on the principal components (on day i) were analysed with regression analysis as described above. Statistical testing was done with R studio (version 3.6.1) using the Base Package, and RColorBrewer package was used in figure making.

3 | RESULTS

3.1 | Dynamics of the mixed layer depth and phytoplankton biomass

During the first half of the summer stratification period in Lake Jyväsjärvi, the daily mean of mixed layer depth (Z_{mix}) ranged from 2.7 to 7.2 m and was on average shallower than the seasonal thermocline (Figures 2 and 3h). Chl-a concentration ($Chla_{vol,z,t}$), O$_2$ saturation (O$_2\%_{z,t}$) and the CDOM content ($CDOM_{z,t}$) were approximately homogenous within the mixed layer and followed its dynamics (Figure 2). $Chla_{vol,z,t}$ values decreased steeply below the diurnal thermocline without a deep Chl-a maximum (Figure 2a). Daily mean phytoplankton biomass in the mixed layer ($Chla_{area}$) ranged from 21 to 115 mg m^{-2} (Figures 1 and 3a; see Figure S3 for the corresponding $Chla_{vol}$ and $Chla_{0-7m}$ range). The daily specific rate of changes in $Chla_{area}$ (r_d) varied between −0.5 and 0.4 d^{-1} (Figure 3b). The lowest $Chla_{area}$ values and the longest period of negative r_d co-occurred when Z_{mix} became shallower and during the warmest air temperatures at the end of July, when a record-breaking heatwave advected hot air from North Africa across western Europe to our study lake (Vautard et al., 2020; Figures 2 and 3, Figure S3).

3.2 | The relationships between meteorological and lake physical parameters

Z_{mix} on day i correlated significantly with many daily mean meteorological parameters on the same day i (Figure 4). The correlation was positive with wind speed (WS) and negative with air pressure (P_{air})
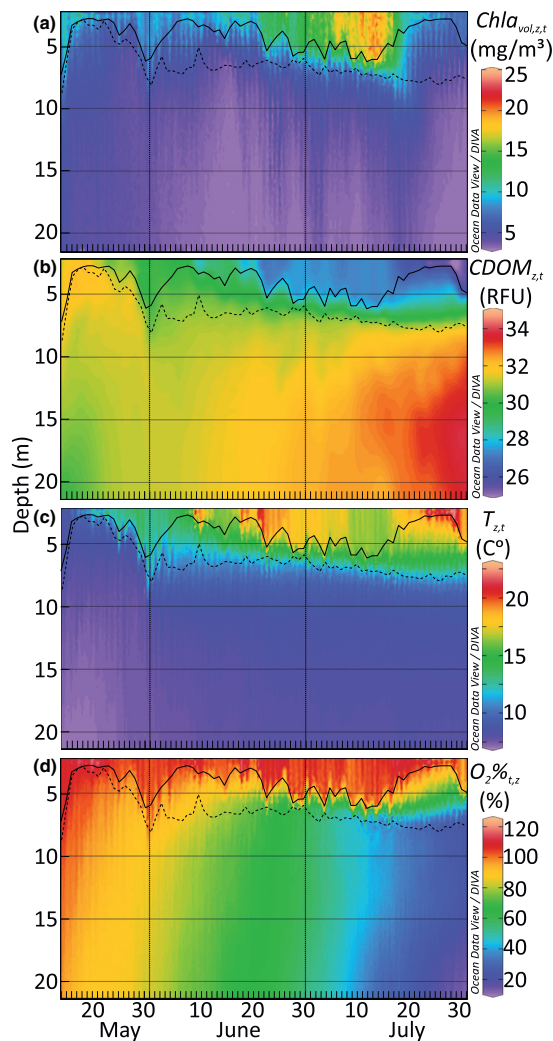
FIGURE 2 (a) Chlorophyll-*a* concentration ($Chla_{vol,z,t}$), (b) CDOM fluorescence ($CDOM_{z,t}$), (c) water temperature ($T_{z,t}$), and (d) oxygen saturation ($O_2\%_{z,t}$) along the study period. Black solid line is the daily mean mixed-layer depth (Z_{mix}) and the dashed line the seasonal thermocline.

and the difference between air temperature and water temperature ($T_{air} - T_{mix}$; Figure 4). Thus, Z_{mix} was deep during high wind speeds, low air pressures and when air was colder than water ($T_{air} - T_{mix} < 0$), which favoured convective mixing (Figures 3 and 4).

Light availability for the phytoplankton in the mixed layer was characterised by the global radiation received by the lake (GR), the vertical attenuation coefficient of light (K_d), CDOM content in the mixed layer ($CDOM_{mix}$), the ratio of euphotic layer depth to Z_{mix} ($Z_{eu}{:}Z_{mix}$) and mean global radiation in the mixed layer (GR_{mix}; Figure 3c,g,j,k,l). GR varied from 0.08 to 0.37 kW/m^2 without a temporal trend during the study period (Figure 3c). High GR values (i.e.,

sunny days) correlated positively with high atmospheric pressures (Figure 4). The values of K_d varied from 1.6 to 2.2 m^{-1}, a higher value meaning a faster light attenuation with depth (Figure 3j). The values of K_d correlated positively with $CDOM_{mix}$ but negatively with GR (Figure 4). The $CDOM_{mix}$ values had a decreasing trend associated with the photobleaching of CDOM in the mixed layer (Figures 2b and 3l). The euphotic layer was typically shallower than the mixed layer ($Z_{eu}{:}Z_{mix}$ was 0.39–1.0, Figure 3g). The $Z_{eu}{:}Z_{mix}$ correlated negatively with WS and K_d and positively with $T_{air} - T_{mix}$, P_{air}, and GR (Figure 4). Thus, light availability in terms of $Z_{eu}{:}Z_{mix}$ was highest on calm, sunny and warm days with low K_d-values (Figures 3 and 4).

3.3 | The dependence of phytoplankton biomass on individual environmental variables

$Chla_{area}$ was high on days with deep Z_{mix}, which explained 69% of the daily variability in $Chla_{area}$ (Figure 5a; Table S2). $Chla_{area}$ was low on days with high $Z_{eu}{:}Z_{mix}$ values (Figure 5b; Table S2). Similarly, $Chla_{area}$ was low on days with high values of GR_{mix}, P_{air}, and $O_2\%_{mix}$ as well as when air temperature was higher than water temperature ($T_{air} - T_{mix} > 0$; Figure 5c,f,g,j; Table S2). $Chla_{area}$ had a non-linear dependence on $CDOM_{mix}$ but no significant dependence on K_d, WS or GR (Figure 5d,e,h,i; Table S2). The same regression analyses with $Chla_{vol}$ and $Chla_{0-7m}$ as response variables gave similar results as those done with $Chla_{area}$ (Figures S4 and S5, Table S3).

Individual explanatory variables on day *i* explained up to 9% of the variation in r_d, i.e., a change in $Chla_{area}$ from day *i* to day *i* + 1 (Figure S6, Table S4). The value of r_d had significant positive dependencies on WS and K_d (Figure S6, Table S4), and significant negative dependencies on Z_{mix}, $T_{air} - T_{mix}$, GR and $O_2\%_{mix}$ (Figure S6, Table S4). Thus, a net increase in $Chla_{area}$ took place after cold days with high wind speed and low solar radiation (Figure S6, Table S4).

3.4 | Dependence of phytoplankton biomass on the principal components of environmental variability

The PCA simplified and reduced the multiple and complex relationships between the meteorological and lake physical factors into two principal components (Figure 6). The first two principal components (PC1 and PC2) of the PCA explained 61% of variation in the environmental parameters on the study days (Figure 6). PC1 explained 43% of the variation and received high loadings from Z_{mix} and related variables such as $T_{air} - T_{mix}$, GR_{mix}, $Z_{eu}{:}Z_{mix}$ and WS (Figure 6). High scores of PC1 indicated deep Z_{mix} on windy days when air (T_{air}) was cooler than the mixed layer (T_{mix}), whereas low PC1 scores indicated shallow Z_{mix} on calm days when air (T_{air}) was warmer than the mixed layer (T_{mix}). PC2 explained 18% of the variation and had high loading from variables associated with light availability ($CDOM_{mix}$, K_d, GR and GR_{mix}; Figure 6). Increasing score of PC2 indicated higher light availability.
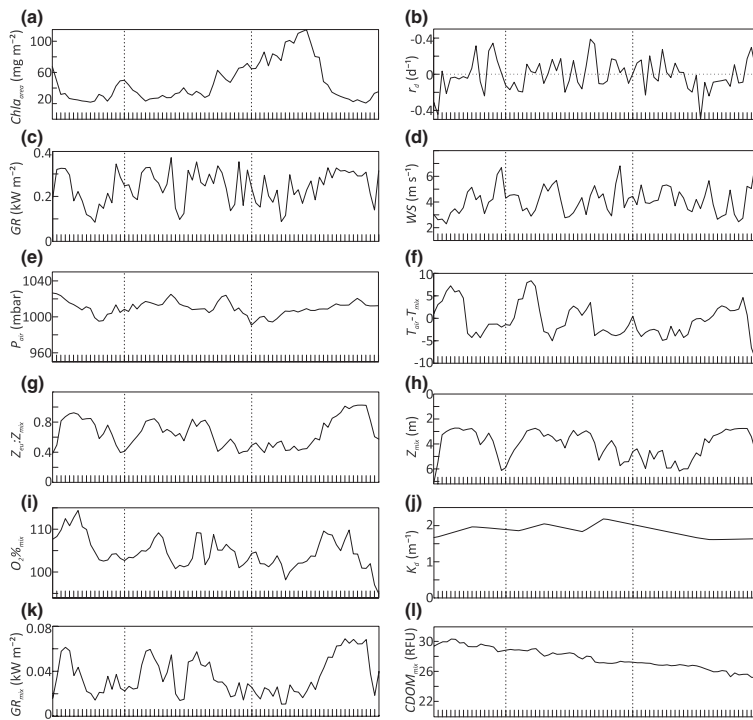
FIGURE 3 Time series of daily mean values of the response (a, b) and explanatory (c–l) parameters used in statistical analyses. Figure 1 explains the parameters and Figure S5 shows the values for T_{air}, T_{mix}, and Z_{eu}.
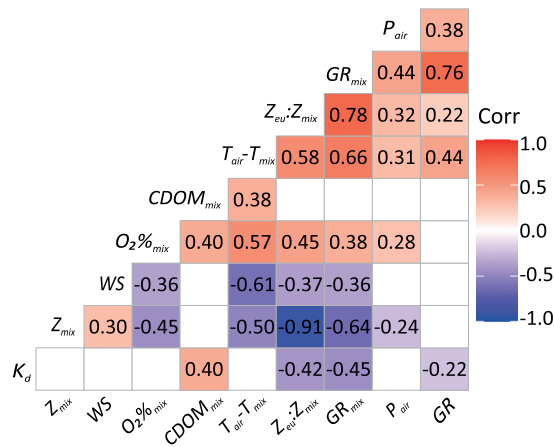

FIGURE 4 Correlation matrix of the meteorological and water quality parameters reported in Figure 3c–l. blue and red colours highlight the values of significant ($p < 0.05$) negative and positive correlation coefficients, respectively.

$Chla_{area}$ on day i was significantly dependent on both principal components on the same day i (Figure 7; Table S5a). The PC1 scores explained 43% of the variability in $Chla_{area}$ according to the non-linear model (Figure 7a; Table S5a) indicating that $Chla_{area}$ was high on days with deep mixed layer characterised by high winds and air temperatures colder than those in water. The PC2 scores explained 25% of the variability in $Chla_{area}$ (Figure 7b; Table S5a) indicating higher $Chla_{area}$ with improving light availability when light levels

were low but low $Chla_{area}$ with the highest light availabilities. The dependencies of $Chla_{vol}$ and $Chla_{0-7m}$ on the PC1 and PC2 scores were similar as found for $Chla_{area}$ (Figure S6, Table S6). The r_d values concerning the changes of $Chla_{area}$ from day i to following day $i+1$ did not show significant dependencies either on the PC1 or PC2 score on day i (Figure 7c,d; Table S5b).

4 | DISCUSSION

Our study shows that during the first half of the summer stratification period in a boreal mesotrophic lake, external meteorological variables (wind speed and $T_{air} - T_{mix}$) are most strongly associated with the depth of the mixed layer, Z_{mix}. Moreover, the variability in phytoplankton biomass depends primarily on the Z_{mix}. In our study, phytoplankton biomass increased with deepening of the mixed layer, caused by higher winds and lower air than water temperature. Instead, phytoplankton biomass decreases when the mixed layer becomes shallower on calm sunny days when air pressure is high and air temperature is warmer than water temperature (e.g. during a heatwave). Light availability showed only a modest influence on phytoplankton biomass.

4.1 | Mixed layer and phytoplankton biomass

The high positive dependence of $Chla_{area}$ on Z_{mix} found in this study is generally consistent with models that predict an increase
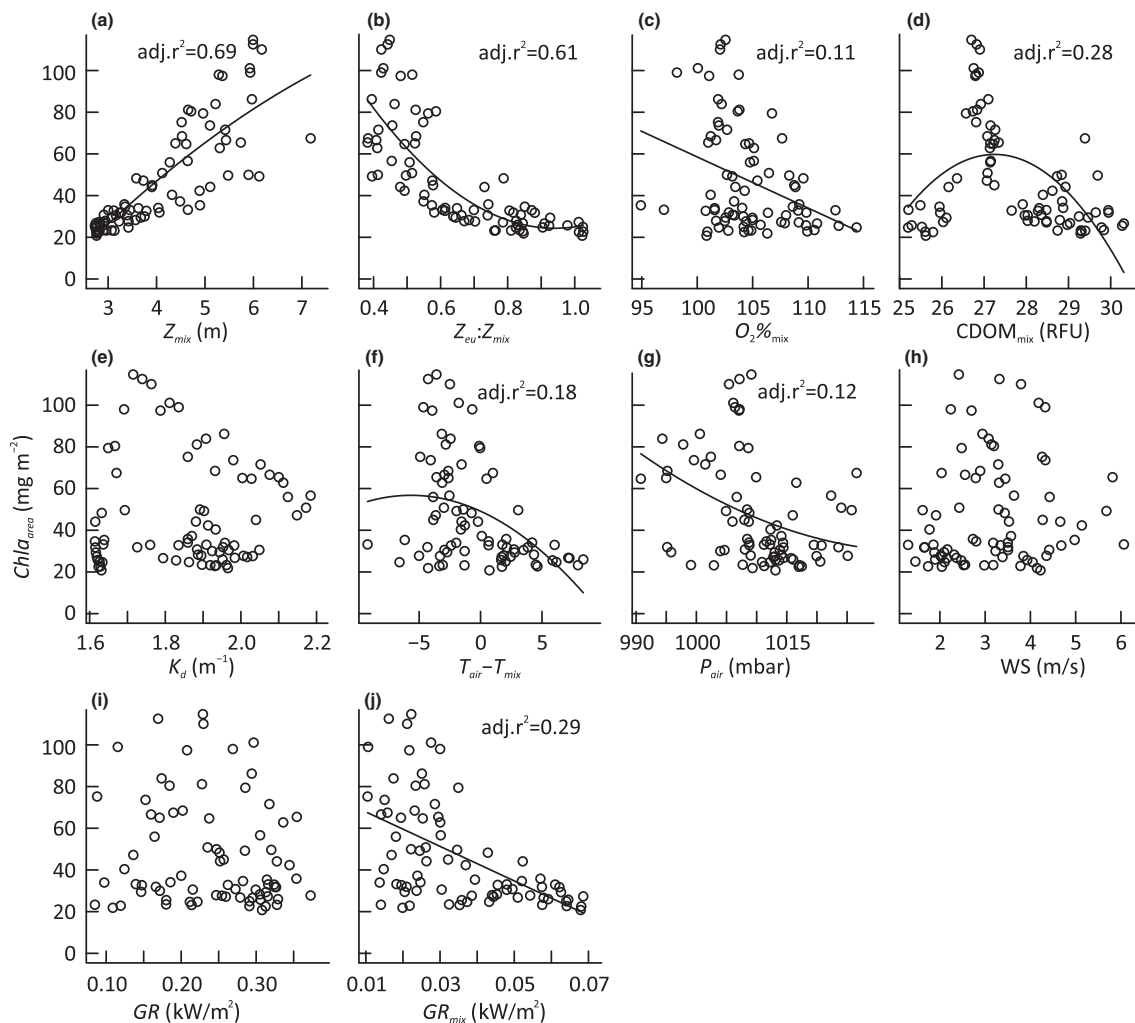
-WILEY-

FIGURE 5 The dependence of $Chla_{area}$ on individual explanatory parameters (Figure 3). The lines and curves show significant linear or non-linear, respectively, dependences, which are reported also in Table S2.

in phytoplankton biomass with a deepening mixed layer (Berger et al., 2006; Diehl, 2002; Mesman et al., 2022). These findings are supported by results from enclosure experiments, where artificial deepening of the mixed layer typically increases phytoplankton growth and biomass (Cantin et al., 2011; Diehl et al., 2002; Giling et al., 2017). Similarly, in 65 European lakes, $Chla_{area}$ increases with Z_{mix} in most (c. 85%) lakes, where Z_{mix} is <8 m like in our study (Berger et al., 2006). In our study, the positive dependence on Z_{mix} was also found for volumetric Chl-a concentration ($Chla_{vol}$) and areal Chl-a concentration at 0–7 m depth ($Chla_{0-7m}$), which do not include Z_{mix} as a multiplier by their definitions, and thereby verify the real dependencies between the phytoplankton biomass and the Z_{mix}. Our study shows that the positive relationship between $Chla_{area}$ and Z_{mix} found in earlier studies concerns also natural day-to-day dynamics in a stratified lake driven by meteorological forcing.

The dependence of $Chla_{area}$ on Z_{mix} can be explained primarily by an improved availability of nutrients from the bottom of (deepening) mixed layer (Diehl, 2002; Giling et al., 2017; Weithoff et al., 2000). Phytoplankton require nutrients to gain in biomass (Falkowski & Raven, 2014). Deep Z_{mix} also reduces sinking losses of phytoplankton out of the mixed layer (Cantin et al., 2011; Ptacnik et al., 2003). In addition, deep Z_{mix} decreases the encounter rate between phytoplankton and grazers and may reduce grazing losses of phytoplankton in the mixed layer (Berger et al., 2006).

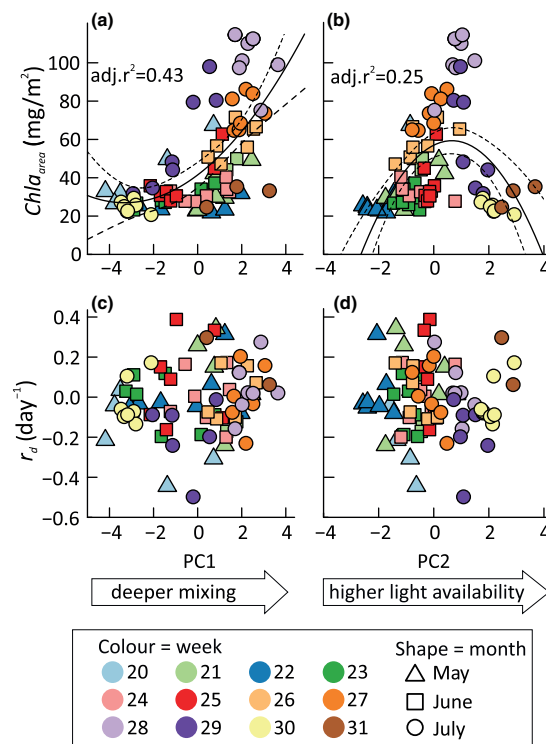## 4.2 | Light availability and phytoplankton biomass

During the first half of the summer stratification period in our study lake, the PC2 component, which expresses light availability,
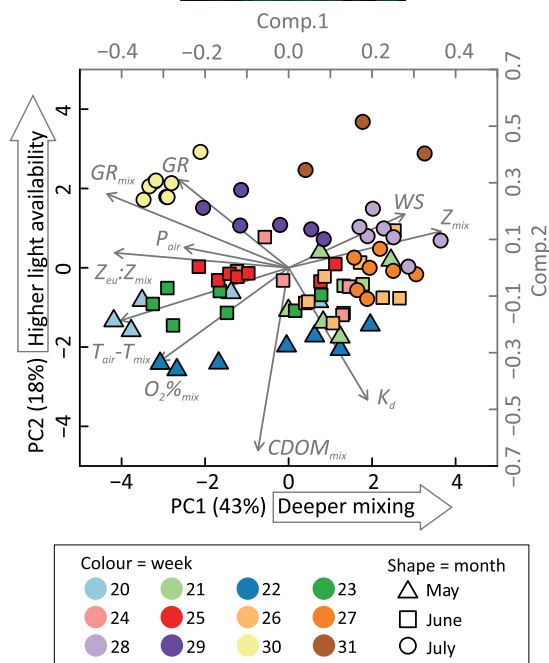
FIGURE 6 Principal component analysis of variability in the environmental parameters (Figure 3c–l) on the study days. The first (PC1) and second (PC2) principal components explain 43% and 18% of variability in the environmental parameters on the study days shown as symbols highlighting month by shape and week by colour. The Comp1 and Comp2 axes quantify the loadings of environmental parameters (arrows) on PC1 and PC2.

FIGURE 7 The dependence of $Chla_{area}$ on day i (Figure 3a) and r_d (i.e., change in $Chla_{area}$ from day i to day $i+1$, Figure 3b) on the PC1 and PC2 scores on day i (Figure 6). The solid and dashed curves show non-linear dependencies and their 95% confidence intervals reported also in Table S5. The symbols are explained in Figure 6.

was not related to the changes in $Chla_{area}$ (i.e. to the values of r_d). Nevertheless, phytoplankton biomass shows a non-linear dependence on PC2 score, where the $Chla_{area}$ has a tendency to increase with improving light availability when light level is poor, characterised by low global radiation (i.e., cloudy days), and high $CDOM_{mix}$ and K_d values. Under the highest light availability, however, $Chla_{area}$ values are also low, creating the overall non-linear shape of the dependency.

The ratio $Z_{eu}:Z_{mix}$ provides essential information about the underwater light conditions for phytoplankton within the mixed layer. In our study lake, the $Z_{eu}:Z_{mix}$ values (c. 0.4–1.0) are larger than c. 0.2, which is a critical value for supporting a net growth of $Chla_{area}$ in various aquatic environments (estuaries, ocean, lakes) according to theoretical models (Diehl, 2002), observations from field (Berger et al., 2006; Cloern, 1987; Sverdrup, 1953) and experiments (Diehl, 2002). When our results are combined with those from earlier studies, they indicate that an increase in Z_{mix} primarily increases $Chla_{area}$ in aquatic ecosystems where the $Z_{eu}:Z_{mix}$ is ≥ c. 0.37 like in our study lake (Cantin et al., 2011; Diehl, 2002; Diehl et al., 2002). When $Z_{eu}:Z_{mix}$ values fall from c. 0.37 towards c. 0.2, light availability becomes a major limiting factor of $Chla_{area}$. In such light limited aquatic ecosystems with $Z_{eu}:Z_{mix} < c.$ 0.2, a shallowing of Z_{mix} can increase the light availability above a critical threshold and

increase $Chla_{area}$ (Cloern, 1987; Diehl et al., 2002; Sverdrup, 1953). Overall, our results and older findings (e.g., Cantin et al., 2011; Diehl et al., 2002) suggest that light availability is not the major controlling factor of phytoplankton biomass in mesotrophic lakes like our study lake in the first half of the summer stratification period.

4.3 | Responses of phytoplankton biomass to warming climate

Our study shows that climatic impact-drivers, wind speed and $T_{air} - T_{mix}$, influence the depth of the mixed layer, which is then strongly associated with phytoplankton biomass during the first half of the summer stratification period in a mesotrophic lake. Our lake is non-eutrophic like most global oceans and lakes, where phytoplankton have been shown to respond negatively to increased surface water temperatures as an indicator of stratification strength (Behrenfeld et al., 2006; Kraemer et al., 2017; Mesman et al., 2021; Mishra et al., 2022; Siemer et al., 2021). This common response indicates that the strengthening of stratification and shallowing of Z_{mix} can reduce nutrient supply to phytoplankton and primarily act on non-eutrophic stratified waters.

We limited our study to the first half of the summer stratification period, when sedimentation of particles reduces the nutrient content of mixed layer and ongoing strengthening of seasonal stratification diminishes upward transport of nutrients. Under these circumstances, heatwaves and atmospheric stilling can reduce Z_{mix} and further diminish upward transport of nutrients to the mixed layer with a negative impact on phytoplankton (Coumou & Rahmstorf, 2012; Deng et al., 2021; Perkins-Kirkpatrick & Lewis, 2020; Woolway et al., 2019; Woolway, Sharma, et al., 2021). These findings suggest that climate change-driven increase in summertime T_{air} and reduced wind speed has an overall tendency to reduce the depth of mixed layer and phytoplankton biomass in non-eutrophic lakes during the first half of the stratification period.

The impact of climatic drivers on phytoplankton may be different or absent during the second half of the stratification season, when the seasonal cooling of T_{air} and reduced solar irradiance increase Z_{mix} towards the autumn turnover. For example, warmer air can lengthen the growth season of phytoplankton and increase phytoplankton biomass in the second part of the stratification period (Kraemer et al., 2017; Wasmund et al., 2019; Yang et al., 2016). Thus, the impact of weather variables altered by climatic change on phytoplankton may be different between the first and second half of the same summer stratification season.

5 | CONCLUSIONS

In this study, we observed a negative response of phytoplankton biomass associated with the mixed layer becoming shallower, caused by increasing air temperature relative to water temperature and declining wind speed; the drivers of climate change. These drivers of climatic change (e.g. experienced as heat waves) can cause oligotrophication during the first half of the stratification period in many boreal lakes without deep chlorophyll maxima, which are non-eutrophic and not limited by light availability like our study lake. Earlier works have shown that elevated surface water temperatures can increase phytoplankton biomass in lakes with extensive external sources of nutrients from a catchment, the atmosphere, N_2 fixing, or hypolimnion through vertical migrations of plankton. Our work highlights a contrasting response by a lake to climate change. These preliminary results are based on observations over one first half of a summer stratification period in one lake. Thus, further work is needed to understand how the characteristics of lakes regulate the responses of lakes to climate change at different phases in the annual cycles of lakes.

AUTHOR CONTRIBUTIONS

Conceptualisation, developing methods: S.A.A., A.V.V., J.S. Conducting the research: S.A.A., A.V.V., J.S.K., J.K. Data analysis: S.A.A., A.V.V. Preparation of figures and tables: S.A.A. Data interpretation, writing: S.A.A., A.V.V., J.S., J.S.K., J.K.

DATA AVAILABILITY STATEMENT

The data that support the findings of this study are available from the corresponding author upon reasonable request.

ORCID

Salla A. Ahonen https://orcid.org/0000-0002-0213-8332
Jukka Seppälä https://orcid.org/0000-0002-1210-9893
Juha S. Karjalainen https://orcid.org/0000-0001-9302-1174
Jonna Kuha https://orcid.org/0000-0001-6476-1077
Anssi V. Vähätalo https://orcid.org/0000-0003-3434-5915

REFERENCES

Behrenfeld, M. J., & Boss, E. S. (2014). Resurrecting the ecological underpinnings of ocean plankton blooms. *Annual Review of Marine Science*, 6, 167–194. https://doi.org/10.1146/annurev-marine-052913-021325

Behrenfeld, M. J., O'Malley, R. T., Siegel, D. A., McClain, C. R., Sarmiento, J. L., Feldman, G. C., Milligan, A. J., Falkowski, P. G., Letelier, R. M., & Boss, E. S. (2006). Climate-driven trends in contemporary ocean productivity. *Nature*, 444, 752–755. https://doi.org/10.1038/nature05317

Berger, S. A., Diehl, S., Kunz, T. J., Albrecht, D., Oucible, A. M., & Ritzer, S. (2006). Light supply, plankton biomass, and seston stoichiometry in a gradient of lake mixing depths. *Limnology and Oceanography, 51*, 1898–1905. https://doi.org/10.4319/lo.2006.51.4.1898

Boehrer, B., & Schultze, M. (2008). Stratification of lakes. *Reviews of Geophysics, 46*, RG2005. https://doi.org/10.1029/2006RG000210

Cantin, A., Beisner, B. E., Gunn, J. M., Prairie, Y. T., & Winter, J. G. (2011). Effects of thermocline deepening on lake plankton communities. *Canadian Journal of Fisheries and Aquatic Sciences, 68*, 260–276. https://doi.org/10.1139/F10-138

Cloern, J. E. (1987). Turbidity as a control on phytoplankton biomass and productivity in estuaries. *Continental Shelf Research, 7*, 1367–1381. https://doi.org/10.1016/0278-4343(87)90042-2

Coumou, D., & Rahmstorf, S. (2012). A decade of weather extremes. *Nature Climate Change, 2*, 491–496. https://doi.org/10.1038/nclimate1452

Deng, K., Azorin-Molina, C., Minola, L., Zhang, G., & Chen, D. (2021). Global near-surface wind speed changes over the last decades revealed by reanalyses and CMIP6 model simulations. *Journal of Climate, 34*, 2219–2234. https://doi.org/10.1175/JCLI-D-20-0310.1

Diehl, S. (2002). Phytoplankton, light, and nutrients in a gradient of mixing depths: Theory. *Ecology, 83*, 386–398.

Diehl, S., Berger, S., Ptacnik, R., & Wild, A. (2002). Phytoplankton, light, and nutrients in a gradient of mixing depths: Field experiments. *Ecology*, *83*, 399–411. https://doi.org/10.2307/2680023

Falkowski, P. G., & Raven, J. A. (2014). *Aquatic photosynthesis*. Princeton University Press.

Field, C. B., Behrenfeld, M. J., Randerson, J. T., & Falkowski, P. (1998). Primary production of the biosphere: Integrating terrestrial and oceanic components. *Science*, *281*, 237–240. https://doi.org/10.1126/science.281.5374.237

Giling, D. P., Nejstgaard, J. C., Berger, S. A., Grossart, H. P., Kirillin, G., Penske, A., Lentz, M., Casper, P., Sareyka, J., & Gessner, M. O. (2017). Thermocline deepening boosts ecosystem metabolism: Evidence from a large-scale lake enclosure experiment simulating a summer storm. *Global Change Biology*, *23*, 1448–1462. https://doi.org/10.1111/gcb.13512

Gray, E., Elliott, J. A., Mackay, E. B., Folkard, A. M., Keenan, P. O., & Jones, I. D. (2019). Modelling lake cyanobacterial blooms: Disentangling the climate-driven impacts of changing mixed depth and water temperature. *Freshwater Biology*, *64*, 2141–2155. https://doi.org/10.1111/fwb.13402

Gronchi, E., Jöhnk, K. D., Straile, D., Diehl, S., & Peeters, F. (2021). Local and continental-scale controls of the onset of spring phytoplankton blooms: Conclusions from a proxy-based model. *Global Change Biology*, *27*(9), 1976–1990. https://doi.org/10.1111/GCB.15521

Huisman, J., Van Oostveen, P., & Weissing, F. J. (1999). Critical depth and critical turbulence: Two different mechanisms for the development of phytoplankton blooms. *Limnology and Oceanography*, *44*, 1781–1787. https://doi.org/10.4319/lo.1999.44.7.1781

Hutchinson, G. E., & Löffler, H. (1956). The thermal classification of lakes. *Proceedings of the National Academy of Sciences of the United States of America*, *42*, 84–86.

Imberger, J. (1985). The diurnal mixed layer. *Limnology and Oceanography*, *30*(4), 737–770. https://doi.org/10.4319/lo.1985.30.4.0737

Imberger, J., & Parker, G. (1985). Mixed layer dynamics in a lake exposed to a spatially variable wind field. *Limnology and Oceanography*, *3*, 473–488. https://doi.org/10.4319/lo.1985.30.3.0473

Imboden, D. M., & Wuest, A. (1995). Mixing mechanisms in lakes. In A. Lerman, D. M. Imboden, & J. R. Gat (Eds.), *Physics and chemistry of lakes*. Springer-Verlag.

Johansson, H., Brolin, A. A., & Håkanson, L. (2007). New approaches to the modelling of lake basin morphometry. *Environmental Modeling & Assessment*, *12*, 213–228. https://doi.org/10.1007/s10666-006-9069-z

Kirillin, G., & Shatwell, T. (2016). Generalized scaling of seasonal thermal stratification in lakes. *Earth-Science Reviews*, *161*, 179–190. https://doi.org/10.1016/j.earscirev.2016.08.008

Kraemer, B. M., Mehner, T., & Adrian, R. (2017). Reconciling the opposing effects of warming on phytoplankton biomass in 188 large lakes. *Scientific Reports*, *7*, 1–7. https://doi.org/10.1038/s41598-017-11167-3

Kuha, J., Arvola, L., Hanson, P. C., Huotari, J., Huttula, T., Juntunen, J., Järvinen, M., Kallio, K., Ketola, M., Kuoppamäki, K., Lepistö, A., Lohila, A., Paavola, R., Vuorenmaa, J., Winslow, L., & Karjalainen, J. (2016). Response of boreal lakes to episodic weather-induced events. *Inland Waters*, *6*, 523–534. https://doi.org/10.5268/IW-6.4.886

Kuha, J. K., Palomäki, A. H., Keskinen, J. T., & Karjalainen, J. S. (2016). Negligible effect of hypolimnetic oxygenation on the trophic state of Lake Jyväsjärvi, Finland. *Limnologica*, *58*, 1–6. https://doi.org/10.1016/j.limno.2016.02.001

Lepori, F., Roberts, J. J., & Schmidt, T. S. (2018). A paradox of warming in a deep peri-alpine lake (Lake Lugano, Switzerland and Italy). *Hydrobiologia*, *824*, 215–228.

MacIntyre, S. (1993). Vertical mixing in a shallow, eutrophic lake: Possible consequences for the light climate of phytoplankton. *Limnology*

and Oceanography, *38*, 798–817. https://doi.org/10.4319/lo.1993.38.4.0798

Macintyre, S., Flynn, K. M., Jellison, R., & Romero, J. R. (1999). Boundary mixing and nutrient fluxes in mono Lake, California. *Limnology and Oceanography*, *44*, 512–529. https://doi.org/10.4319/lo.1999.44.3.0512

Magee, M. R., & Wu, C. H. (2017). Response of water temperatures and stratification to changing climate in three lakes with different morphometry. *Hydrology and Earth System Sciences*, *21*, 6253–6274. https://doi.org/10.5194/hess-21-6253-2017

Mesman, J. P., Ayala, A. I., Goyette, S., Kasparian, J., Marcé, R., Markensten, H., Stelzer, J. A. A., Thayne, M. W., Thomas, M. K., Pierson, D. C., & Ibelings, B. W. (2022). Drivers of phytoplankton responses to summer wind events in a stratified lake: A modeling study. *Limnology and Oceanography*, *67*, 856–873. https://doi.org/10.1002/lno.12040

Mesman, J. P., Stelzer, J. A. A., Dakos, V., Goyette, S., Jones, I. D., Kasparian, J., McGinnis, D. F., & Ibelings, B. W. (2021). The role of internal feedbacks in shifting deep lake mixing regimes under a warming climate. *Freshwater Biology*, *66*, 1021–1035. https://doi.org/10.1111/fwb.13704

Minor, E. C., Austin, J. A., Sun, L., Gauer, L., Zimmerman, R. C., & Mopper, K. (2016). Mixing effects on light exposure in a large-lake epilimnion: A preliminary dual-dye study. *Limnology and Oceanogrpahy*, *14*, 542–554. https://doi.org/10.1002/lom3.10111

Mishra, R. K., Jena, B., Venkataramana, V., Sreerag, A., Soares, M. A., & AnilKumar, N. (2022). Decadal changes in global phytoplankton compositions influenced by biogeochemical variables. *Environmental Research*, *206*, 112546. https://doi.org/10.1016/j.envres.2021.112546

Monismith, S. G., & MacIntyre, S. (2009). The surface mixed layer in lakes and reservoirs. In G. E. Linkens (Ed.), *Encyclopedia of inland waters*. Academic Press.

Nelson, D. M., & Brand, L. E. (1979). Cell division periodicity in 13 species of marine phytoplankton on a light: Dark cycle. *Journal of Phycology*, *15*, 67–75. https://doi.org/10.1111/J.1529-8817.1979.TB02964.X

O'Neil, J. M., Davis, T. W., Burford, M. A., & Gobler, C. J. (2012). The rise of harmful cyanobacteria blooms: The potential roles of eutrophication and climate change. *Harmful Algae*, *14*, 313–334. https://doi.org/10.1016/J.HAL.2011.10.027

Perkins-Kirkpatrick, S. E., & Lewis, S. C. (2020). Increasing trends in regional heatwaves. *Nature Communications*, *11*, 1–8. https://doi.org/10.1038/s41467-020-16970-7

Persson, I., & Jones, I. D. (2008). The effect of water colour on lake hydrodynamics: A modelling study. *Freshwater Biology*, *53*, 2345–2355. https://doi.org/10.1111/j.1365-2427.2008.02049.x

Ptacnik, R., Diehl, S., & Berger, S. (2003). Performance of sinking and nonsinking phytoplankton taxa in a gradient of mixing depths. *Limnology and Oceanography*, *48*, 1903–1912. https://doi.org/10.4319/lo.2003.48.5.1903

Shatwell, T., Thiery, W., & Kirillin, G. (2019). Future projections of temperature and mixing regime of European temperate lakes. *Hydrology and Earth System Sciences*, *23*, 1533–1551. https://doi.org/10.5194/hess-23-1533-2019

Siemer, J. P., Machin, F., González-Vega, A., Arrieta, J. M., Gutiérrez-Guerra, M. A., Pérez-Hernández, M. D., … Fraile-Nuez, E. (2021). Recent trends in SST, Chl-a, productivity and wind stress in upwelling and open ocean areas in the upper eastern North Atlantic subtropical gyre. *Journal of Geophysical Research: Oceans*, *126*, e2021JC017268. https://doi.org/10.1029/2021JC017268

Spigel, R. H., & Imberger, J. (1987). Mixing processes relevant to phytoplankton dynamics in lakes. *New Zealand Journal of Marine and Freshwater Research*, *21*, 361–377. https://doi.org/10.1080/00288330.1987.9516233

Stetler, J. T., Girdner, S., Mack, J., Winslow, L. A., Leach, T. H., & Rose, K. C. (2021). Atmospheric stilling and warming air temperatures drive

long-term changes in lake stratification in a large oligotrophic lake. *Limnology and Oceanography, 66*, 954–964.

Straile, D., Jöhnk, K., & Rossknecht, H. (2003). Complex effects of winter warming on the physicochemical characteristics of a deep lake. *Limnology and Oceanography, 48*, 1432–1438.

Sverdrup, H. U. (1953). On the conditions of the vernal blooming of phytoplankton. *Journal Du Conseil International Pour l'Éxploration de La Mer, 18*, 287–295.

Vautard, R., Van Aalst, M., Boucher, O., Drouin, A., Haustein, K., Kreienkamp, F., Van Oldenborgh, G. J., Otto, F., Ribes, A., Robin, Y., Schneider, M., Soubeyroux, J.-M., Stott, P., Seneviratne, S., Vogel, M., & Wehner, M. (2020). Human contribution to the record-breaking June and July 2019 heatwaves in Western Europe. *Environmental Research Letters, 15*. https://doi.org/10.1088/1748-9326/aba3d4

Wasmund, N., Nausch, G., Gerth, M., Busch, S., Burmeister, C., Hansen, R., & Sadkowiak, B. (2019). Extension of the growing season phytoplankton in the western Baltic Sea in response to climate change. *Marine Ecology Progress Series, 622*, 1–16. https://doi.org/10.3354/meps12994

Weithoff, G., Lorke, A., & Walz, N. (2000). Effects of water-column mixing on bacteria, phytoplankton, and rotifers under different levels of herbivory in a shallow eutrophic lake. *Oecologia, 125*, 91–100. https://doi.org/10.1007/PL00008896

Wetzel, R. G. (2001). *Limnology: Lake and River Ecosystems*. (3rd ed.). (pp. 1006). Academic Press.

Winder, M., & Sommer, U. (2012). Phytoplankton response to a changing climate. *Hydrobiologia, 698*, 5–16. https://doi.org/10.1007/s10750-012-1149-2

Winslow, L., Read, J., Woolway, R., Brentrup, J., Leach, T., Zwart, J., Albers, S., & Collinge, D. (2019). rLakeAnalyzer: Lake physics tools. *R package version* 1.11.4.1. https://github.com/GLEON/rLakeAnalyzer/issues

Woolway, R. I., Jennings, E., Shatwell, T., Golub, M., Pierson, D. C., & Maberly, S. C. (2021). Lake heatwaves under climate change. *Nature, 589*, 402–407. https://doi.org/10.1038/s41586-020-03119-1

Woolway, R. I., Merchant, C. J., Van Den Hoek, J., Azorin-Molina, C., Nõges, P., Laas, A., Mackay, E. B., & Jones, I. D. (2019). Northern hemisphere atmospheric stilling accelerates lake thermal responses to a warming world. *Geophysical Research Letters, 46*, 11983–11992. https://doi.org/10.1029/2019GL082752

Woolway, R. I., Sharma, S., Weyhenmeyer, G. A., Debolskiy, A., Golub, M., Mercado-Bettín, D., Perroud, M., Stepanenko, V., Tan, Z., Grant, L., Ladwig, R., Mesman, J., Moore, T. N., Shatwell, T., Vanderkelen, I., Austin, J. A., DeGasperi, C. L., Dokulil, M., La Fuente, S., … Jennings, E. (2021). Phenological shifts in lake stratification under climate change. *Nature Communications, 12*, 1–11. https://doi.org/10.1038/s41467-021-22657-4

Yang, Y., Colom, W., Pierson, D., & Pettersson, K. (2016). Water column stability and summer phytoplankton dynamics in a temperate Lake (lake Erken, Sweden). *Inland Waters, 6*, 499–508. https://doi.org/10.1080/IW-6.4.874

SUPPORTING INFORMATION

Additional supporting information can be found online in the Supporting Information section at the end of this article.